

**A COMPREHENSIVE  
VIBRATION ASSESSMENT PROGRAM  
FOR  
PALO VERDE  
NUCLEAR GENERATING STATION  
UNIT 1  
(SYSTEM 80 PROTOTYPE)**

**EVALUATION OF PREDICTIONS  
AND PRE-CORE HOT FUNCTIONAL  
MEASUREMENT AND INSPECTION  
PROGRAMS**

**FINAL REPORT**

**JANUARY 1985**

 **POWER  
SYSTEMS**  
COMBUSTION ENGINEERING, INC.

8503140219 850307  
PDR ADOCK 0500052B  
E PDR

## LEGAL NOTICE

THIS REPORT WAS PREPARED AS AN ACCOUNT OF WORK SPONSORED BY COMBUSTION ENGINEERING, INC. NEITHER COMBUSTION ENGINEERING NOR ANY PERSON ACTING ON ITS BEHALF:

A. MAKES ANY WARRANTY OR REPRESENTATION, EXPRESS OR IMPLIED INCLUDING THE WARRANTIES OF FITNESS FOR A PARTICULAR PURPOSE OR MERCHANTABILITY, WITH RESPECT TO THE ACCURACY, COMPLETENESS, OR USEFULNESS OF THE INFORMATION CONTAINED IN THIS REPORT, OR THAT THE USE OF ANY INFORMATION, APPARATUS, METHOD, OR PROCESS DISCLOSED IN THIS REPORT MAY NOT INFRINGE PRIVATELY OWNED RIGHTS; OR

B. ASSUMES ANY LIABILITIES WITH RESPECT TO THE USE OF, OR FOR DAMAGES RESULTING FROM THE USE OF, ANY INFORMATION, APPARATUS, METHOD OR PROCESS DISCLOSED IN THIS REPORT.

A COMPREHENSIVE VIBRATION ASSESSMENT  
PROGRAM FOR PALO VERDE NUCLEAR GENERATING  
STATION UNIT 1

(SYSTEM 80 PROTOTYPE)

EVALUATION OF PREDICTIONS  
AND PRE-CORE HOT FUNCTIONAL  
MEASUREMENT AND INSPECTION  
PROGRAMS  
FINAL REPORT

JANUARY, 1985

TABLE OF CONTENTS

<u>SECTION</u>	<u>PAGE</u>
TABLE OF CONTENTS . . . . .	i
LIST OF TABLES . . . . .	iii
LIST OF FIGURES . . . . .	iv
SUMMARY . . . . .	vii
1.0 INTRODUCTION . . . . .	1-1
1.1 ABSTRACT . . . . .	1-1
1.2 CVAP PROGRAM . . . . .	1-1
1.2.1 ANALYSIS . . . . .	1-1
1.2.2 MEASUREMENT . . . . .	1-2
1.2.3 INSPECTION . . . . .	1-2
1.2.4 EVALUATION . . . . .	1-3
1.3 ACCEPTANCE CRITERIA FOR TEST DATA . . . . .	1-3
1.4 EFFECT OF ASME WINTER 1982 ADDENDA ON ACCEPTANCE CRITERIA . . . . .	1-4
2.0 ANALYSIS PROGRAM . . . . .	2-1
2.1 INTRODUCTION . . . . .	2-1
2.2 ANALYSIS . . . . .	2-1
2.2.1 CORE SUPPORT BARREL . . . . .	2-1
2.2.2 LOWER SUPPORT STRUCTURE . . . . .	2-16
2.2.3 UPPER GUIDE STRUCTURE . . . . .	2-24
2.3 SUMMARY . . . . .	2-34
3.0 MEASUREMENT PROGRAM . . . . .	3-1
3.1 INTRODUCTION . . . . .	3-1
3.2 INSTRUMENTATION . . . . .	3-1
3.3 DATA ACQUISITION . . . . .	3-1
3.4 TEST CONDITIONS . . . . .	3-4

TABLE OF CONTENTS (Cont'd)

<u>SECTION</u>	<u>PAGE</u>
3.5 DATA REDUCTION. . . . .	3-5
3.5.1 CORE SUPPORT BARREL. . . . .	3-6
3.5.2 LOWER SUPPORT STRUCTURE. . . . .	3-7
3.5.3 UPPER GUIDE STRUCTURE. . . . .	3-9
3.6 SUMMARY . . . . .	3-10
4.0 INSPECTION PROGRAM. . . . .	4-1
4.1 INTRODUCTION . . . . .	4-1
4.2 DISCUSSION . . . . .	4-1
4.3 INSPECTION . . . . .	4-2
4.3.1 REACTOR VESSEL. . . . .	4-2
4.3.2 CORE SUPPORT BARREL EXTERIOR. . . . .	4-3
4.3.3 UNDER THE CSB AND ALIGNMENT KEYS. . . . .	4-4
4.3.4 CORE SUPPORT BARREL INTERIOR. . . . .	4-4
4.3.5 UNDER THE UPPER GUIDE STRUCTURE . . . . .	4-5
4.3.6 UPPER GUIDE STRUCTURE EXTERIOR. . . . .	4-5
4.3.7 HOLDDOWN RING . . . . .	4-6
4.3.8 REACTOR VESSEL CLOSURE HEAD . . . . .	4-6
4.4 SUMMARY. . . . .	4-7
5.0 EVALUATION PROGRAM. . . . .	5-1
5.1 INTRODUCTION . . . . .	5-1
5.2 COMPARISON OF PREDICTIONS & MEASURED DATA. . . . .	5-1
5.2.1 CORE SUPPORT BARREL . . . . .	5-1
5.2.2 LOWER SUPPORT STRUCTURE . . . . .	5-5
5.2.3 UPPER GUIDE STRUCTURE . . . . .	5-7
5.3 EVALUATION . . . . .	5-10
5.3.1 STRUCTURAL ADEQUACY OF PEACTOR INTERNALS. . . . .	5-10
5.3.2 MARGINS OF SAFETY . . . . .	5-12
5.3.3 ANALYTICAL & TEST METHODS . . . . .	5-12
5.4 CONCLUSIONS. . . . .	5-13
REFERENCES. . . . .	5-16

## TABLES

	<u>Page</u>
I	Summary of Predicted and Measured Stresses. . . . . xi
II	Summary of System 80 CVAP Instrumentation . . . . . xii
1.3-1	Response Instrumentation Data Acceptance Criteria . . . . . 1-6
2.2-1	CSB Hydraulic Loading . . . . . 2-7
2.2-2	CSB Annulus Liquid Frequencies. . . . . 2-8
2.2-3	CSB Frequencies in Air and Water. . . . . 2-9
2.2-4	LSS Deterministic Hydraulic Loading . . . . . 2-17
2.2-5	LSS Random Hydraulic Loading. . . . . 2-18
2.2-6	UGS Deterministic Hydraulic Loading . . . . . 2-25
2.2-7	UGS Random Hydraulic Loading. . . . . 2-26
2.3-1	Design and CVAP Peak Stress Summary . . . . . 2-35
3.2-1	CVAP Instrumentation . . . . . 3-12
3.4-1	Original Test Conditions. . . . . 3-20
3.4-2	Modified Test Conditions. . . . . 3-21
3.5-1	CVAP Transducer History . . . . . 3-22
3.5-2	Spectral Density Data Reduction. . . . . 3-24
3.5-3	CSB Total RMS Response. . . . . 3-25
3.5-4	Inlet Pressure Breakdown (P2) . . . . . 3-26
3.5-5	Snubber Displacement Breakdown (A3) . . . . . 3-27
3.5-6	Upper Flange Strain Breakdown (S1). . . . . 3-28
3.5-7	LSS Total RMS Response . . . . . 3-29
3.5-8	Instrument Tube Pressure Breakdown (P12). . . . . 3-30
3.5-9	LSS Displacement Breakdown (A11). . . . . 3-31
3.5-10	Instrument Tube Strain Breakdown (S14). . . . . 3-32
3.5-11	UGS Total RMS Response. . . . . 3-33
3.5-12	Upper Plate Pressure Breakdown (P13). . . . . 3-34
3.5-13	Tube Midspan Displacement Breakdown (A7). . . . . 3-35
3.5-14	Guide Tube Strain Breakdown (S9). . . . . 3-36
5.3-1	Summary of Margins of Safety. . . . . 5-15

## FIGURES

	<u>PAGE</u>
I	System 80 Vertical Arrangement. . . . . xiii
1.1-1	Reactor Vessel Arrangement. . . . . 1-7
1.1-2	Comprehensive Vibration Assessment Program. . . . . 1-8
2.1-1	Summary of Analytical Methodology . . . . . 2-3
2.1-2	Core Support Barrel . . . . . 2-4
2.1-3	Lower Support Structure . . . . . 2-5
2.1-4	Upper Guide Structure . . . . . 2-6
2.2-1	CSB Circumferential Pressure Distribution . . . . . 2-10
2.2-2	CSB Axial Pressure Distribution . . . . . 2-11
2.2-3	CSB Modeshapes. . . . . 2-12
2.2-4	CSB Max Strain - Upper Flange . . . . . 2-13
2.2-5	CSB Max Strain - Mid Plane. . . . . 2-14
2.2-6	CSB Snubber Displacements . . . . . 2-15
2.2-7	LSS Assy Frequencies & Modeshapes . . . . . 2-19
2.2-8	ICI Tube Frequencies & Modeshapes . . . . . 2-20
2.2-9	ICI Tube Strain - S13 . . . . . 2-21
2.2-10	ICI Tube Strain - S14 . . . . . 2-22
2.2-11	ICI Support Plate - Displacements . . . . . 2-23
2.2-12	UGS Shroud Tube - Frequencies & Modeshapes. . . . . 2-27
2.2-13	UGS Tube Bank - Frequencies & Modeshapes. . . . . 2-28
2.2-14	UGS Assembly - Frequencies & Modeshapes . . . . . 2-29
2.2-15	UGS Guide Tube Strain - S9 & S11. . . . . 2-30
2.2-16	UGS Guide Tube Strain - S10 & S12 . . . . . 2-31
2.2-17	UGS Guide Tube Displacement - Midspan . . . . . 2-32
2.2-18	Fuel Alignment Plate Displacement . . . . . 2-33

FIGURES (Cont'd)

	<u>PAGE</u>
3.2-1	Transducer Axial Locations. . . . . 3-13
3.2-2	Circumferential Locations of Nozzles. . . . . 3-14
3.2-3	Input Function Transducers. . . . . 3-15
3.2-4	Response Measurement Transducers. . . . . 3-15
3.2-5	LSS Assembly Instrumentation. . . . . 3-16
3.2-6	UGS Instrumentation - Circumferential Locations . . . . . 3-17
3.2-7	UGS Instrumentation - Axial Locations . . . . . 3-18
3.3-1	Data Acquisition System . . . . . 3-19
3.5-1	Pressure PSD (P2) - Test Condition 6. . . . . 3-37
3.5-2	Pressure PSD (P2) - Test Condition 8. . . . . 3-38
3.5-3	Pressure PSD (P2) - Test Condition 11 . . . . . 3-39
3.5-4	Pressure PSD (P2) - Test Condition 15 . . . . . 3-40
3.5-5	Pressure PSD (P4) - Test Condition 15 . . . . . 3-41
3.5-6	Pressure PSD (P2) - Test Condition 15 . . . . . 3-42
3.5-7	Pressure PSD (P4 & P5) - Test Condition 15 . . . . . 3-43
3.5-8	Coherence/Phase (P4 & P5) - Test Condition 15 . . . . . 3-44
3.5-9	Pressure PSD (P4 & P5) - Test Condition 15 . . . . . 3-45
3.5-10	Coherence/Phase (P4 & P7) - Test Condition 15 . . . . . 3-46
3.5-11	Pressure PSD (P4 & P8) - Test Condition 15. . . . . 3-47
3.5-12	Coherence/Phase (P4 & P8) - Test Condition 15 . . . . . 3-48
3.5-13	Displacement PSD (A3 & A4) - Test Condition 1 . . . . . 3-49
3.5-14	Coherence/Phase (A3 & A4) - Test Condition 1. . . . . 3-50
3.5-15	Strain PSD - 0 to 50 HZ (S2 & S6) - Test Condition 15 . . . 3-51
3.5-16	Coherence/Phase (S2 & S6) - Test Condition 15 . . . . . 3-52
3.5-17	Strain PSD - 0 to 500 HZ (S2) - Test Condition 15 . . . . . 3-53
3.5-18	Strain PSD - 0 to 500 HZ (S6) - Test Condition 15 . . . . . 3-54
3.5-19	Coherence - 0 to 500 HZ (S2 & S6) - Test Condition 15 . . . 3-55
3.5-20	Time History - Pump Start (S5) - Test Condition 15. . . . . 3-56
3.5-21	Pressure PSD - 0 to 500 HZ (P12) - Test Condition 15. . . . 3-57
3.5-22	Pressure PSD - 0-50 HZ (P12) - Test Condition 15. . . . . 3-58
3.5-23	Acceleration PSD - 0 to 500 HZ (A11) - Test Condition 15. . 3-59



FIGURES (Cont'd)

	<u>PAGE</u>
3.5-24	Acceleration PSD - 0 to 50 HZ (A11) - Test Condition 15. . . 3-60
3.5-25	Strain PSD - 0 to 500 HZ (S14) - Test Condition 6. . . . . 3-61
3.5-26	Time History - Pump Start (A11) - Test Condition 15. . . . . 3-62
3.5-27	Pressure PSD - 0 to 500 HZ (P13) - Test Condition 15 . . . 3-63
3.5-28	Pressure PSD - 0 to 500 HZ (P11) - Test Condition 11 . . . 3-64
3.5-29	Acceleration PSD - 0 to 50 HZ (A5) - Test Condition 15 . . 3-65
3.5-30	Strain PSD - 0 to 500 HZ (S11) - Test Condition 15 . . . . . 3-66
3.5-31	Time History - Pump Start (S11) - Test Condition 15. . . . . 3-67
3.5-32	Guide Tube APD (A5) - Test Condition 15. . . . . 3-68
3.5-33	Guide Tube APD (S12) - Test Condition 15 . . . . . 3-69
5.2-1	UGS Random Pressure Comparison (P13) - Test Condition 15 . 5-11

## SUMMARY

In accordance with the United States Nuclear Regulatory Commission Regulatory Guide 1.20 (Ref. 1) a Comprehensive Vibration Assessment Program (CVAP) has been developed for Palo Verde Nuclear Generating Station Unit 1. This plant is prototypical of Combustion Engineering's 3800 Mwt System 80 pressurized water reactor (Figure I).

The purpose of the CVAP is to verify the structural integrity of the reactor internals to flow induced loads prior to commercial operation. The dynamic flow related loads considered are associated with normal steady state operation and anticipated operating transients.

This comprehensive program, for a reactor prototype, consists of four individual Analysis, Measurement, Inspection, and Evaluation programs. The Analysis program provides theoretical evidence of the structural integrity of the internals and serves as a basis for both the Measurement and Inspection programs. Results of these programs form a basis for assessing, in the Evaluation program, the margins of safety for the reactor internals. Detailed descriptions of the Analysis, Measurement and Inspection programs are found in Reference 2.

The Evaluation program includes analysis and critical review of the data obtained in both the Measurement and Inspection programs and comparison of these data with predictions of the Analysis program. This evaluation includes an assessment of the methods used to predict the response of the internals to dynamic forces and the resulting margins of safety. Preliminary and final reports of this evaluation are to be submitted to the Nuclear Regulatory Commission, as specified in Regulatory Guide 1.20, after completion of all precritical testing. The preliminary report was submitted in January of 1984 (Ref. 3). This report contains the required final evaluation.

Analyses were completed for the flow induced loading dynamic response of the two safety related core support assemblies; the core support barrel assembly (core support barrel and lower support structure) and upper guide structure assembly (Figure I).

Maximum predicted stresses, summarized in Table I, are the alternating stress intensities due to flow induced dynamic loads predicted for CVAP test conditions corresponding to normal operation.

A measurement program was developed based on results of these analyses. The purpose of this program is to obtain data on both random and deterministic excitation (pressure) and structural response (displacement, strain and acceleration). Instrumentation, consisting of pressure transducers, strain gages, accelerometers, and displacement transducers has been specified for each of the assemblies. A summary of the instrumentation is given in Table II.

Pre-core hot functional testing was started on May 13, 1983 and completed July 8, 1983.

Testing was done at steady state and transient (pump startup and shutdown) conditions corresponding to normal and part loop operation, except for 500°F four pump operation. The period of data acquisition for the CVAP was from May 15 to June 3, 1983. Approximately 1200 hours of pre-core flow testing were completed insuring that the components were subjected to more than  $10^6$  cycles of vibration before inspection.

Data were acquired to compare with predicted values of hydraulic forcing functions and structural response. Transducer signals were conditioned and recorded on magnetic tape for post test reduction and analysis. Response during testing was monitored online and the signals evaluated for spectral content. Root mean square values of the signals related to structural response were computed following each test and compared to an acceptance criterion based on the endurance stress from the ASME Code (Ref. 4). Maximum measured values of stress are listed in Table I at the predicted maximum stress locations. In all cases the measured values of stress were less than the acceptance limits. Evaluation of the test data shows that the measured stresses are less than the predicted values.

A pre-core inspection of the internals was performed before initiation and after completion of all pre-core flow tests. In both cases, the internals were positioned to permit visual inspection of the specified locations (Ref. 2). Major load bearing surfaces, contact surfaces, welds, maximum stress locations identified in the analysis program and the CVAP instrumentation, mountings, and conduits were examined. A photographic record was made of all observations.

Comparison of results of the visual inspection before and after pre-core testing indicated no signs of abnormal wear or contact for any of the core support structures. However, cracks were found in the heat affected zones near the welds of seven Control Element Assembly (CEA) extension shaft guides and ten connecting web locations in the CEA Shroud Assembly. Evidence of these cracks was reported to the NRC (Ref. 9) and a program was successfully carried out to determine the cause of the cracking and to institute design modifications. The redesigned CEA shroud package was instrumented and tested to verify the adequacy of the design modifications. This testing was addressed in a separate report (Ref. 8).

Post test disassembly of the reactor coolant circulating pumps revealed damage to the impeller blades on two of the four pumps. This condition was reported to the NRC (Ref. 9) and a program was successfully carried out to institute design modifications which corrected the problem. This program is addressed in a separate report (Ref. 7). The adequacy of these design modifications was verified during the Demonstration Testing done in July of 1984. Response of the UGS was similar in both the CVAP and Demonstration Testing (Ref. 8) thereby indicating that the Reactor Coolant Pump (RCP) blade failures had no significant effect on the magnitude of the flow loading imposed on the reactor internals during the CVAP. Hydraulic loading was found to agree well with predictions.

Evaluation of the comparisons of analytical predictions, test measurements, and visual inspection results leads to the conclusion that the System 80 Prototype Reactor Internals are structurally adequate and acceptable for long term operation. Measured response strains were all smaller than predicted resulting in fatigue margins of safety which are more than adequate (see Table 5.3-1). Methods employed in the various phases (Analysis, Test, and Inspection) of this CVAP are valid and sufficient to meet the requirements of Reg. Guide 1.20 (Ref. 1).

TABLE I  
SUMMARY OF PREDICTED AND MEASURED STRESSES

<u>Component</u>	<u>Predicted Stress (psi)</u>	<u>Measured Stress (psi)</u>
Core Support Barrel	[	]
Upper Guide Structure		
Lower Support Structure		

Predicted Stress = Peak alternating stress at CVAP test conditions of 4 pump operation, 564°F.

Measured Stress = 3.0 times root mean square values of measured strain, converted to stress, at CVAP test conditions of 4 pump operation, 564°F, times the appropriate stress concentration factor.

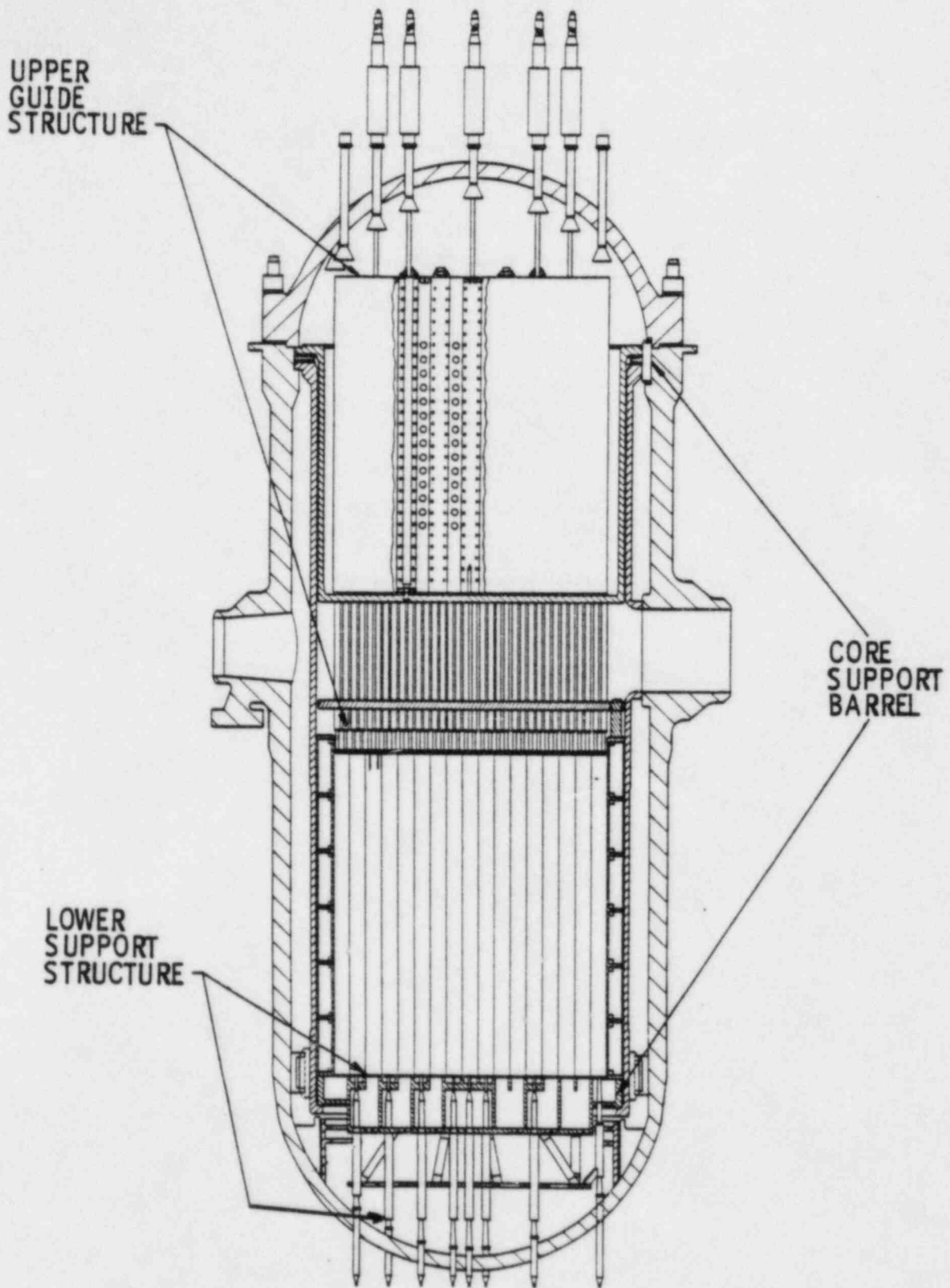
TABLE II

SUMMARY OF SYSTEM 80 CVAP INSTRUMENTATION

<u>MAJOR COMPONENTS</u>	<u>TRANSDUCER</u>	<u>INPUT FUNCTIONS</u>		<u>RESPONSE</u>		
		<u>PRIMARY FUNCTION</u>	<u>QTY.</u>	<u>TRANSDUCER</u>	<u>PRIMARY FUNCTION</u>	<u>QTY.</u>
Core Support Barrel	P. T.	Axial Dist.	2	S. G.	Shell Mode Response	4
		Circumferential Dist.	3	2-D Accl.	5-300 Hz Response (Beam & Shell Modes)	1
		Coherence Area	2	E. D. D.	0.1-10 Hz Response (Beam Mode)	3
		Transient	1	S. G.	CSB Stress State Below Upper Flange	4
		Inlet Pressure	1			
Upper Guide Structure	P. T.	CEA Shroud Tube Loading (Max. Crossflow Velocity Location)	2	2-d Accl.	CEA Shroud Tube Response	5
		UGS Support Plate Loading	1	S. G.	CEA Shroud Tube Stress State	4
				3-D Accl.	Fuel Alignment Plate Vertical and Radial Response	1
Lower Support Structure	P. T.	ICI Tube-58 (Max. Turbulent Load)	1	S. G.	Axial Stress and Response of ICI Tube 58	2
				2-D Accl.	Lateral response of LSS	1
Summary		Pressure Transducers	13	2-D Accelerometers		7
				3-D Accelerometers		1
				Eddy Type Disp. Device		3
				Strain Gages		14
		Total (Input)	13	Total (Response)		25

Total Instruments 38

P. T. Pressure Transducer  
 S. G. Strain Gage  
 E. D. D. Eddy Type Displacement Device  
 Accl. Accelerometer (2-D, Two Directions, 3-D, Three Directions)



SYSTEM 80 VERTICAL ARRANGEMENT SHOWING ASSEMBLIES  
INSTRUMENTED FOR CVAP

FIGURE I



## 1.0 INTRODUCTION

### 1.1 ABSTRACT

A comprehensive vibration assessment program (CVAP) has been developed for Palo Verde Nuclear Generating Station Unit 1, in accordance with NRC Regulatory Guide 1.20, Rev. 2 (Ref. 1). This reactor is classified as the prototype for Combustion Engineering's System 80 NSSS design. This program, is intended to satisfy the requirements of a CVAP for a prototype reactor as defined in Ref. 1. Reactor vessel arrangement is shown in Figure 1.1-1.

### 1.2 CVAP PROGRAM

The purpose of the CVAP is to verify the structural integrity of the reactor internals to flow induced vibrations prior to commercial operation. This program was implemented during pre-operational and initial start-up testing of Palo Verde Unit 1. An overview of the program is shown in Figure 1.1-2.

The CVAP consists of four separate programs (a) analysis program, (b) measurement program, (c) inspection program, (d) evaluation program.

These programs include:

#### 1.2.1 Analysis Program

Analytical and empirical methods were used to predict the steady state and transient flow induced loads (i.e., forcing functions). Dynamic response of the reactor internals components were then analytically determined for those forcing functions which correspond to pre-operational and initial start-up, test, and normal operating conditions.

This program includes theoretical predictions of the forcing functions and associated structural responses, definition of test acceptance criteria, and the basis for the establishment of the criteria. A summary of this program is given in Section 2.0.

#### 1.2.2 Measurement Program

This program includes an experimental program incorporating accelerometers, pressure transducers, and strain gages, which permitted the recording of time dependent accelerations, pressures, and strains at specific locations. The type, number, and position of the instruments were based upon the results of the analysis program. These measurements were made during pre-core, pre-critical testing. A summary of this program is presented in Section 3.

#### 1.2.3 Inspection Program

A visual inspection program, including photographic documentation, was implemented at both the start and conclusion of the vibration measurement program. Specific locations were inspected for evidence of contact and wear and for effects of vibration. These locations include contact and potential contact surfaces between all major load bearing reactor internal components, highly stressed locations identified in the analysis program, lateral, vertical, and torsional restraints, locking and bolting components, specific welds, and CVAP instrumentation housings, mountings, and conduits.

Testing was of sufficient duration to assure satisfaction of the requirement that critical components be subjected to a minimum of  $10^6$  cycles of vibration before post test inspection. Results of the inspection program are given in Section 4.0.

#### 1.2.4 Evaluation Program

This program includes the analysis and review of data obtained in both the measurement and inspection programs and comparison of these data with predictions from the analysis program. The results of these comparisons are used to assess the methods employed to predict the response of the internals to dynamic forces and to verify the margin of safety of the structure associated with normal steady-state and anticipated transient operation over the service life of the reactor.

This report presents the predicted structural responses determined in the analysis program and compares them to the findings of the measurement and inspection programs. The comparison of predictions to measurements is used to verify the adequacy of the structure to withstand long term operation. The results of this program are found in Section 5.0.

#### 1.3 ACCEPTANCE CRITERIA FOR TEST DATA

Per Regulatory Guide 1.20 an acceptance criteria is defined for the measured stress. The definition is based upon the ASME endurance limit stress for fatigue (Ref. 4). The maximum allowable readings for the response instrumentation are specified based on this acceptance criteria.

It is convenient to define an acceptance criterion that is independent of the statistical nature of the response and can be applied in both random and deterministic situations. This is conservative in the case of deterministic response.

The acceptance criterion is defined equal to one third the endurance stress limit of 26,000 psi, or approximately 8,700 psi. Limiting values based on this criteria are listed in Table 1.3-1 as determined in Ref. 2.

The Acceptance Criteria for test data was established in the Analysis Phase and summarized in Section 1.3 above. This criteria was based upon the fatigue endurance limit presented in the ASME code 1977 Edition (Ref. 4) which is identical to the ASME code 1974 Edition Limits required by CESSAR (Ref. 13) to be used for the verification of ANPP. The Winter 1982 Addenda to the code revised the fatigue "endurance limits" from the 26,000 psi at  $10^6$  cycles 1977 value to 21,850 psi at  $10^{11}$  cycles for the stress range predicted and measured in these structures. This would reduce the acceptance stress of 8,700 psi to 7,300 psi RMS. The revised acceptance criteria is still considerably above the highest predicted peak stress of [ ] psi which was high compared to measured data (see Table I). Because the measured values of peak stress are so low, there is very little difference in the Margin of Safety computed using either the original endurance limit or the revised value from the Winter '82 Addenda (Ref. 14).

Reduced values of strain and displacement Acceptance Criteria resulting from this change in the "endurance limit" are shown below:

<u>RESPONSE INSTRUMENTATION DATA ACCEPTANCE CRITERIA USING WINTER '82 ADDENDA</u>			
<u>Assembly</u>	<u>Type</u>	<u>Number</u>	<u>Criteria</u>
CSB	SG	S1 to S8	270 micro-in/in
	AC	A1	.030 in.
	DT	A2 to A4	.030 in.
UGS	SG	S9 to S12	270 micro-in/in
	AC	A5 to A9	.0155 in.
	AC	A10	.0155 in.
LSS	SG	S13,S14	270 micro-in/in
	AC	A11	.0092 in.

Measured values are all well below these allowable levels. It may therefore be concluded that the revised fatigue limits according to the ASME Winter 1982 Addenda have no effect on measured values meeting Acceptance Criteria and negligible effect on Margins of Safety calculated for the components based on measured data.

TABLE 1.3-1  
RESPONSE INSTRUMENTATION  
DATA ACCEPTANCE CRITERIA

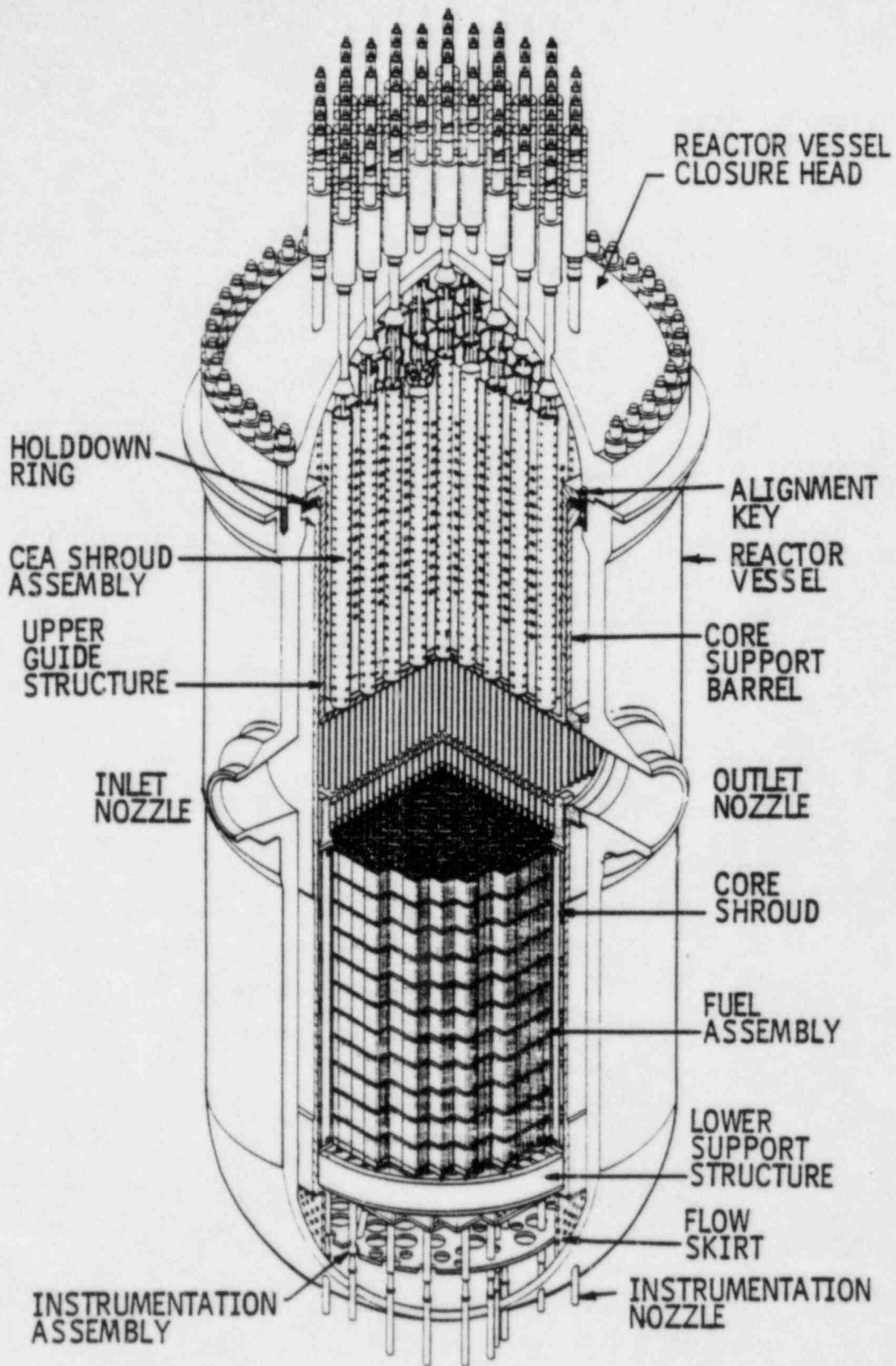
<u>Assembly</u>	<u>Type</u>	<u>Number</u>	<u>Criteria*</u>
CSB	SG	S1 to S8	320 micro-in/in
	AC	A1	.030 in.
	DT	A2 to A4	.030 in.
UGS	SG	S9 to S12	320 micro-in/in
	AC	A5 to A9	.0185 in.
	AC	A10	.0185 in.
LSS	SG	S13, S14	320 micro-in/in
	AC	A11	.011 in.

\* Limits are all based on 1/3 the endurance limit of 26,000 psi except for the CSB displacement (A1 to A4) which is based on a clearance at the snubbers of  $\pm .015$  inches. Acceptance values for the UGS and LSS accelerometers are based on motion of the assembly relative to the upper guide structure cylinder and the core support barrel, respectively.

SG = Strain Gauge

AC = Accelerometer

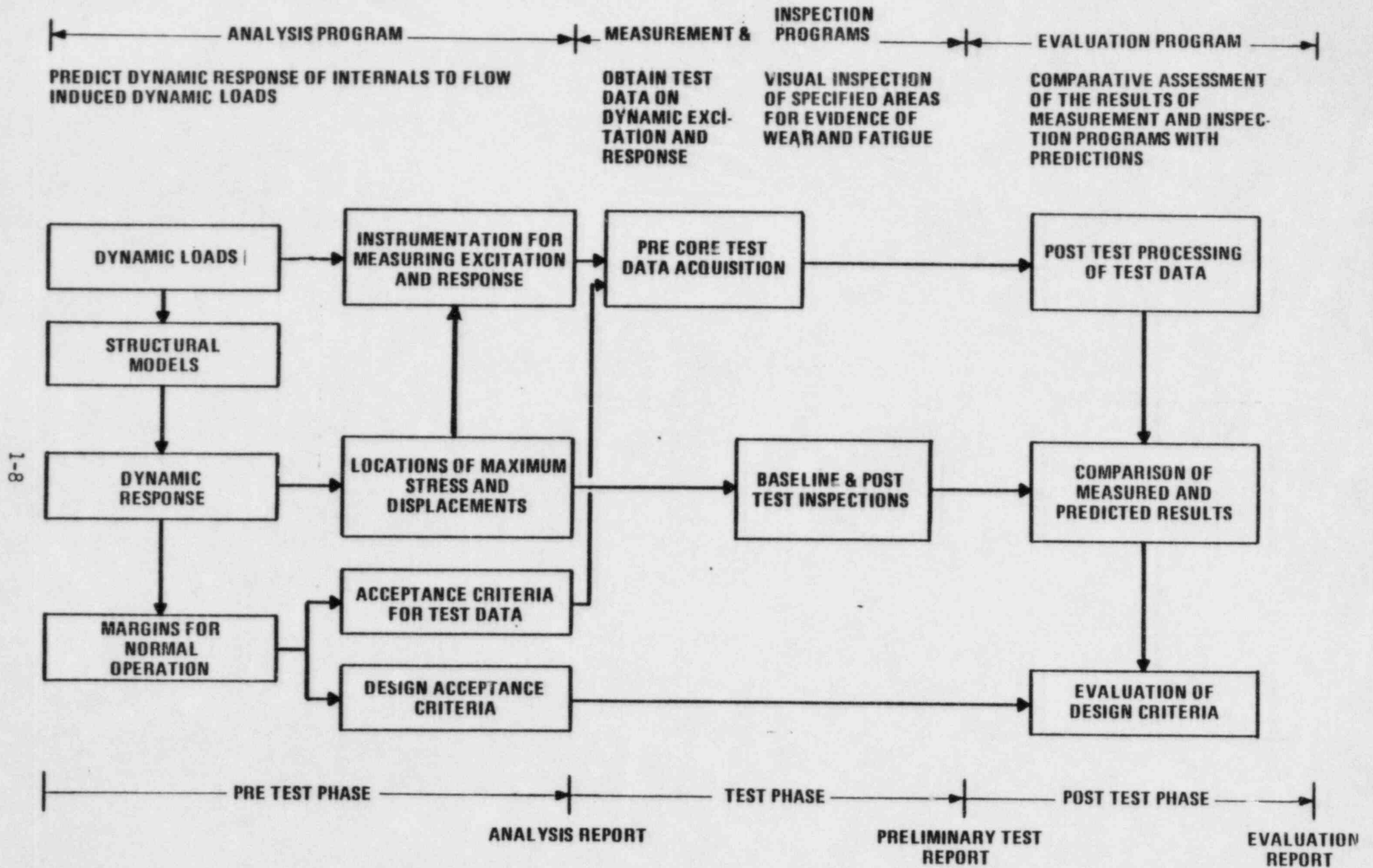
DT = Displacement Transducer



REACTOR VESSEL ARRANGEMENT

FIGURE 1.1-1

**FIGURE 1.1-2  
COMPREHENSIVE VIBRATION ASSESSMENT PROGRAM**



1-8



## 2.0 ANALYSIS PROGRAM

The methodology used to calculate the dynamic response of the core support structures to flow induced loads is divided into three parts; calculation of the hydraulic loads, (or forcing functions), analysis of the structures to determine their modal characteristics, (e.g., frequencies and mode shapes), and finally, calculation of the dynamic response (e.g., displacement, strain, and stress).

### 2.1 INTRODUCTION

Dynamic response of the core support structure assemblies is a function of the magnitude, frequency, and spatial distribution of the flow induced loads and the modal frequencies and mode shapes of the assemblies. The procedures used to compute this response are shown in Figure 2.1-1. Details of the analyses are given in Reference 2. The assemblies considered in the analysis are shown in Figures 2.1-2 through 2.1-4. Summaries of the results from Ref. 2 are given in Sections 2.2.1, 2.2.2 and 2.2.3.

### 2.2 ANALYSIS

#### 2.2.1 Core Support Barrel (CSB)

Deterministic loads on the CSB are caused by propagation of pump induced periodic variations in pressure through the reactor vessel-CSB annulus.

Random excitation, assumed to have a constant amplitude versus frequency (white noise), is due to turbulence induced by flow in the reactor vessel-CSB annulus.

Predicted values of Random and Deterministic loading on the CSB are shown in Table 2.2-1. The loading distributions are shown in Figures 2.2-1 and 2.2-2.

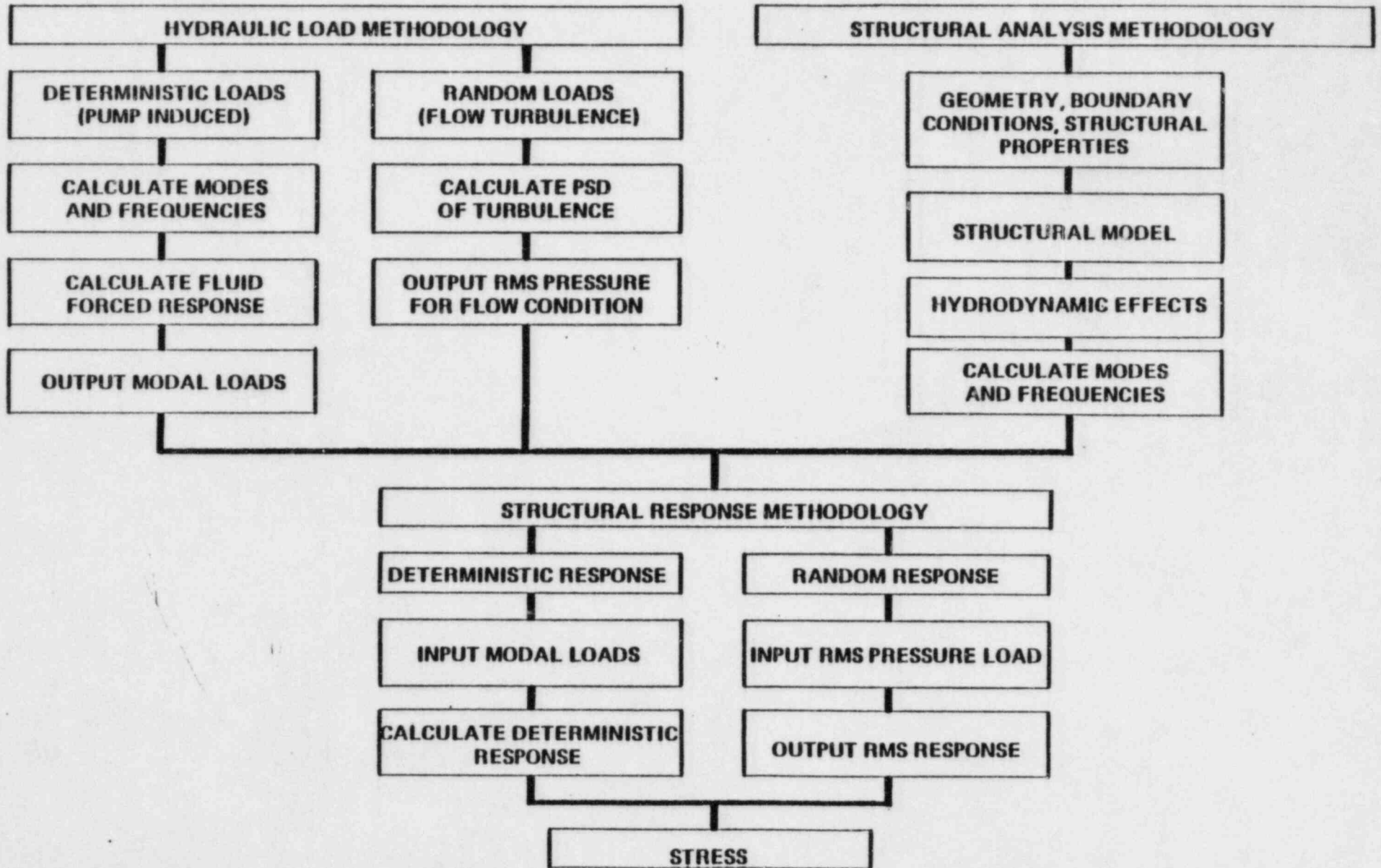
Liquid natural frequencies in the CSB annulus are important in assessing the response of the CSB to deterministic loading. Predicted values of these frequencies are presented in Table 2.2-2.

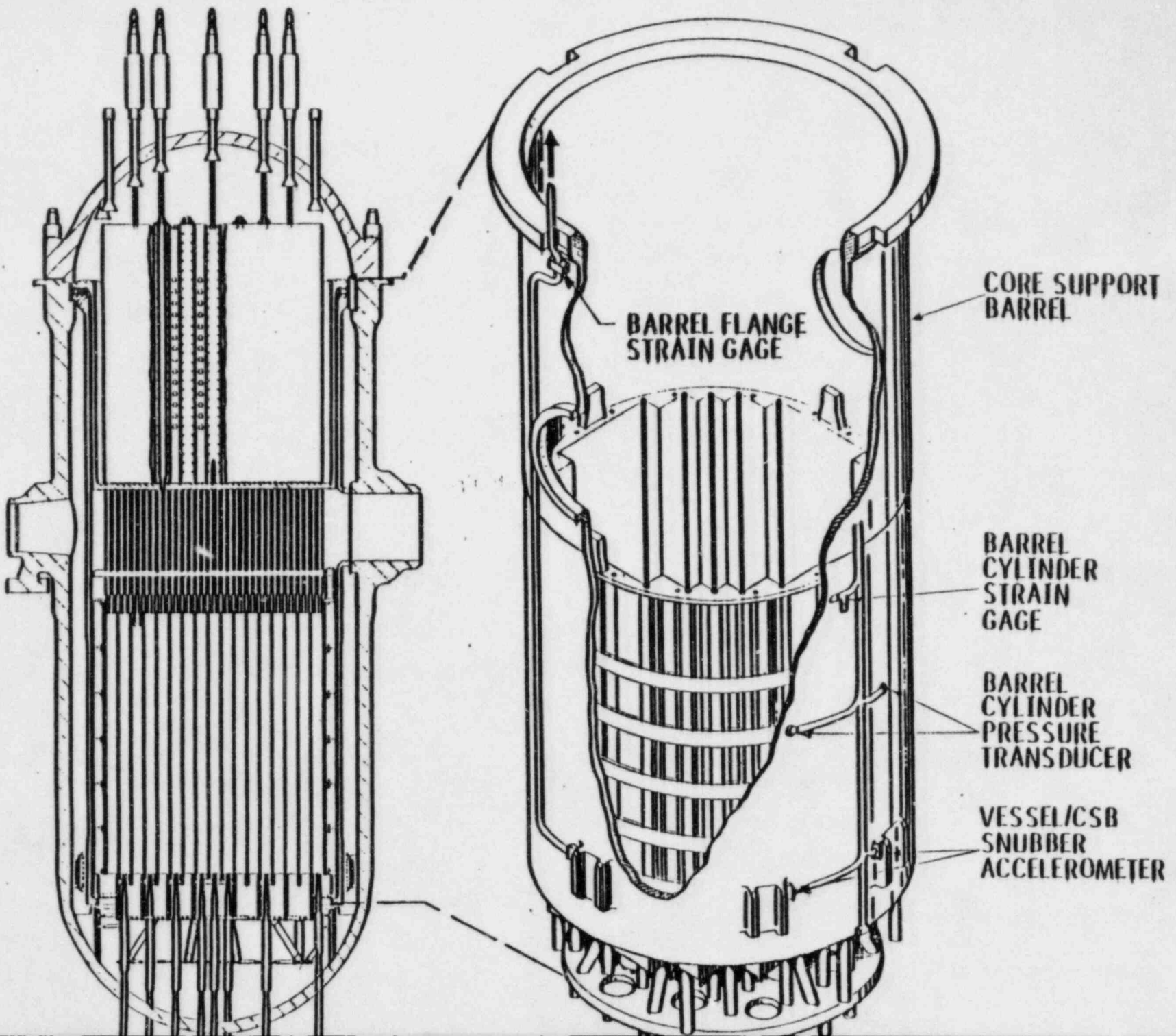
Modeshapes and frequencies of the CSB are computed for the first four beam and shell modes. Predicted frequencies are shown in Table 2.2-3 and the modeshapes are presented in Figure 2.2-3.

Dynamic response of the CSB to the imposed loading is computed using all of the forcing functions and system characteristics noted above. The predicted values of these response strains and displacements at the instrument locations are shown in Figures 2.2-4 to 2.2-6.

FIGURE 2.1-1

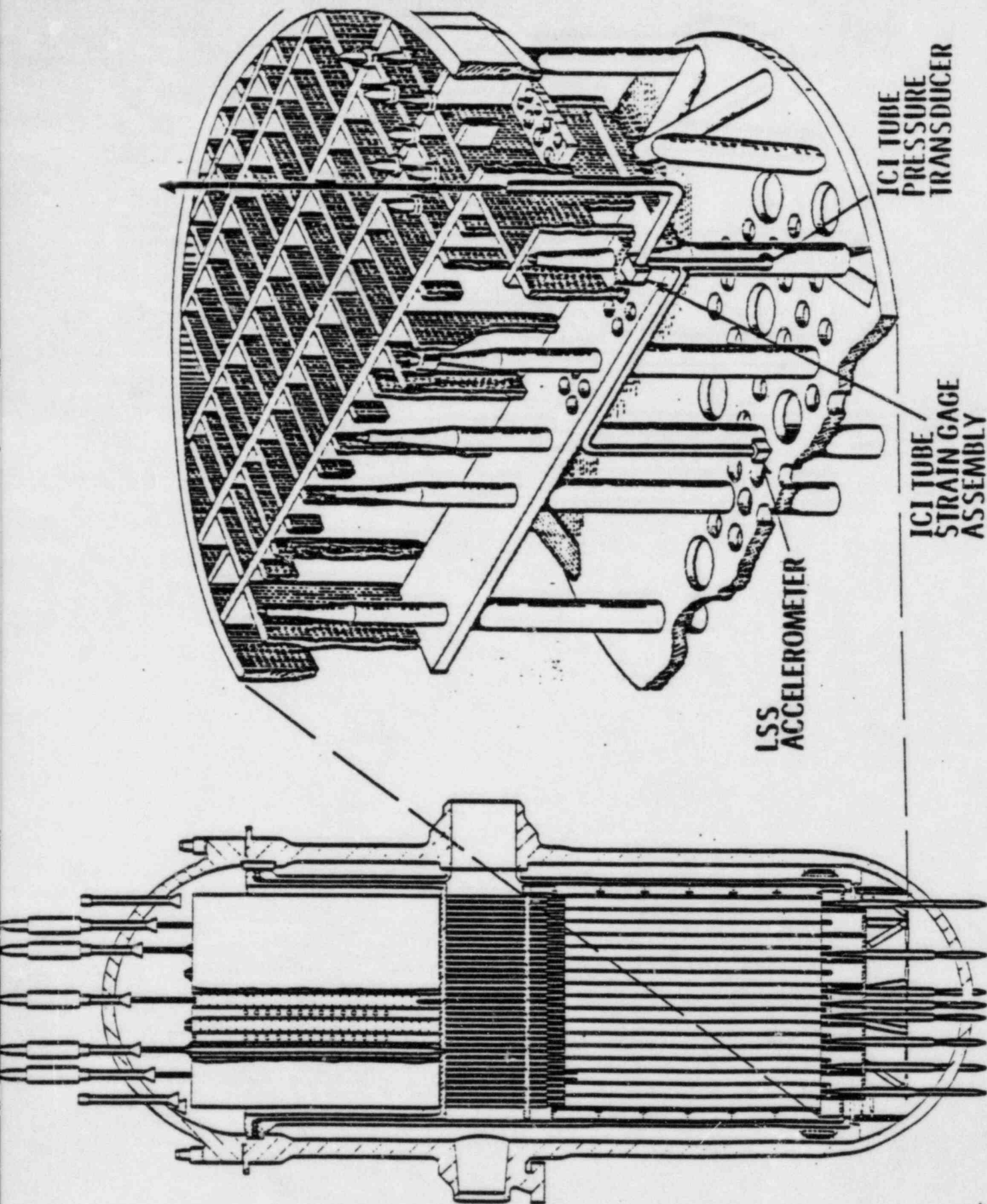
SUMMARY OF ANALYTICAL METHODOLOGY





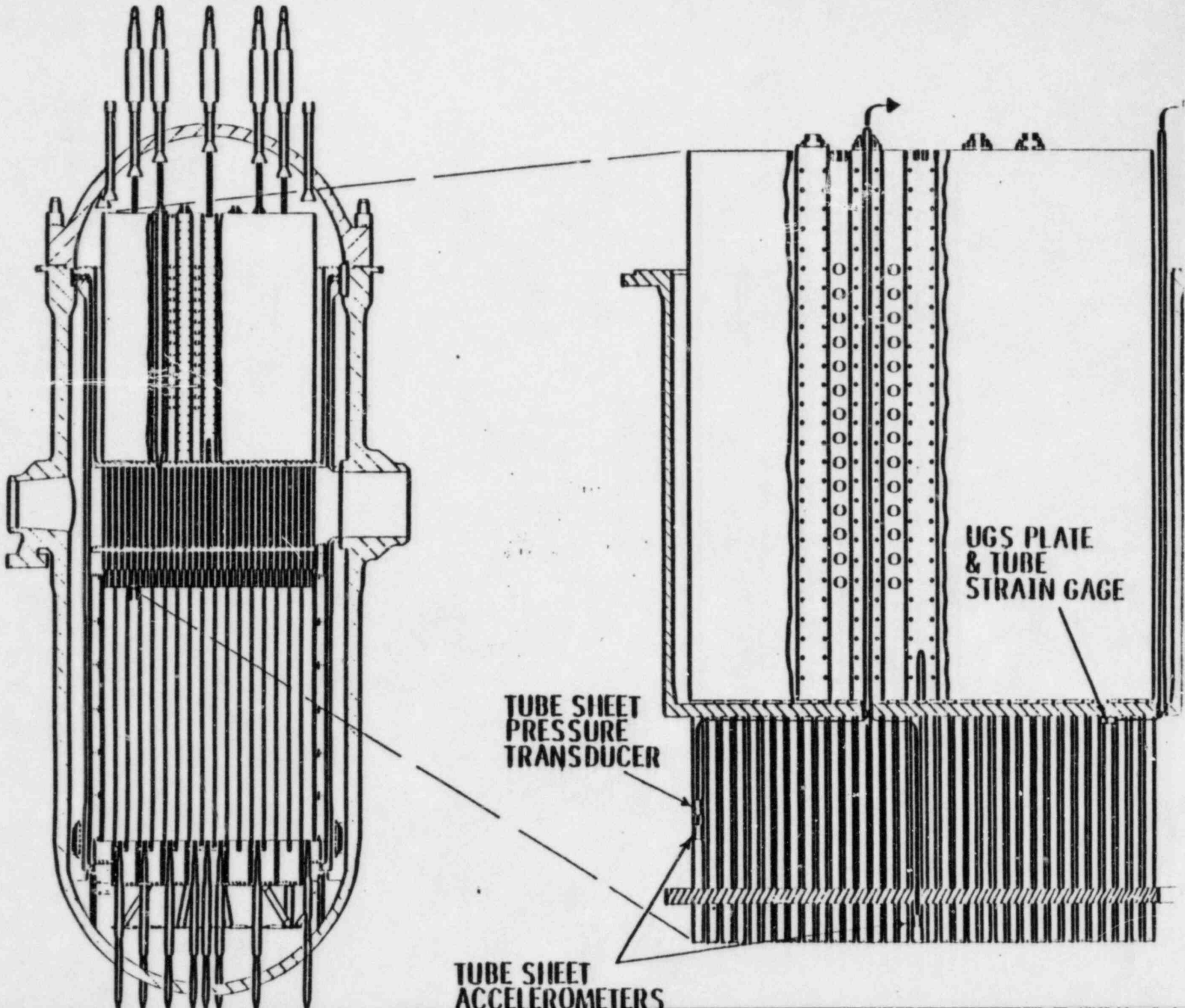
CORE SUPPORT BARREL & INSTRUMENTATION

FIGURE 2.1-2



LOWER SUPPORT STRUCTURE & INSTRUMENTATION

FIGURE 2.1-3



UPPER GUIDE STRUCTURE & INSTRUMENTATION

FIGURE 2.1-4

TABLE 2.2-1

RANDOM FLUCTUATING PRESSURE ON CORE SUPPORT BARREL,  
POWER SPECTRAL DENSITY (PSI<sup>2</sup>/HZ)

Temperature °F	No. Pumps	Random Pressure PSD Psi <sup>2</sup> /Hz
564	4	[ ]
	3	
	2	
500	4	
	3	
	2	
260	3	
	2	
200	3	
	2	

MAXIMUM PUMP INDUCED PERIODIC PRESSURE  
 ON CORE SUPPORT BARREL AT PRESSURE  
TRANSDUCER LOCATIONS P1 & P2 (PSI)

Temperature °F	No. Pumps	Rotor Speed 20 Hz	2 x RS 40 Hz	Blade Passing Frequency 120 Hz	2 x BPF 240 Hz
564	4	[ ]			
	3				
	2				
500	4				
	3				
	2				
260	3				
	2				
200	3				
	2				
<200	1				

TABLE 2.2-2

LIQUID (564°F) NATURAL FREQUENCIES IN CSB ANNULUS

f (HZ)	N = 1	N = 2	N = 3	N = 4
M = 1				
M = 2				
M = 3				
M = 4				

N = Circumferential Modes

M = Axial Modes



TABLE 2.2-3

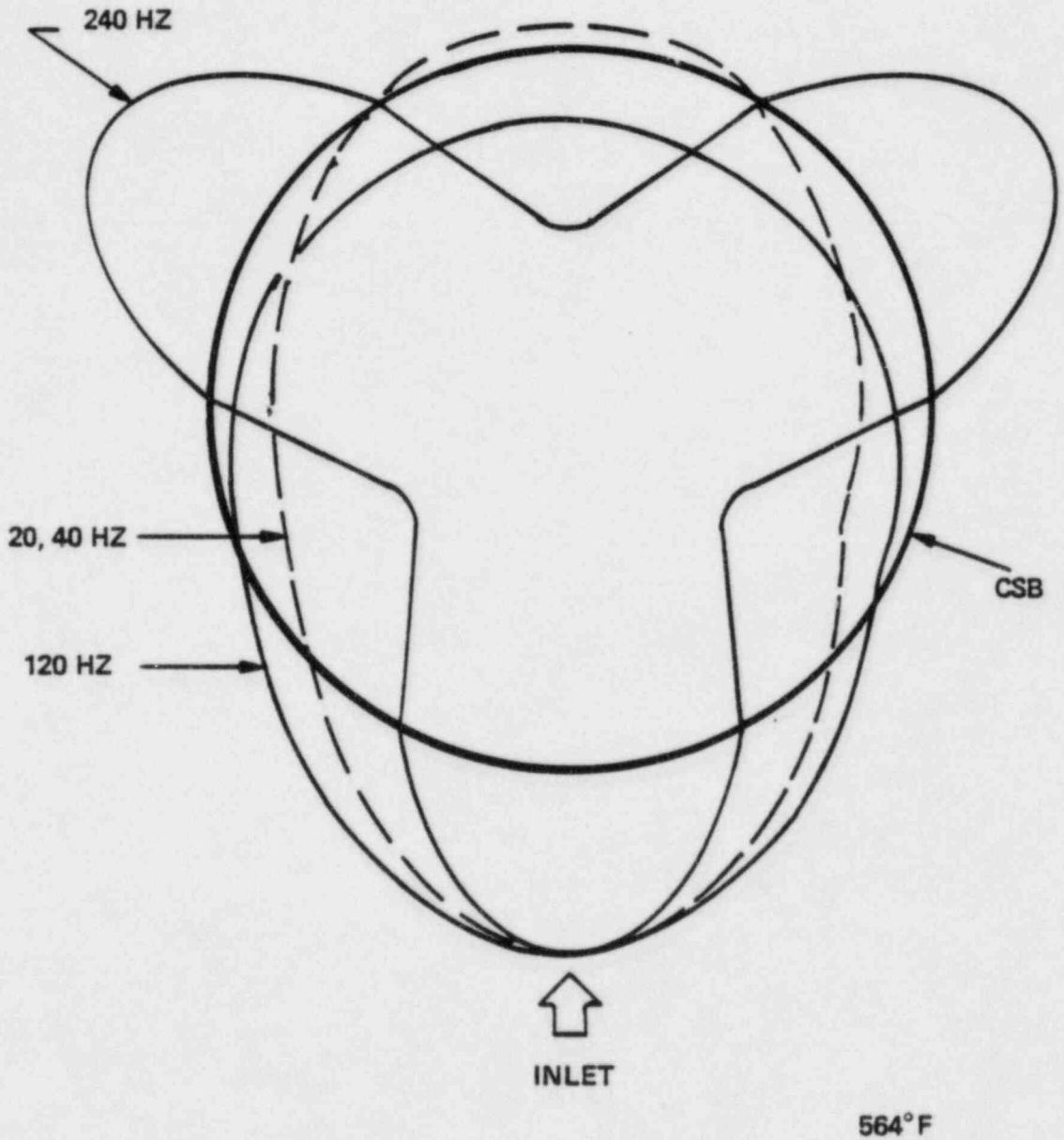
PRE-CORE CSB FREQUENCIES IN AIR  
AND IN WATER  
(564°F)

$f(\text{Hz})$ air / $f(\text{Hz})$ water	N = 1	N = 2	N = 3	N = 4
M = 1 <hr/> M = 2 <hr/> M = 3 <hr/> M = 4				

N = Circumferential Modes

M = Axial Mode

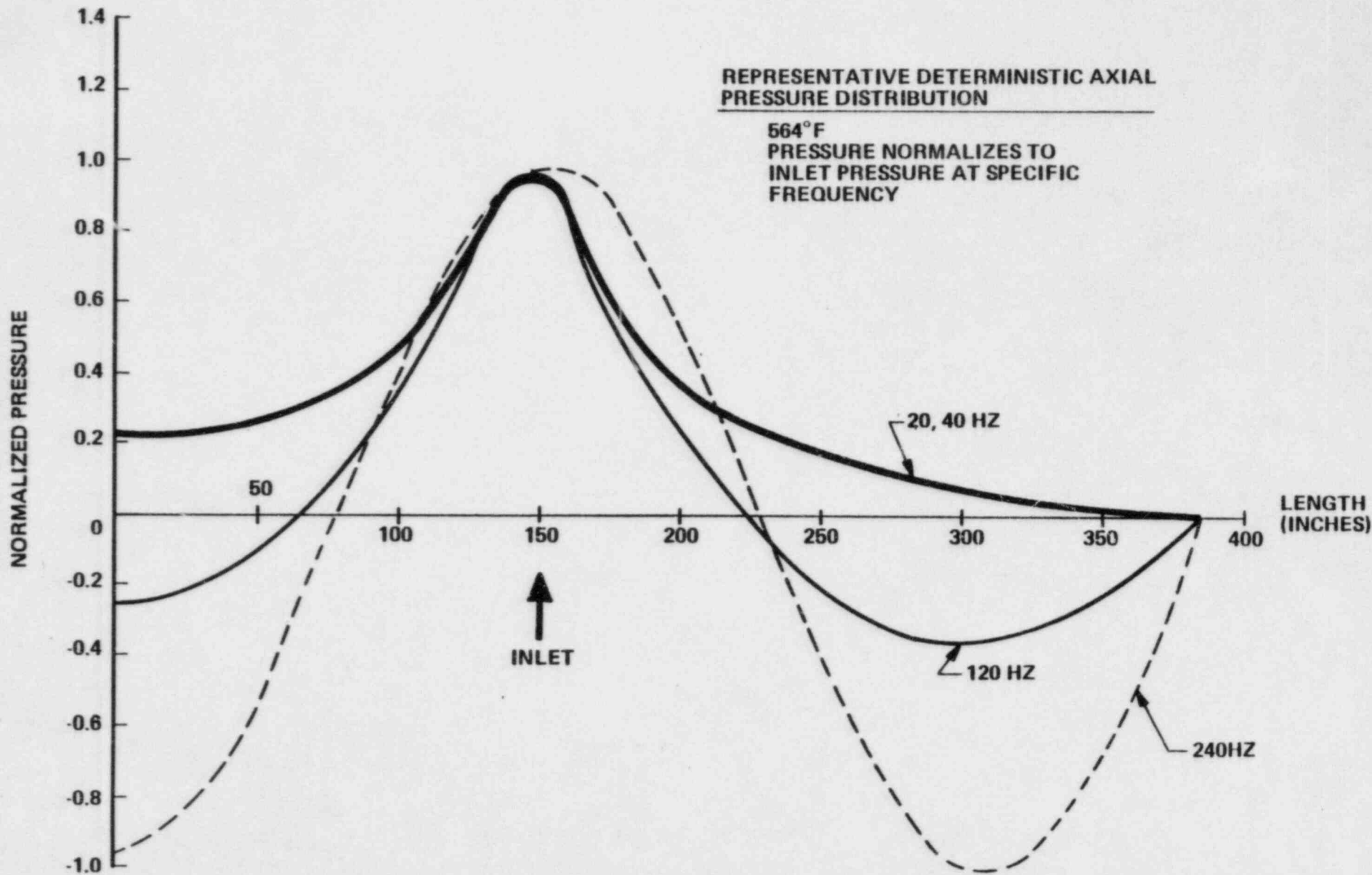
REPRESENTATIVE CIRCUMFERENTIAL DETERMINISTIC  
PRESSURE DISTRIBUTION



CIRCUMFERENTIAL VARIATION IN PRESSURE

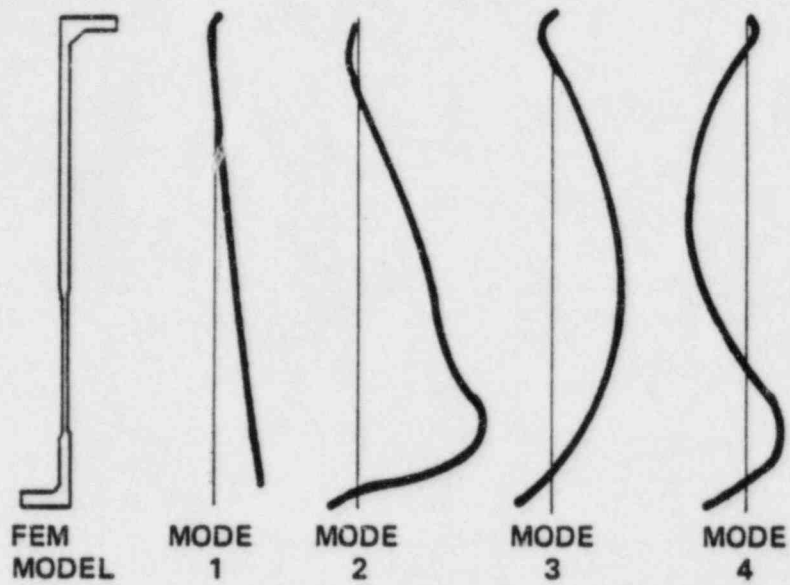
FIGURE 2.2-1

2-11

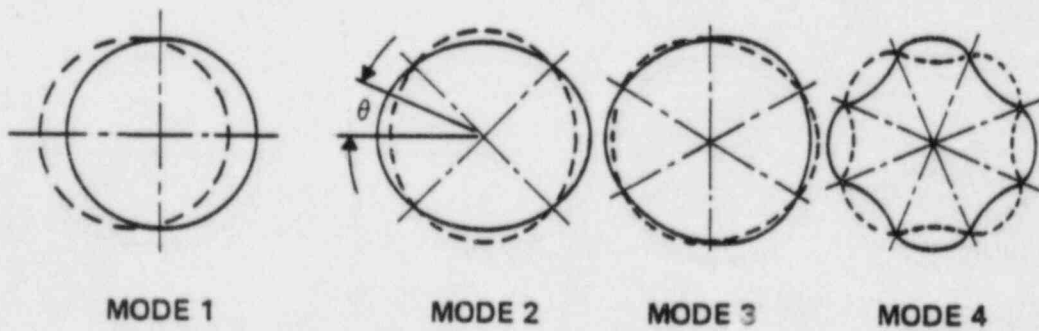


AXIAL VARIATION IN PRESSURE

FIGURE 2.2-2



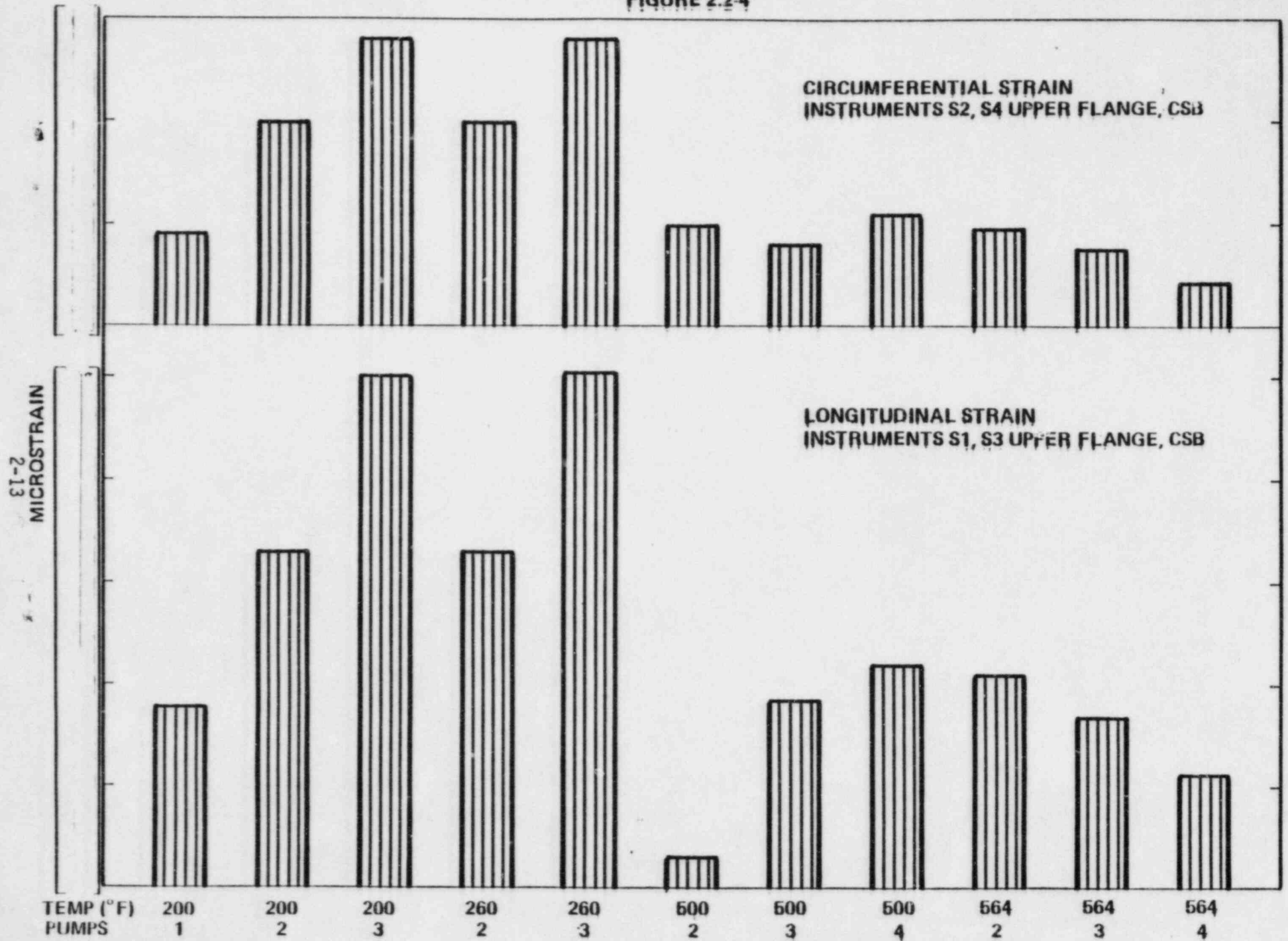
CSB BEAM MODESHAPES



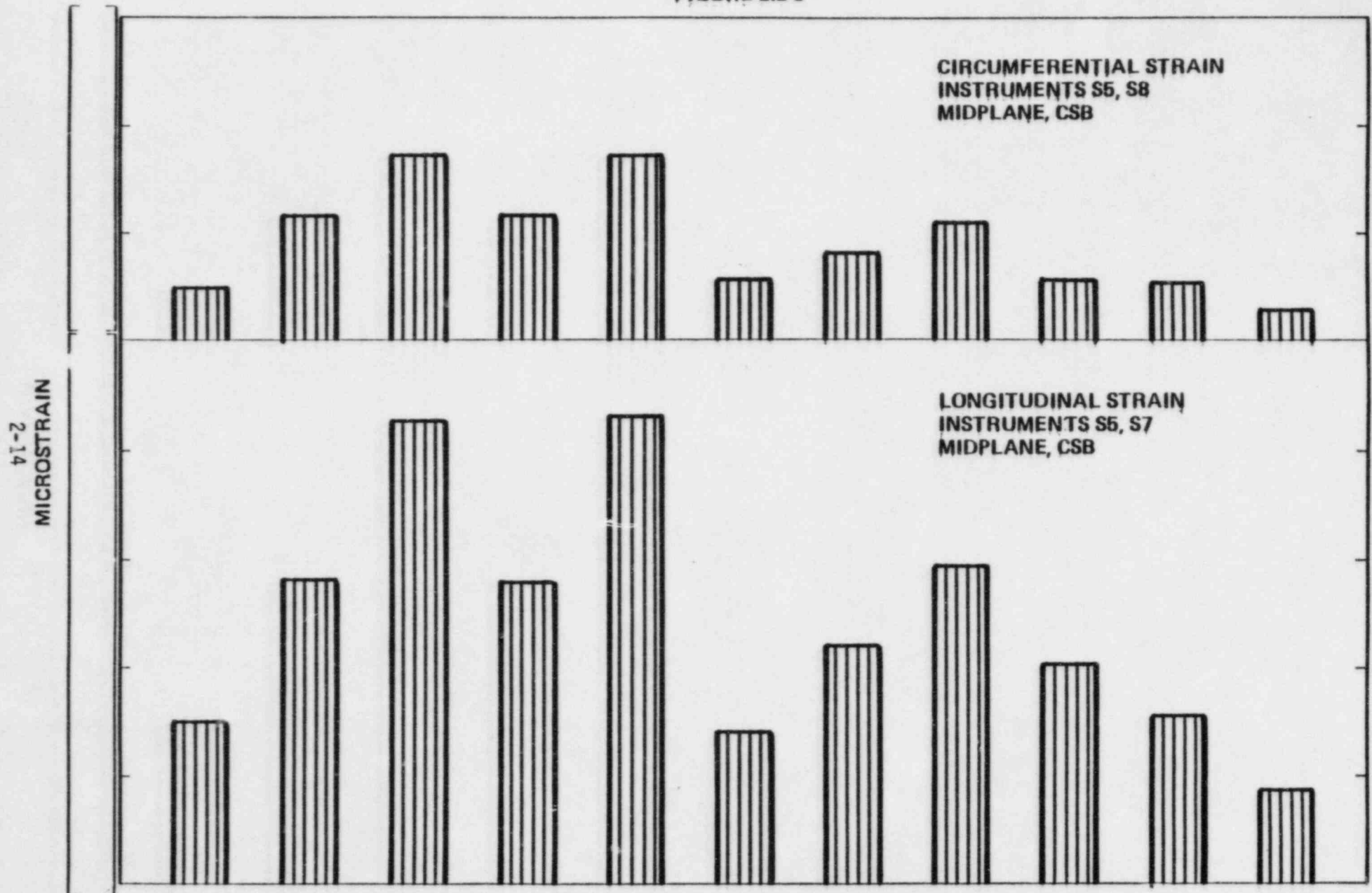
CSB SHELL MODESHAPES

FIGURE 2.2-3

CSB: MAXIMUM STRAIN - UPPER FLANGE  
 FIGURE 2.2-4



CSB: MAXIMUM STRAIN - MID PLANE  
 FIGURE 2.2-5



TEMP (°F)

200

200

200

260

260

500

500

500

564

564

564

1

2

3

2

3

2

3

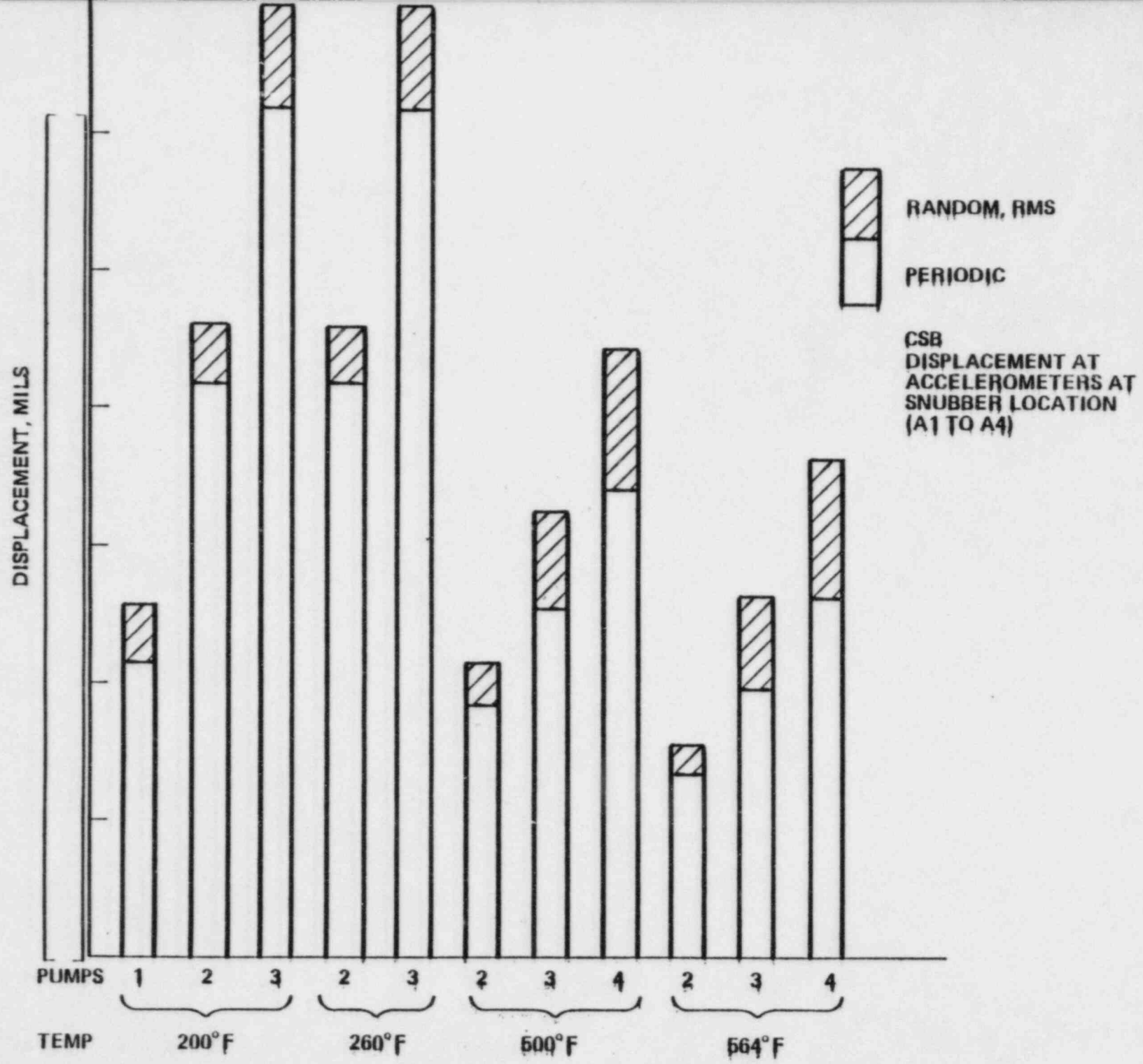
4

2

3

4

CSB: MAXIMUM DISPLACEMENT AT BOTTOM OF BARREL: INSTRUMENTS A1-A4  
 FIGURE 2.2-6  
 2-15



### 2.2.2 Lower Support Structure

Deterministic loading in this area causes a dynamic response of the entire instrument nozzle assembly as well as the individual ICI support tubes. Assembly loading is from pump pulsations acting across the ICI tubes as well as vertically on the Instrument Support Plate. Individual tubes are exposed to periodic pump pulsations and vortex shedding. Design analysis showed ICI tube 58 to be a most highly stressed member of the assembly. These individual ICI tubes are also exposed to random excitation from flow turbulence.

Predicted Deterministic and Random flow loadings on ICI tube 58 are presented in Tables 2.2-4 and 2.2-5, respectively.

Modeshapes and frequencies of the Instrument Nozzle Assembly of the LSS and the individual ICI tubes were determined by analysis and verified by modal testing. Predicted modeshapes and frequencies are shown in Figures 2.2-7 and 2.2-8.

Dynamic response of the LSS is computed using the forcing functions and system characteristics discussed above. The predicted values of these strains and displacements at the instrument locations are shown in Figures 2.2-9 to 2.2-11.



TABLE 2.2-4

PUMP PULSATION PRESSURES  
ON ICI TUBE 58 (PSI)

<u>Temperature °F</u>	<u>No. Pumps</u>	<u>ICI Tube 58</u>	
		<u>120Hz</u>	<u>240Hz</u>
564	4 3 2		
500	4 3 2		
260	3 2		
200	3 2		

PERIODIC LIFT/DRAG ON ICI TUBE 58  
DUE TO VORTEX SHEDDING (PSI)

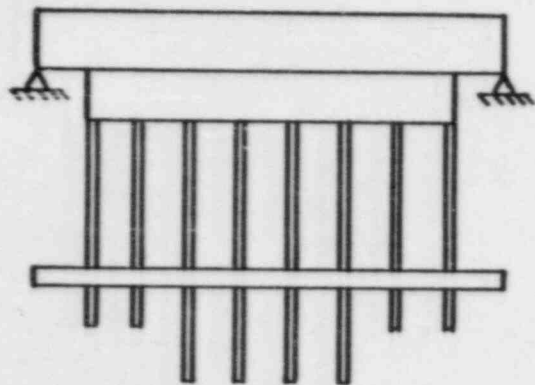
<u>Temperature °F</u>	<u>No. Pumps</u>	<u>Vortex Shedding Frequency</u>	<u>Lift Load</u>	<u>Drag Load</u>
		<u>Hz</u>	<u>(PSI)</u>	<u>(PSI)</u>
564	4 3 2			
500	4 3 2			
260	3 2			
200	3 2			

NOTE: 20 HZ AND 40 HZ PUMP PULSATION LOADINGS ARE NEGLIGIBLE.

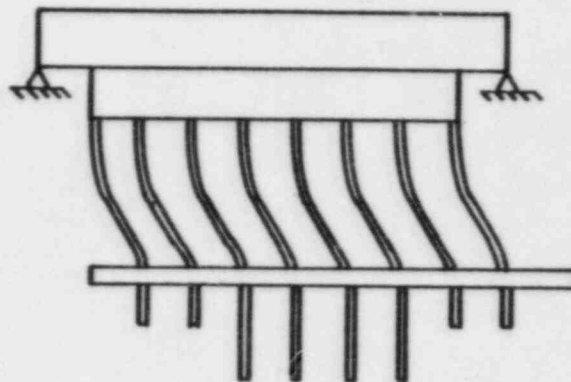
TABLE 2.2-5

RANDOM FLUCTUATING PRESSURE ON ICI  
TUBE 58

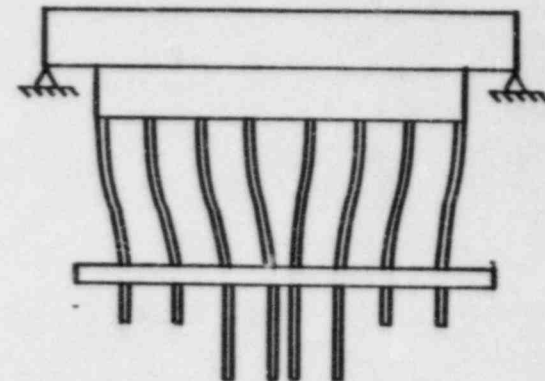
Temperature °F	No. Pump	Random Pressure PSD Psi <sup>2</sup> /Hz
564	4	[ ]
	3	
	2	
500	4	
	3	
	2	
260	3	
	2	
200	3	
	2	



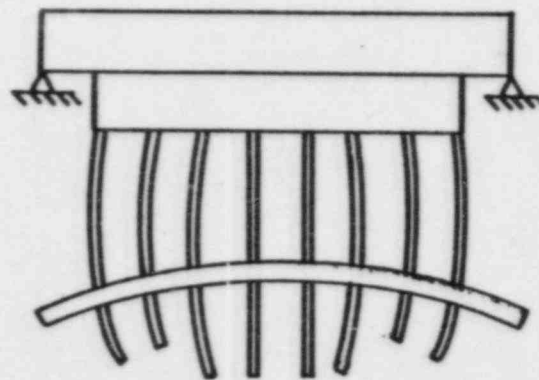
INSTRUMENT NOZZLE ASSEMBLY



MODE 1 - LATERAL  
[ · HZ ]



MODE 2 - LATERAL  
[ · HZ ]



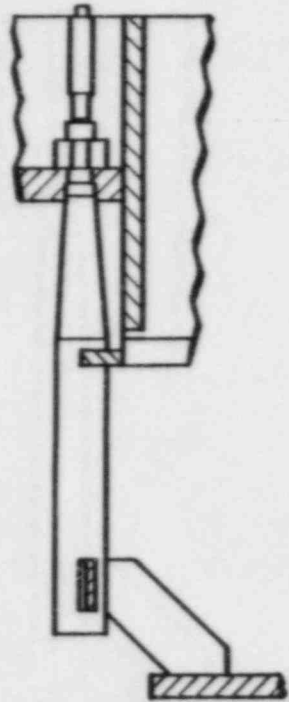
MODE 1 - VERTICAL  
[ · HZ ]

2-19

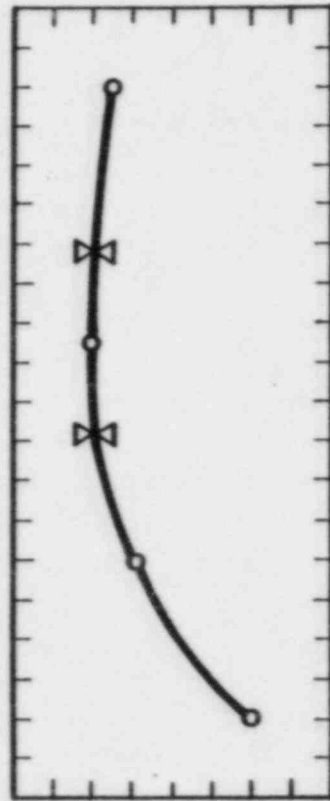
LSS ASSEMBLY -  
MODESHAPES AND FREQUENCIES  
FIGURE 2.2-7

ICI TUBE MODE SHAPES AND FREQUENCIES  
FIGURE 2.2-8

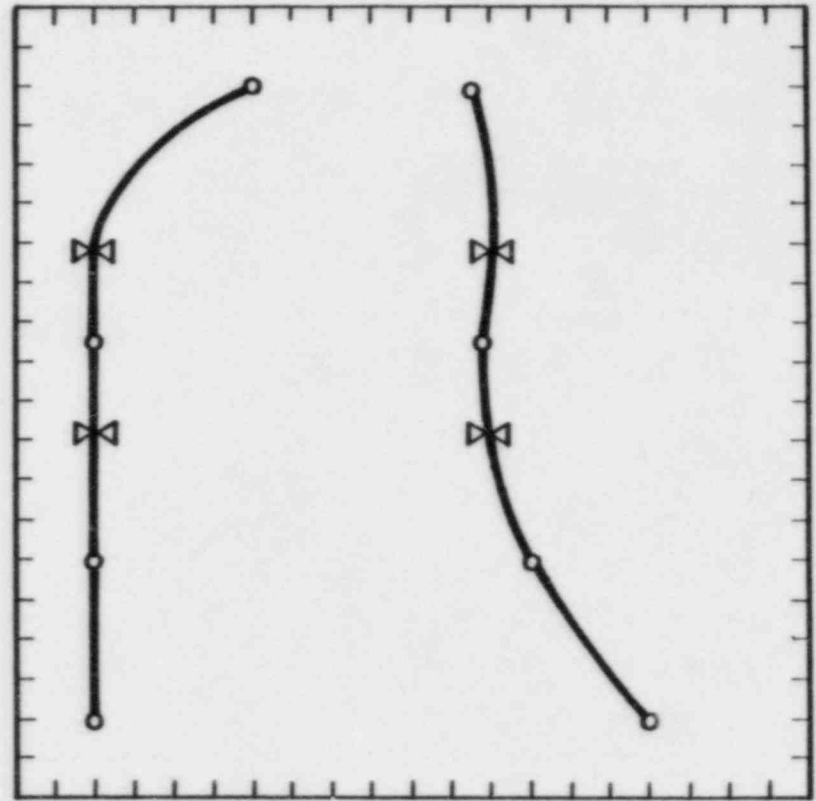
2-20



ICI NOZZLE  
TYPE D



MODE 1  
[ HZ]



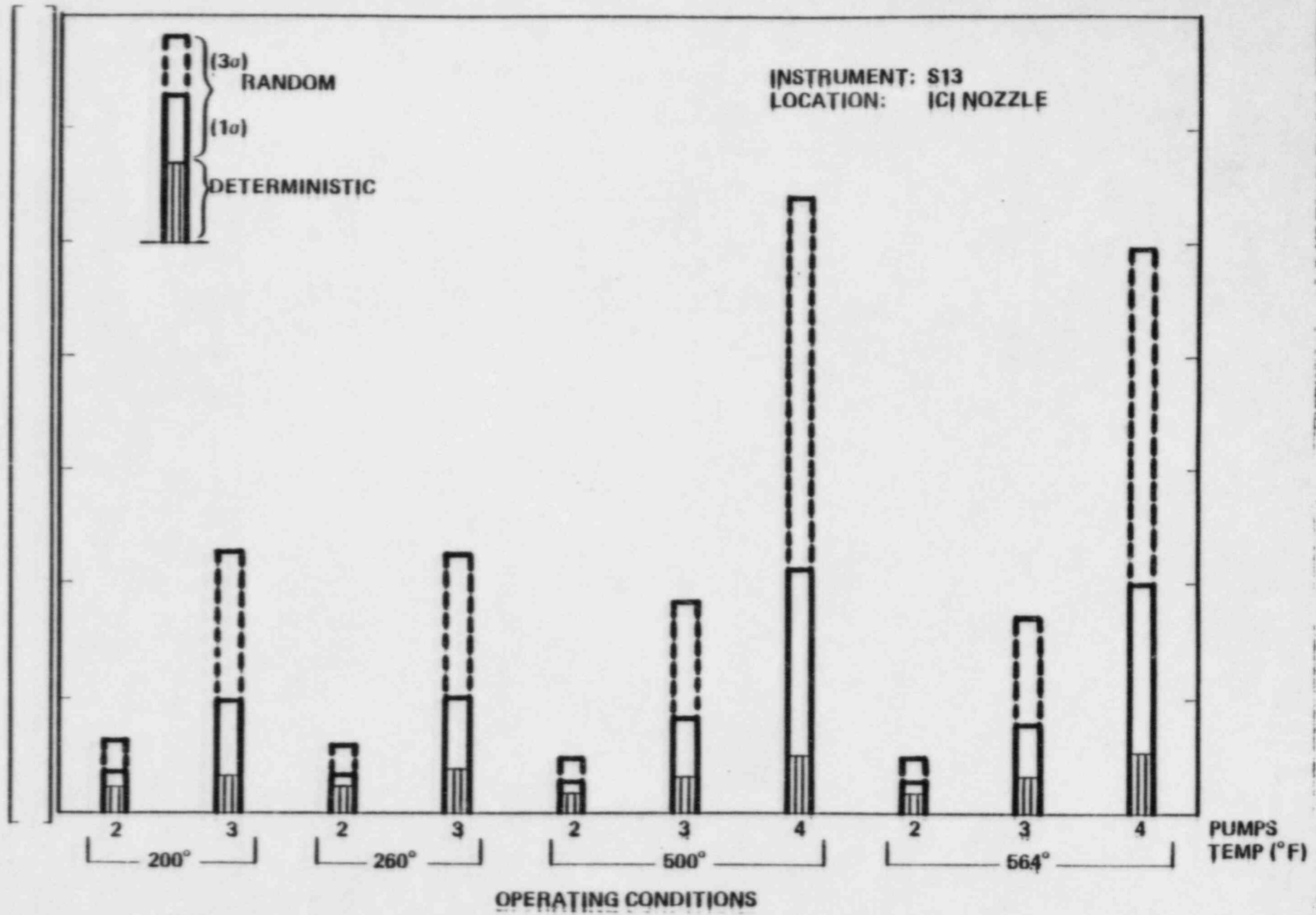
MODE 2  
[ HZ]

MODE 3  
[ HZ]

MODESHAPES AND FREQUENCIES

2-21

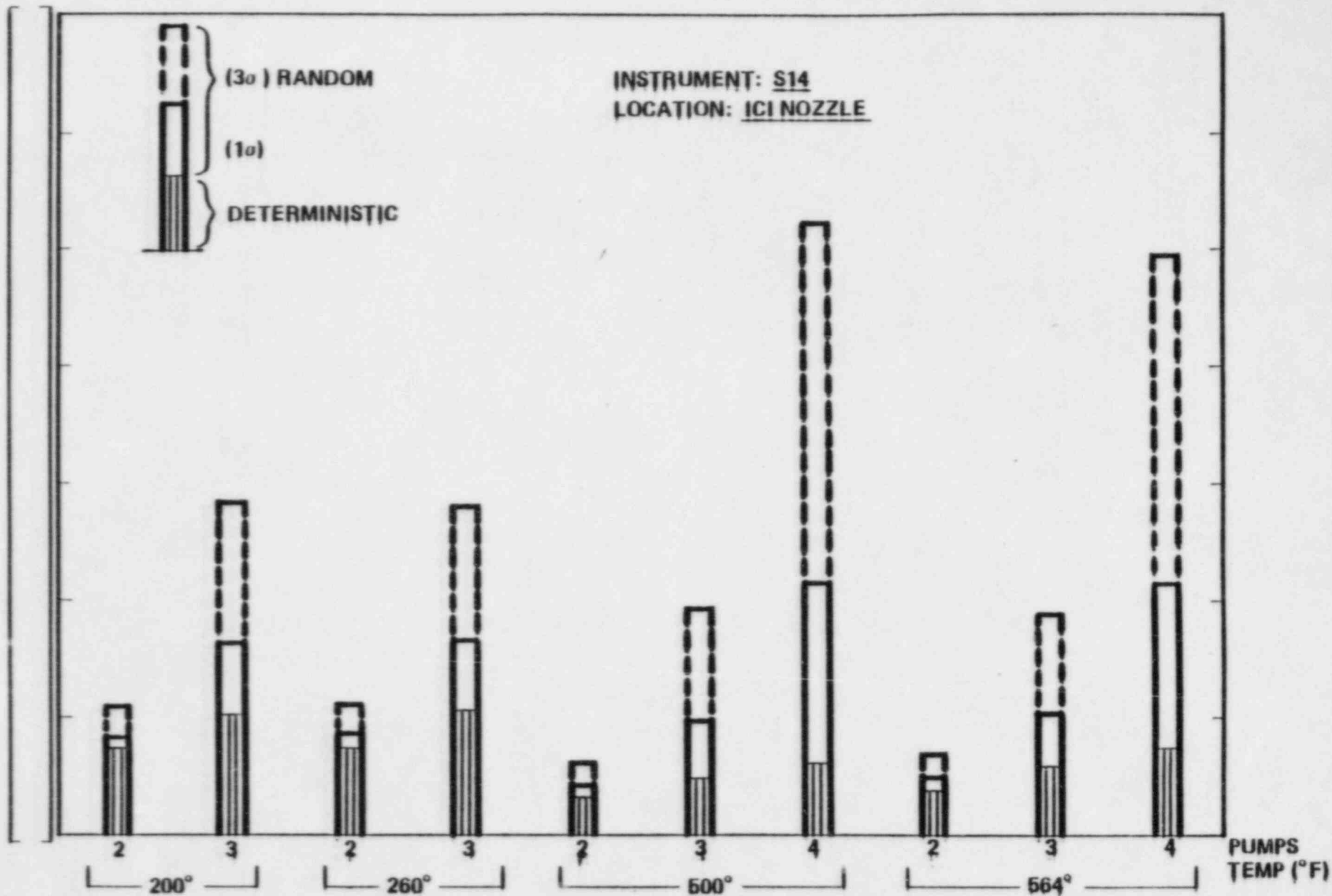
MICROSTRAIN  $\sim \mu\epsilon$



ICI TUBE STRAIN; INSTRUMENT S13  
FIGURE 2.2-9

2-22

MICROSTRAIN  $\sim \mu\epsilon$

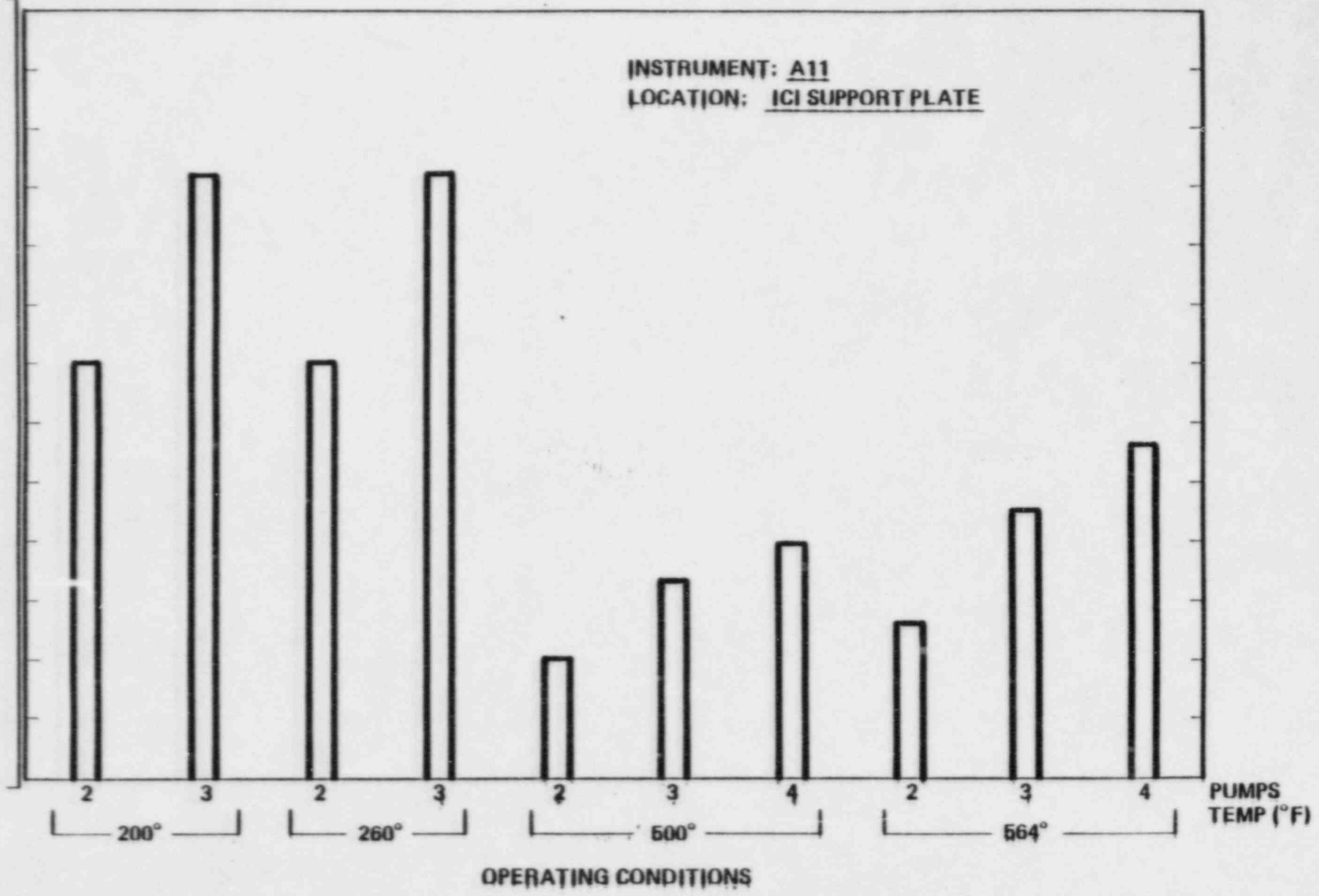


OPERATING CONDITIONS

ICI TUBE STRAIN; INSTRUMENT S14  
FIGURE 2.2-10

DISPLACEMENT ~ INCHES RMS  
2-23

INSTRUMENT: A11  
LOCATION: ICI SUPPORT PLATE



ICI SUPPORT PLATE; DISPLACEMENT; INSTRUMENT A11  
FIGURE 2.2-11

### 2.2.3 Upper Guide Structure

Response to deterministic forcing functions will result in structural response of the entire shroud tube assembly as well as of the individual tubes. The only significant periodic loading is due to pump pressure pulsations.

The upper guide structure will not respond to random excitation as a complete assembly but rather will experience local disturbances of individual components within the assembly. The results of flow testing conducted on a 1/4 scale shroud tube assembly model in conjunction with analysis are utilized to determine the random responses of the shroud tubes and support plates.

This flow testing indicated the most adversely loaded portions of the assembly to be the shroud tubes located near the outlet nozzle. Predicted values of pump pulsations and random flow turbulence are presented in Tables 2.2-6 and 2.2-7.

Modeshapes and frequencies of the structure are determined analytically using finite elements and classical methods. Predictions of these modeshapes and frequencies for the assembly and the individual tubes are shown in Figures 2.2-12 to 2.2-14.

Dynamic response of the UGS is computed using the scale model test data, forcing functions and system characteristics noted above. The predicted values of these strains and displacements are displayed in Figures 2.2-15 to 2.2-18.



TABLE 2.2-6

PUMP PULSATION LOADS ON THE UPPER GUIDE  
STRUCTURE COMPONENTS (PSI)

Temperature °F	No. Pumps	Pressure Pulsations			
		20 HZ	40 HZ	120 HZ	240 HZ
564	4	[			]
	3				
	2				
500	4				
	3				
	2				
260	3				
	2				
200	3				
	2				

TABLE 2.2-7

UGS RANDOM HYDRAULIC LOADING  
OF GUIDE TUBES AND SUPPORT PLATE

FREQUENCY (HZ)	PRESSURE PSD (PSI <sup>2</sup> /HZ)
[ ]	

Note: Values represent continuous pressure PSD which decreases with increasing frequency.

UGSSP

FAP

TYPICAL SHROUD TUBE



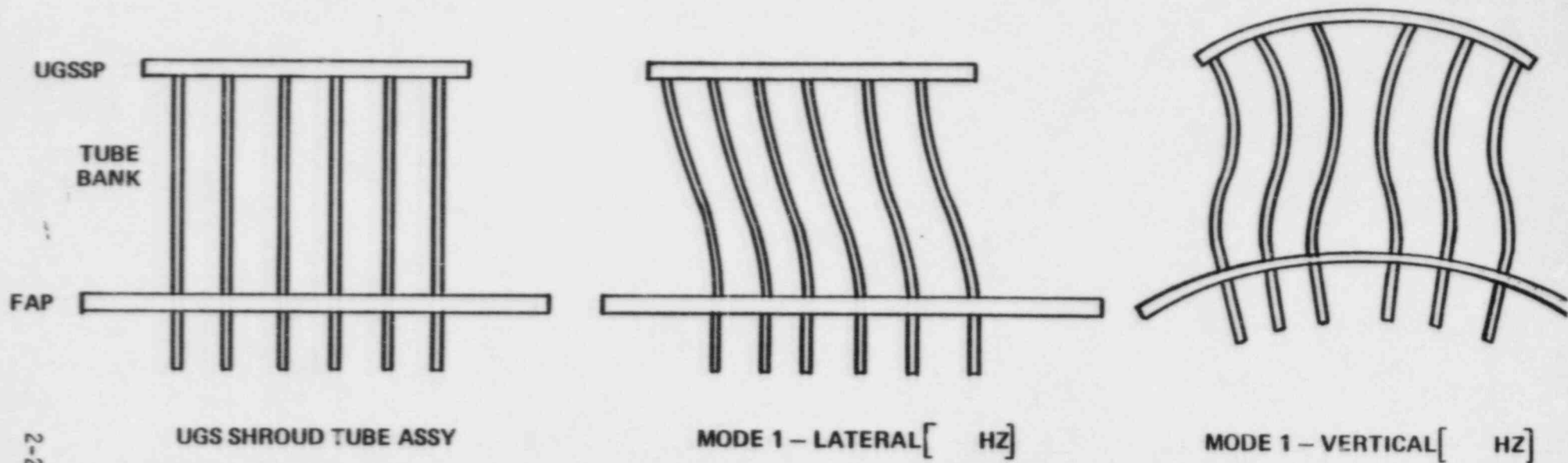
[ MODE 1  
HERTZ ]

[ MODE 2  
HERTZ ]

[ MODE 3  
HERTZ ]

[ MODE 4  
HERTZ ]

UGS GUIDE TUBE  
NATURAL FREQUENCIES & MODESHAPES  
FIGURE 2.2-12



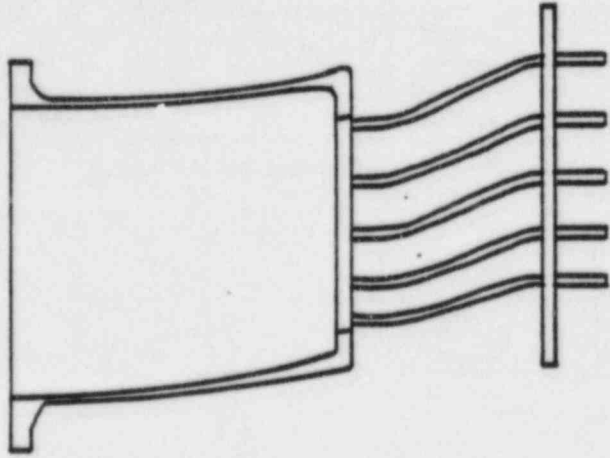
2-28

UGS TUBE BANK ASSY NATURAL FREQUENCIES & MODESHAPES

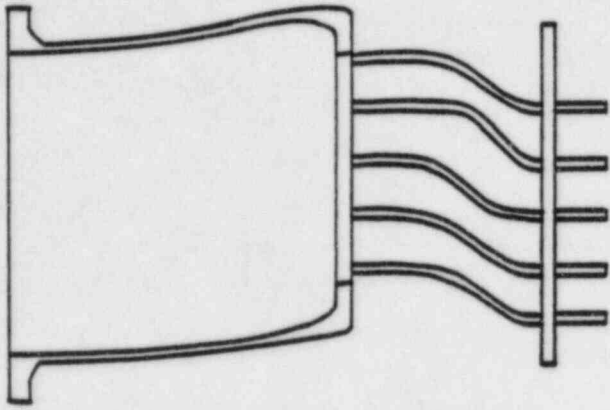
FIGURE 2.2-13

LATERAL

MODE 1 - [    ] HZ

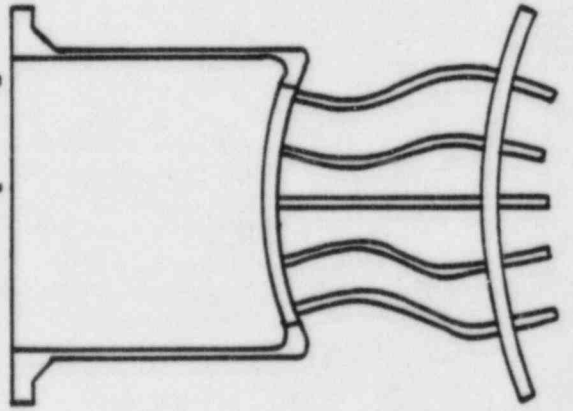


MODE 2 - [    ] HZ

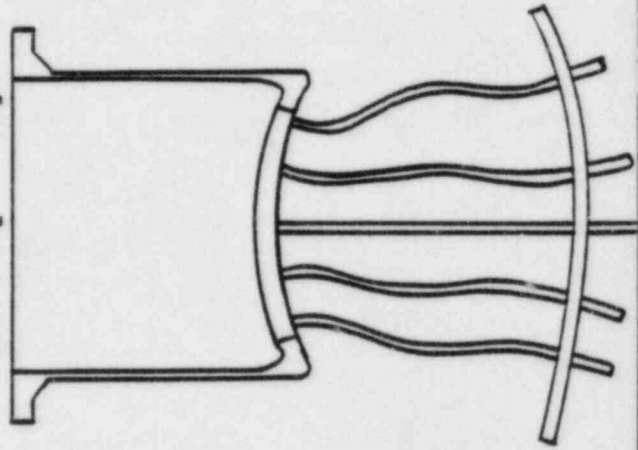


VERTICAL

MODE 1 - [    ] HZ



MODE 2 - [    ] HZ

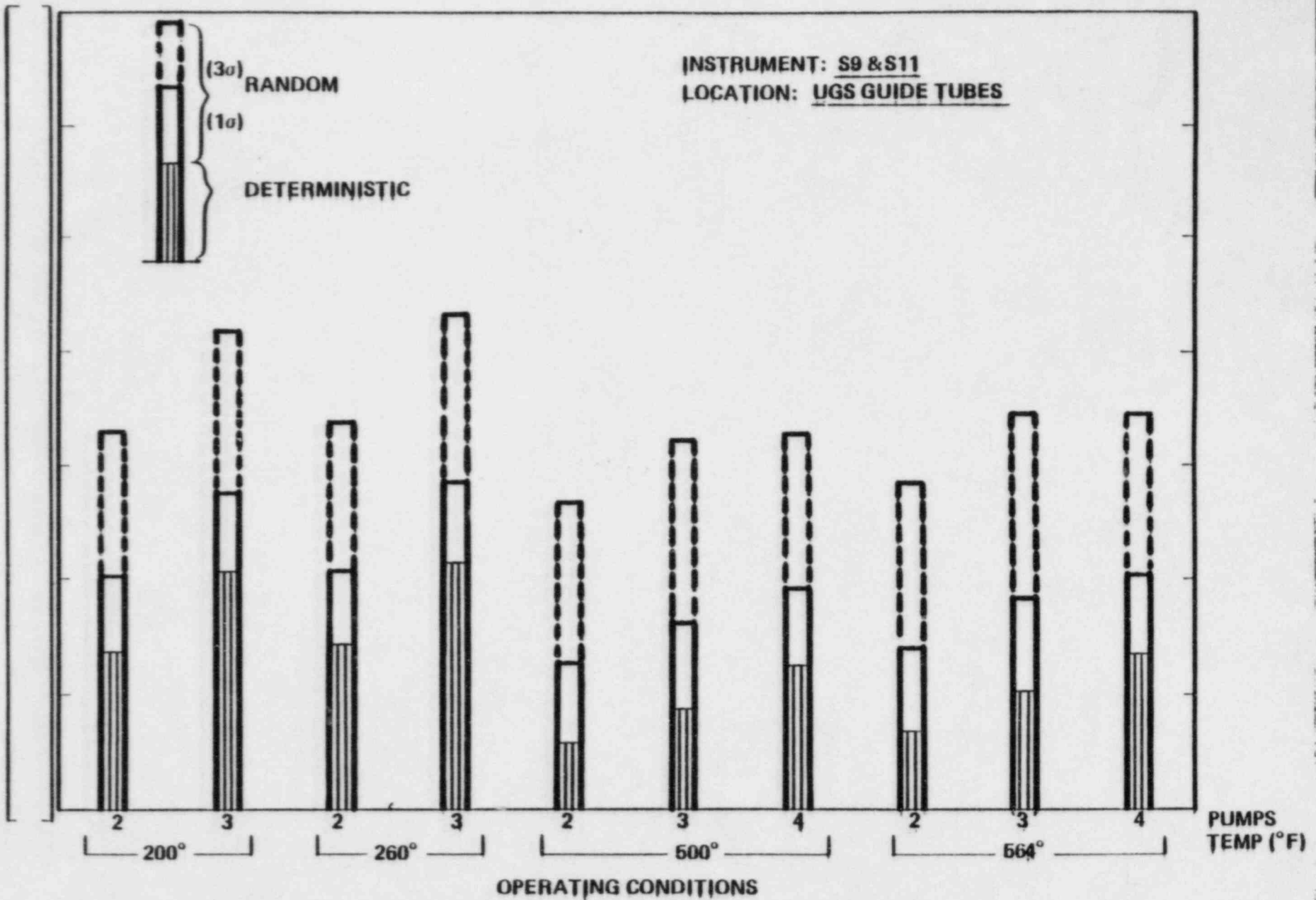


UGS ASSY  
MODE SHAPES AND  
FREQUENCIES

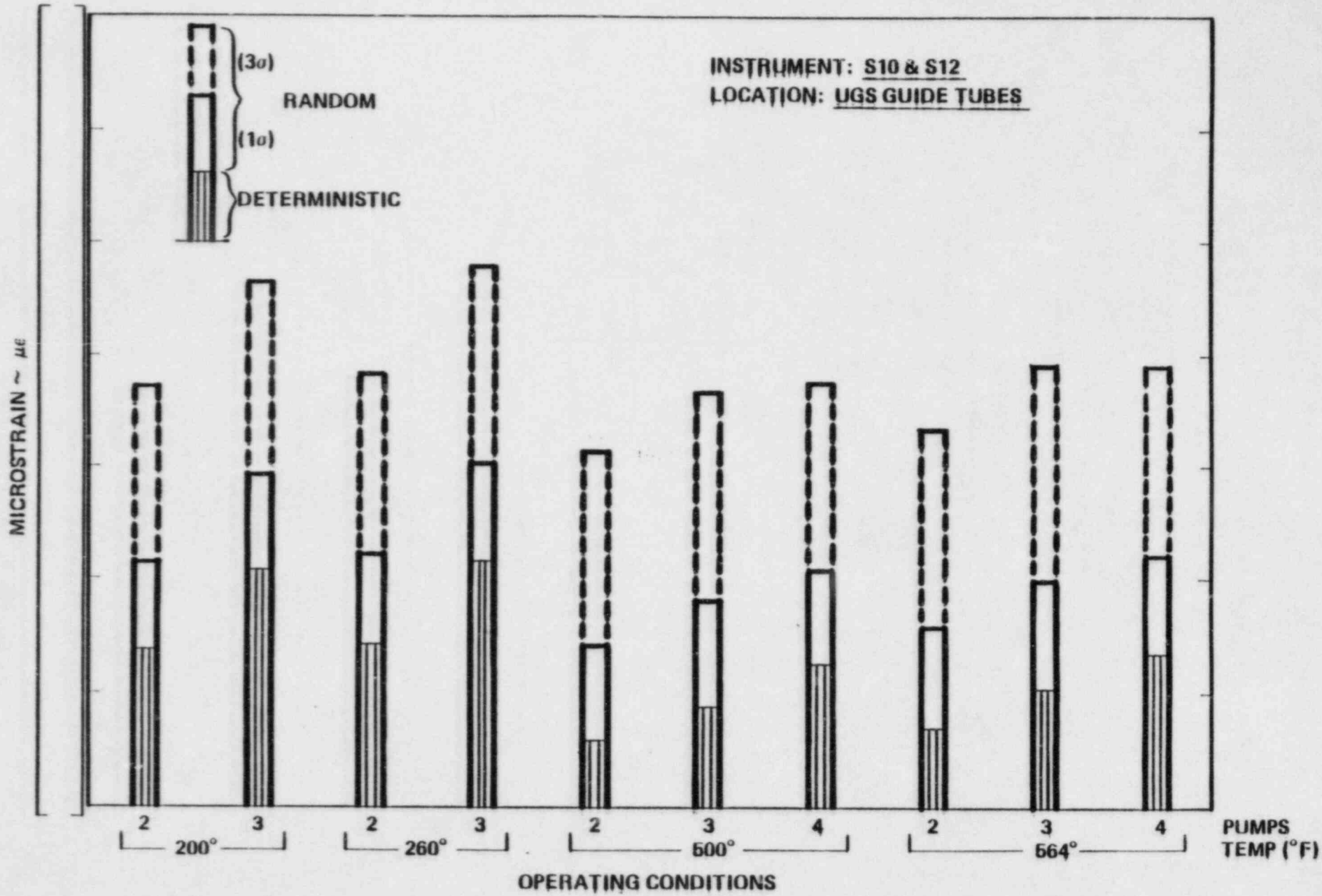
UGS ASSEMBLY; MODE SHAPES AND FREQUENCIES  
FIGURE 2.2-14

2-30

MICROSTRAIN  $\sim \mu\epsilon$

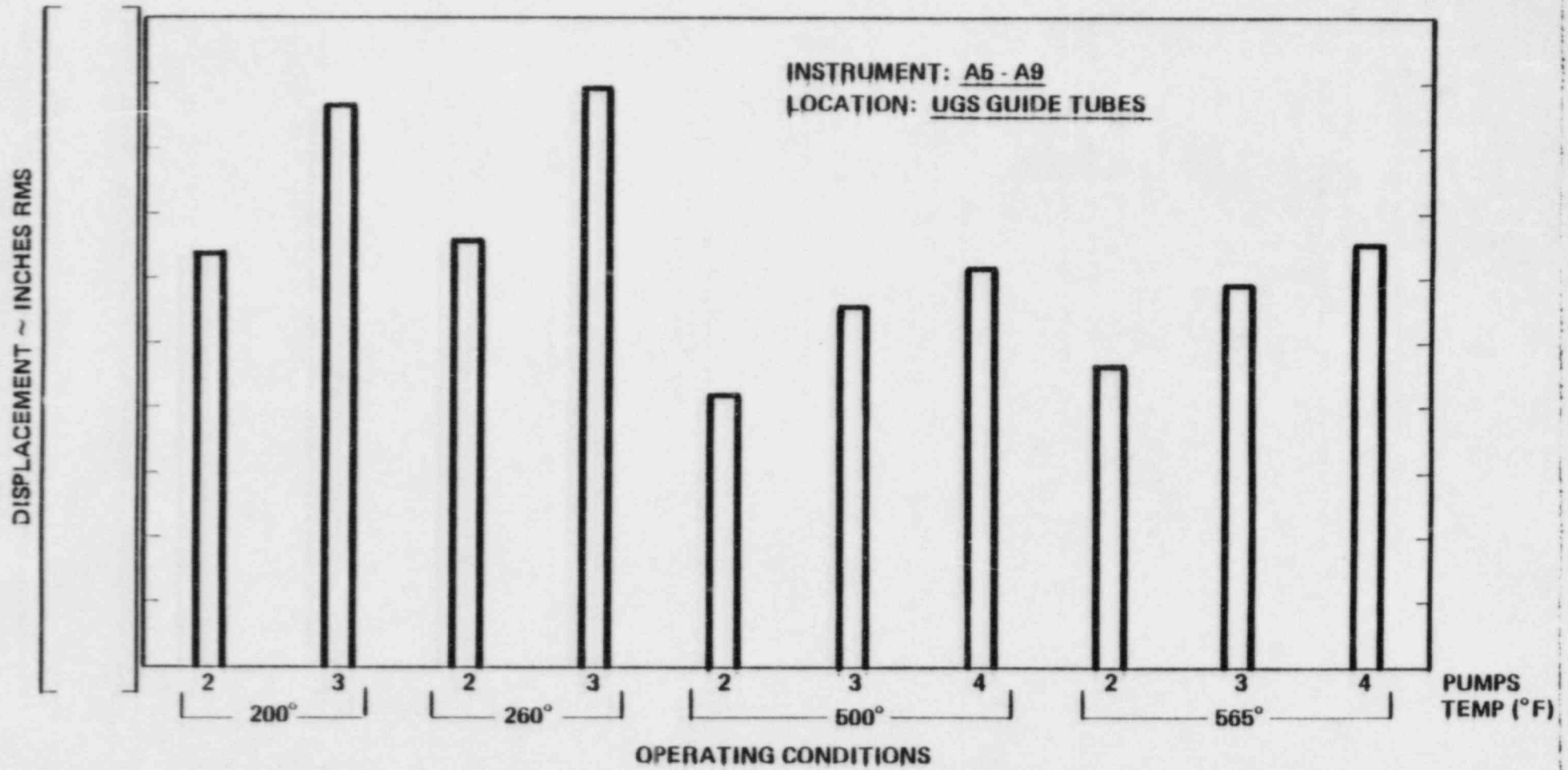


UGS GUIDE TUBES; STRAIN; INSTRUMENTS S9, S11  
FIGURE 2.2-15



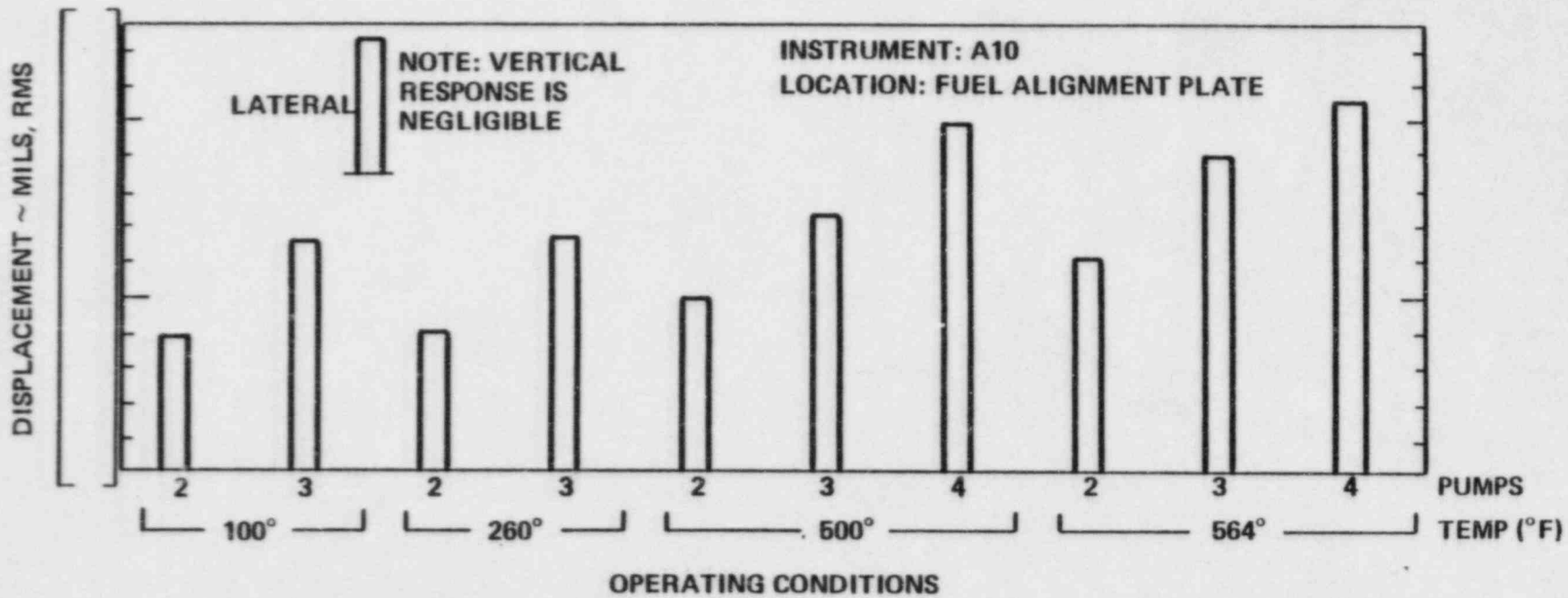
UGS GUIDE TUBES; STRAIN; INSTRUMENTS S10, S12  
 FIGURE 2.2-16

2-32



UGS GUIDE TUBES; DISPLACEMENT; INSTRUMENTS A5 TO A9  
FIGURE 2.2-17





FUEL ALIGNMENT PLATE DISPLACEMENT; INSTRUMENT A10  
FIGURE 2.2-18

The Analysis Program provides a means of determining the hydraulic forcing functions, structural characteristics of the components, and dynamic response strains and displacements of the core support structures. Details of this program are given in Ref. 2. The predicted values of pressure, strains and displacements at the instrument locations are summarized from Ref. 2 and presented in the preceding sections. Peak values for CVAP conditions are predicted to be lower than design levels as shown in Table 2.3-1. The fatigue margin is also predicted to be ample in all cases.

TABLE 2.3-1  
DESIGN AND CVAP PREDICTED PEAK STRESS SUMMARY

Component	Location	Peak Alternating Stress* (psi)		Fatigue Margin
		Design	CVAP	
CSB	Upper Flange (S2,S4)	[		]
LSS	ICI Nozzle (S13,S14)			
UGS	CEA Shroud (S10-S12) Tubes			

2-35

Fatigue Margin = Endurance Limit (26,000 psi)/Peak Alternating Stress

\* At conditions of Normal Operation (4 pumps, 564°F)

## 3.0 MEASUREMENT PROGRAM

### 3.1 INTRODUCTION

The objective of the measurements program is to obtain sufficient data to confirm predictions at operating conditions of steady state and transient normal operation. This confirmation requires data related to both the flow induced hydraulic loads (forcing functions) and the dynamic response of the structural components. Hence instrumentation is necessary to measure flow and response data. The measurements program was planned with adequate instrumentation to record the information necessary, with appropriate data reduction, to compare predicted and measured values of response and verify the margin of safety for long term operation.

### 3.2 INSTRUMENTATION

Instrumentation is summarized in Table 3.2-1 with locations shown in Figures 3.2-1 to 3.2-7.

### 3.3 DATA ACQUISITION

The CVAP data acquisition system is designed to record the electrical signals from transducers, mounted on the reactor internals, on magnetic tape. These tape recordings are the inputs used by various off-line processing techniques. The recorded time histories were examined for both amplitude and frequency content.

The CVAP data acquisition system has the capability to simultaneously record 54 channels of conditioned transducer signals on a 14 single track one inch instrumentation grade analog tape recorder. The transducer signals were recorded on tape using a Pulse Code Modulation (PCM) technique. PCM involves frequency filtering and analog-to-digital (A/D) conversion of the continuous transducer time

history prior to tape recording. Several transducer channels are then combined by an encoder into a serial bit stream. This data bit stream with necessary encoder framing information is then recorded on a single recorder track. The particular PCM scheme for CVAP uses nine tracks of the recorder. Each track has the encoded A/D values for six transducer signals. The PCM A/D rate and word length have been selected to allow a data channel frequency response of 0-500 Hertz and amplitude resolution of  $\pm 0.98$  millivolts ( $< \pm .05\%$  full scale). In order to achieve these operating specifications the PCM system requires a tape speed of 30 inches/second. The analog tape reels used during CVAP accommodated 24 minutes of data recording. For data monitoring a PCM-decommutator (decom) system was used during the test. This system enabled test personnel to monitor the recorded transducer signals, and verify the operation of the recording system.

The analog tape recorder, the PCM encoding and decom systems, signal conditioning and auxiliary test equipment are rack mounted in three standard electronic equipment cabinets. The cabinets are equipped with levelers, casters and lifting eye bolts to insure portability. The data acquisition system is shown in Figure 3.3-1.

The three phases of CVAP data acquisition include: documentation, calibration, and data monitoring.

Each transducer and its associated cables were uniquely identified. The transducer and cables associated with a signal conditioner were logged in the transducer hook-up log. This identifies a signal path at every connection from the transducer to tape recorder. The accuracy of this hook-up log was verified by acquisition personnel during instrumentation hook-up and checkout. Any deviations from the initial hook-up made during testing were noted and verified.

The integrity of the transducers and connecting cables was monitored through leadwire insulation and transducer capacitance measurements. These checks were made and recorded in the transducer characteristics log. Additionally, twice a day, strain gage transducers were shunt calibrated at the bridge amplifier and these shunt calibration voltages recorded on the characteristics log. Overall system calibration was made by switching all signal conditioners into calibrate mode and a short tape recording was made. An entry for each system calibration was made in the CVAP data log.

When a test condition was set and in the judgement of the acquisition engineer, the acquisition system was ready, a data recording was made. The signal level of each transducer channel was monitored while setting the signal conditioning amplifier gains for optimum output levels. The strain gage amplifiers were balanced and the sensitivity of all charge amplifier verified. An entry was then made in the CVAP data log, a sequential test number assigned, tape footage, and time of day noted and all signal conditioning gains entered. Additional comments were made in the data log when necessary.

A recording session was started with a voice recording on tape detailing the test number, test conditions, data, time, and tape footage. Other pertinent information was included as necessary in the voice recording. As the recording proceeds the PCM-decom system was used to monitor the signals recorded on tape. Each signal was monitored on-line to verify the recording process and the adequacy of the data signal level.

### 3.4 TEST CONDITIONS

Internal vibration data required for the CVAP was obtained at Palo Verde from May 15 to June 3, 1983 during pre-core hot functional testing. Thirty-eight (38) instruments were monitored during various temperature plateaus and pump combinations.

The test acceptance criteria was incorporated into APS Hot Functional Test Procedure (Ref. 5). This procedure also specified the use of APS personnel to act as a test coordinator and QA/AC inspector.

The original test conditions are specified in Table 3.4-1. Data for conditions 1 through 7 was obtained without any difficulty. Test conditions 8 through 15 required modification (Table 3.4-2) as described below:

Substitution of Pump 2-B for 1-B in condition 8 due to pump seal problems. Failure of Pump 1-B seal required modification of test conditions 11 through 15 (Table 3.4-2). To circumvent the use of Pump 1-B, test conditions 9 and 10, which called for four-pump operation, at 500°F were deleted. Upon reaching the 565°F plateau, the 2 and 3 pump, conditions 11, 12 and 14 were then completed. Test condition 13 was scheduled to be tested, as it was the sequential step between 12 and 14. However, due to a site power failure after obtaining data for condition 12, this sequence was no longer obtainable and, as a result, condition 13 was deleted. Pump 1-B was temporarily repaired and the four-pump (condition 15) 565°F data was then obtained.

In addition to the official test conditions of 1 through 15, data was taken for the case of no pumps operating to determine the background noise effects. It was observed from this that 60 HZ

electrical noise was present in the strain gage readings as both even and odd multiples of the harmonic while accelerometer and pressure readings contained only odd multiples of the 60 HZ electrical noise.

### 3.5 DATA REDUCTION

Data was reduced on-line during the tests for selected instrumentation to determine if the response was within the acceptance limits (Table 1.3-1). This reduction included calculation of the RMS values for both the response and forcing function instrumentation. In addition, a spectrum analyzer was used to examine the spectral characteristics of selected instruments. After completion of the testing the total data package, recorded on magnetic tape, was returned to C-E Windsor for thorough data reduction and evaluation. This manipulation of the data included the determination of the Power Spectral Densities (PSD), coherence and phase plots for a large number of instruments and test conditions. Additional work was done to separate Random and Deterministic portions of response PSD's, plot Transient Time Histories, and to determine the Amplitude Probability Densities (APD) in the Upper Guide Structure region.

The amount and variety of data reduced is indicative of the scope of the CVAP program. These quantities of reduced data are used to verify the predicted values of pressure, acceleration (displacement), and strain presented in Section 2.0. The comparable measured values are presented in Sections 3.5.1 to 3.5.3 below. Predicted and measured values are compared and evaluated in Section 5.0.

Of the 47 instrument channels used to acquire test data, 19 failed during the CVAP. An instrument history is shown in Table 3.5-1. Although this appears to be a high failure rate, Table 3.5-1 indicates that failures occurred only at the start of testing



(3 instruments) and after the high temperature plateau (500°F) had been reached. This allowed for the collection of a considerable amount of data from virtually all the instruments prior to the majority of failures. Because of this and the level of instrument redundancy, the data acquired for the CVAP is sufficient to confirm the structural adequacy of the System 80 internals.

### 3.5.1 Core Support Barrel

Data measured on the Core Support Barrel was obtained using the instrumentation shown and listed in Section 3.2. This measured data was reduced and examined for the various instruments as shown in Table 3.5-2.

The Power Spectral Densities (PSD), Coherence, and Phase were reduced and plotted in the 0-500 HZ frequency range for all instruments at all test conditions. In addition 0-50 HZ plots were obtained for all instruments for Test Condition 15. The total RMS responses found at the various instruments are tabulated in Table 3.5-3. This table is used to determine response trends and maximums at the various instruments. Because of the low frequency of many of the response modes of the CSB, and the dual nature of the forcing function, a more detailed break down of the response RMS was made. This detailed breakdown illustrated the relative deterministic and random contributions at various pump related frequencies, total deterministic response, total random response, and the total RMS response. Electrical noise can also be calculated from these quantities using the equation:

$$\text{ELECTRICAL NOISE} = \sqrt{(\text{RMS TOTAL})^2 - (\text{RMS TOTAL RANDOM})^2 - (\text{RMS TOTAL DETERMINISTIC})^2}$$

Typical tabulations of this type are shown in Table 3.5-4 (inlet pressure - P2), Table 3.5-5 (snubber displacement - A3), and Table 3.5-6 (upper flange strain - S1).

PSD plots of inlet pressure (P2) are shown in Figures 3.5-1 to 3.5-3. These plots represent 3 pump operations at different temperature conditions and are used to evaluate random and deterministic hydraulic loading at various temperatures. Figures 3.5-4 and 3.5-5 show the 4 pump, 565°F normal operating inlet load at P2 and P4 respectively. Details of the 0-50 HZ frequency range loading at P2 are shown in Figure 3.5-6.

Figures 3.5-7 to 3.5-12 present the PSD, Coherence and Phase plots for the cluster of pressure transducers P4, P5, P7 & P8 in the 0-50 HZ frequency range. These are used to evaluate the random turbulence coherence lengths.

Typical plots of the PSD, Coherence and Phase for displacement transducers A3 & A4 are shown in Figures 3.5-13 and 3.5-14. These are used to identify modeshapes, frequencies and snubber response displacements.

PSD, Coherence and Phase plots in Figures 3.5-15 thru 3.5-19 are used to show the broad band and low frequency response strains in the CSB at S2 & S6.

Figure 3.5-20 is a typical time history envelope of the response strains in the CSB during the pump start up transients. This and other similar plots are used to evaluate transient response as compared to steady state response.

### 3.5.2 Lower Support Structure

Instrumentation on the Lower Support Structure consists of the 5 transducer channels listed and shown in Section 3.2. Measured data

from these instruments was reduced and examined as shown in Table 3.5-2. Strain gage S13 failed prior to testing and S14 failed at the 500°F plateau.

The Power Spectral Densities (PSD), Coherence, and Phase were reduced and plotted in the 0-500 HZ frequency range for all instruments at all test conditions. The total RMS responses found from these plots are tabulated in Table 3.5-7. This table is used to determine general trends in the test conditions. A further breakdown of data is made to determine the random and periodic content of the responses. These breakdowns are listed in Table 3.5-8 (hydraulic pressure - P12), Table 3.5-9 (LSS displacement - A11), and Table 3.5-10 (instrument tube strain - S14).

Pressure loading on the LSS instrument tube #58 is shown from 0-500 HZ in the PSD plot of Figure 3.5-21. Details of the 0-50 HZ low frequency region are shown in Figure 3.5-22. These plots are typical for the condition of 4 pump, 565°F normal operation.

Acceleration of the LSS Assembly for normal operating conditions from 0-500 HZ is shown in Figure 3.5-23. Response at the pump pulsation frequencies is apparent. Low frequency (0-50 HZ) response acceleration of the assembly clearly shows the influence of CSB motion in the plot of Figure 3.5-24.

A typical wide band strain PSD plot is shown in Figure 3.5-25. This type of plot is used to determine the response strain in the instrumentation tube for comparison with predicted levels.

A time history envelope of LSS Assembly response to pump start up conditions is shown in Figure 3.5-26. This and other similar plots are used to evaluate transient behavior as compared to steady state conditions.

### 3.5.3 Upper Guide Structure

The instrumentation on the Upper Guide Structure consists of the 20 transducer channels listed and shown in Section 3.2. These 20 channels are composed of accelerometers (13 channels), pressure (3 channels), and strain (4 channels). Measured data from these instruments was reduced and examined as shown in Table 3.5-2. Upon reaching the high temperature region of testing (564°F) successive failures accounted for 7 accelerometer channels, 2 pressure channels, and 1 strain channel.

The Power Spectral Densities (PSD), Coherence, and Phase were reduced and plotted in the 0-500 HZ frequency range for all instruments at all test conditions. Total RMS responses found from these plots are tabulated in Table 3.5-11. This table is used to provide an overview of the UGS behavior as a function of temperature and number of pumps operating. A further breakdown of data is made to determine the random and periodic content of the responses. Typical listings of these breakdowns are shown in Table 3.5-12 (hydraulic pressure - P13), Table 3.5-13 (tube midspan displacement - A7), and Table 3.5-14 (guide tube strain - S9). Additional data plots were made in the 0-50HZ frequency range for Test Condition 15 normal operating conditions for the purposes of examining low frequency modes of the UGS assembly.

Pressure loading on the UGS upper plate from 0-500 HZ is shown in the PSD plot of Figure 3.5-27. Figure 3.5-27 presents a similar PSD plot of the pressure on a guide tube in the UGS tube bank for comparison with that of the upper plate.

The response frequency of the UGS assembly is shown in the 0-50 HZ acceleration PSD plot of Guide Tube accelerometer A5 presented in Figure 3.5-29.

A typical wide band strain PSD plot is shown in Figure 3.5-30 for guide tube #3. This type of plot is used to determine response frequencies and strains for comparison with predicted values.

A time history envelope of guide tube response to pump start up conditions is shown in Figure 3.5-31. This and other similar plots are used to evaluate transient response as compared to steady state response.

Figures 3.5-32 and 3.5-83 show Amplitude Probability Distributions for guide tube acceleration and strain respectively. These are used to verify the absence of any fluid elastic instability mechanisms in the UGS tube bank.

### 3.6 SUMMARY

The Measurement Program provides a means of measuring the forcing functions, structural characteristics of the components, and dynamic response strains and displacements of the core support structures. Adequate instrumentation was provided to record data sufficient to verify the predicted quantities discussed in Section 2.0. Although the instrument history shown in Table 3.5-1 indicates a number of failures, considerable data was obtained prior to the loss of the majority of these instruments. Because of this and the level of instrument redundancy, the data acquired during the CVAP is sufficient to confirm the structural adequacy of the reactor internals.

Conditions representing the normal operating range of temperature, pressure, number of pumps, steady state and transient combinations were tested as shown in Table 3.4-2. Data was recorded during this testing, partially reduced on-line to check with acceptance criteria, and returned to C-E Windsor for thorough data evaluation. Complete reduction and evaluation of this data included Power Spectral Density (PSD), Coherence, and Phase plots for wide band

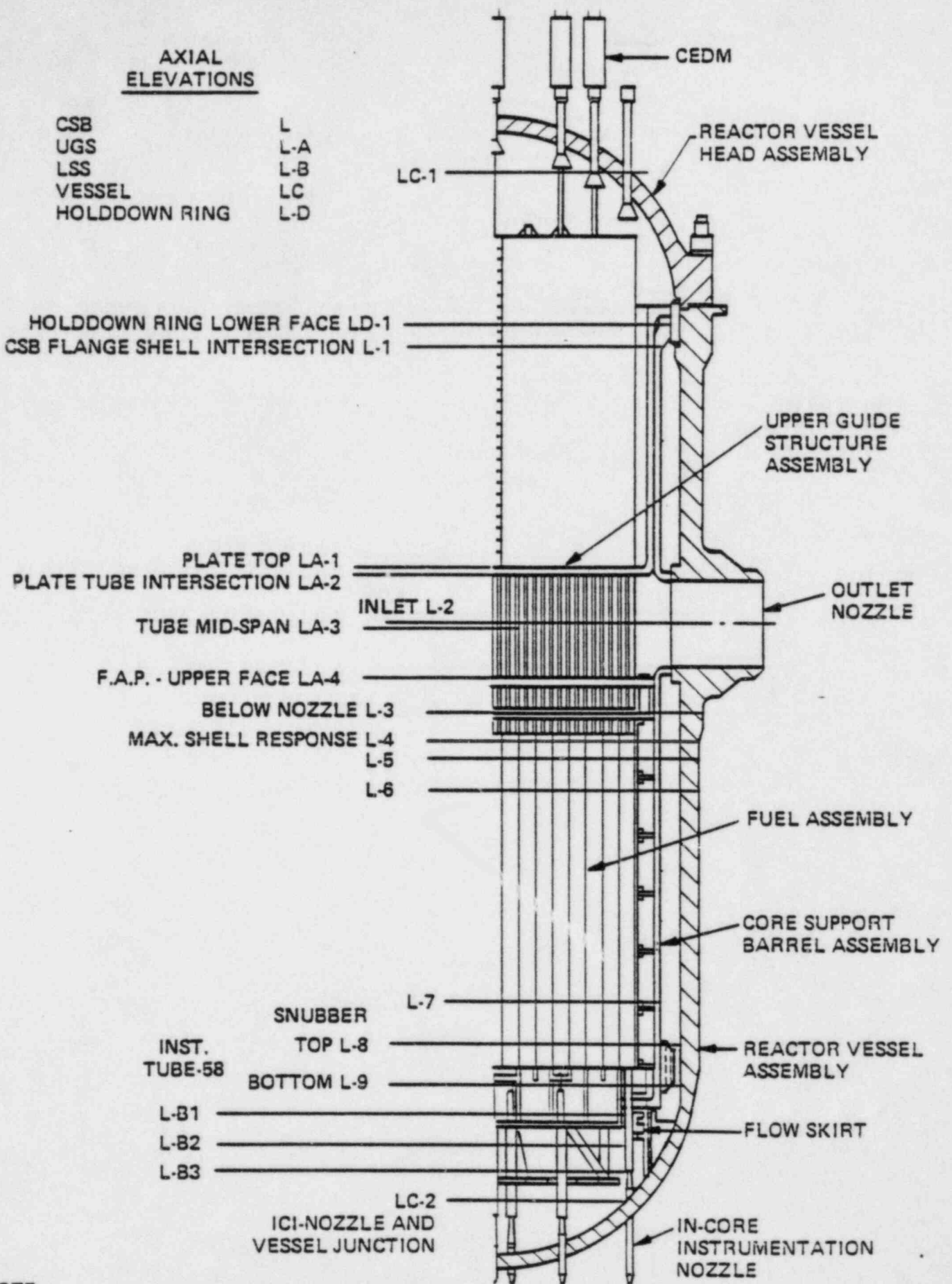
(0-500 HZ) and low frequency (0-50 HZ) conditions; breakdown of RMS response into Random and Deterministic portions; Time History plots of instrument response during transient conditions; and Amplitude Probability Distributions to determine signal characteristics. This data was used for the verification of the structure through comparison with analytical predictions in the Evaluation Program (Section 5.0). Portions of this reduced data are presented in the previous section (Section 3.5). This data provides the basis for the evaluations in Section 5.0.

TABLE 3.2-1  
CVAP INSTRUMENTATION

Assembly	Type	ID No.	Channels	Location (Fig. 3.2.1 & 3.2-2)
Core Support Barrel (Fig. 3.2-3 3.2-4)	1. Pressure Transducer	P1	1	CSB 120° Inlet
	2. Pressure Transducer	P2	1	CSB 300° Inlet
	3. Pressure Transducer	P3	1	CSB 300° Level 7
	4. Pressure Transducer	P4	1	CSB 300° Level 4
	5. Pressure Transducer	P5	1	CSB 270° Level 4
	6. Pressure Transducer	P6	1	CSB 270° Level 4
	7. Pressure Transducer	P7	1	CSB 300° Level 5
	8. Pressure Transducer	P8	1	CSB 300° Level 6
	9. Pressure Transducer	P9	1	CSB 240° Inlet
	10. Strain Gage	S1	1	CSB 180° Key Way
	11. Strain Gage	S2	1	
	12. Strain Gage	S3	1	CSB 270° Key Way
	13. Strain Gage	S4	1	
	14. Strain Gage	S5	1	CSB 180° Level 4
	15. Strain Gage	S6	1	
	16. Strain Gage	S7	1	CSB 270° Level 4
	17. Strain Gage	S8	1	
	18. Biaxial Accelerometer	A1	2	CSB 180 Snubber
	19. Displacement Transducer	A2	1	CSB 0° Snubber
	20. Displacement Transducer	A3	1	CSB 120° Snubber
	21. Displacement Transducer	A4	1	CSB 240° Snubber
Upper Guide Structure (Fig. 3.2-6 3.2-7)	22. Pressure Transducer	P10	1	UGS 180°-270° Tube 3
	23. Pressure Transducer	P11	1	UGS 180°-270° Tube 6
	38. Pressure Transducer	P13	1	UGS Plate
	24. Strain Gage	S9	1	UGS 180°-270° Tube 6
	25. Strain Gage	S10	1	
	26. Strain Gage	S11	1	UGS 0°-90° Tube 3
	27. Strain Gage	S12	1	
	28. Biaxial Accelerometer	A5	2	UGS 180°-270° Tube 3
	29. Biaxial Accelerometer	A6	2	UGS 180°-270° Tube 4
	30. Biaxial Accelerometer	A7	2	UGS 180°-270° Tube 6
	31. Biaxial Accelerometer	A8	2	UGS 180°-270° Tube 10
32. Biaxial Accelerometer	A9	2	UGS 180°-270° Tube 37	
33. Triaxial Accelerometer	A10	3	UGS 180°-270° Tube 187	
Lower Support Structure (Fig. 3.2-5)	34. Pressure Transducer	P12	1	LSS Ins. Guide Tube 58
	35. Strain Gage	S13	1	LSS Ins. Guide Tube 58
	36. Strain Gage	S14	1	
	37. Biaxial Accelerometer	A11	2	LSS ICI Support Plate
Totals			38	47

**AXIAL  
ELEVATIONS**

CSB	L
UGS	L-A
LSS	L-B
VESSEL	LC
HOLDDOWN RING	L-D

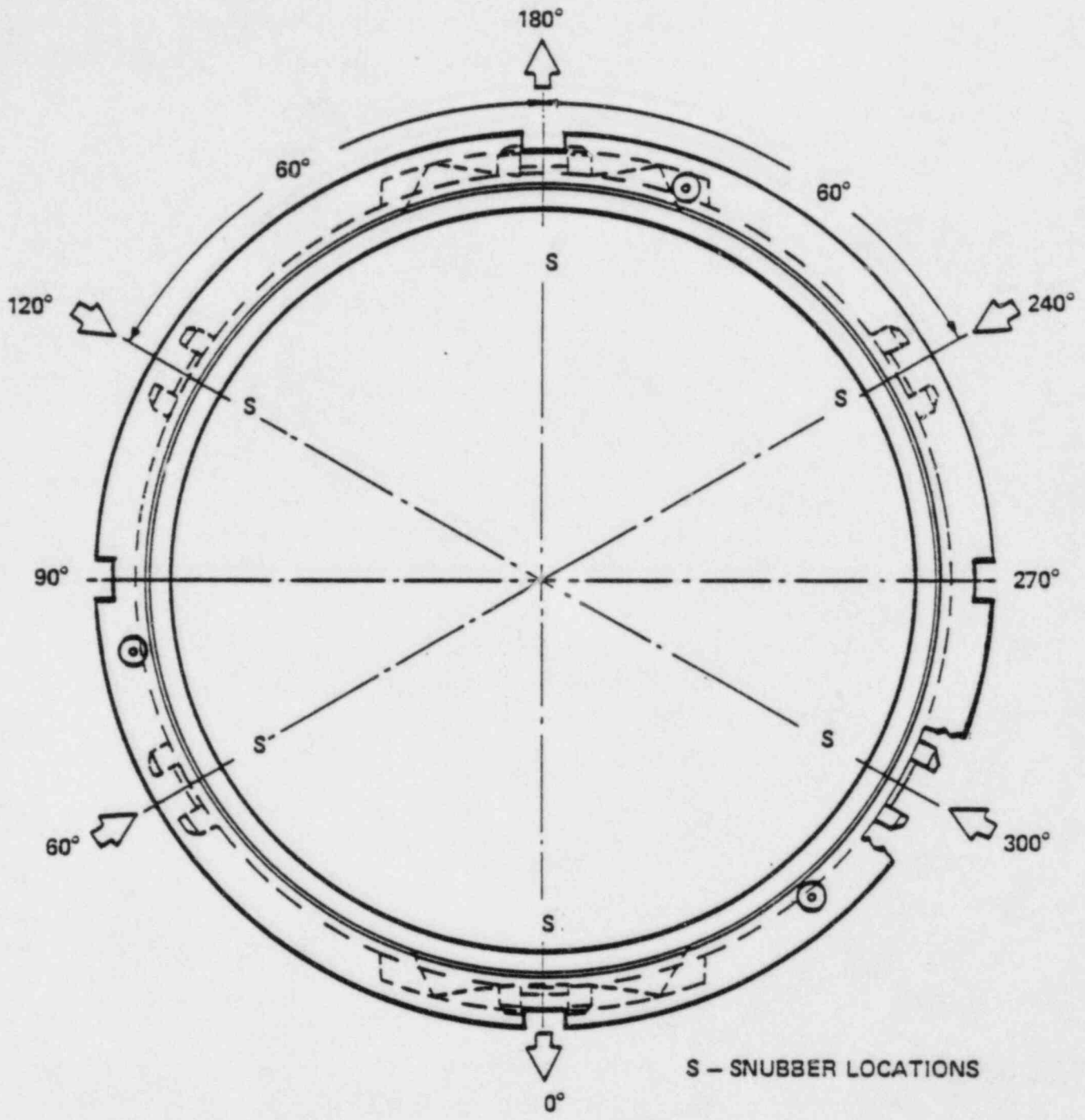


**NOTE:**

L-4 = FROM TOP OF CSB  
L-7 = FROM BOTTOM OF CSB

**TRANSDUCER AXIAL LOCATIONS  
FIGURE 3.2-1**





CIRCUMFERENTIAL LOCATIONS  
OF INLET AND OUTLET NOZZLES

FIGURE 3.2-2

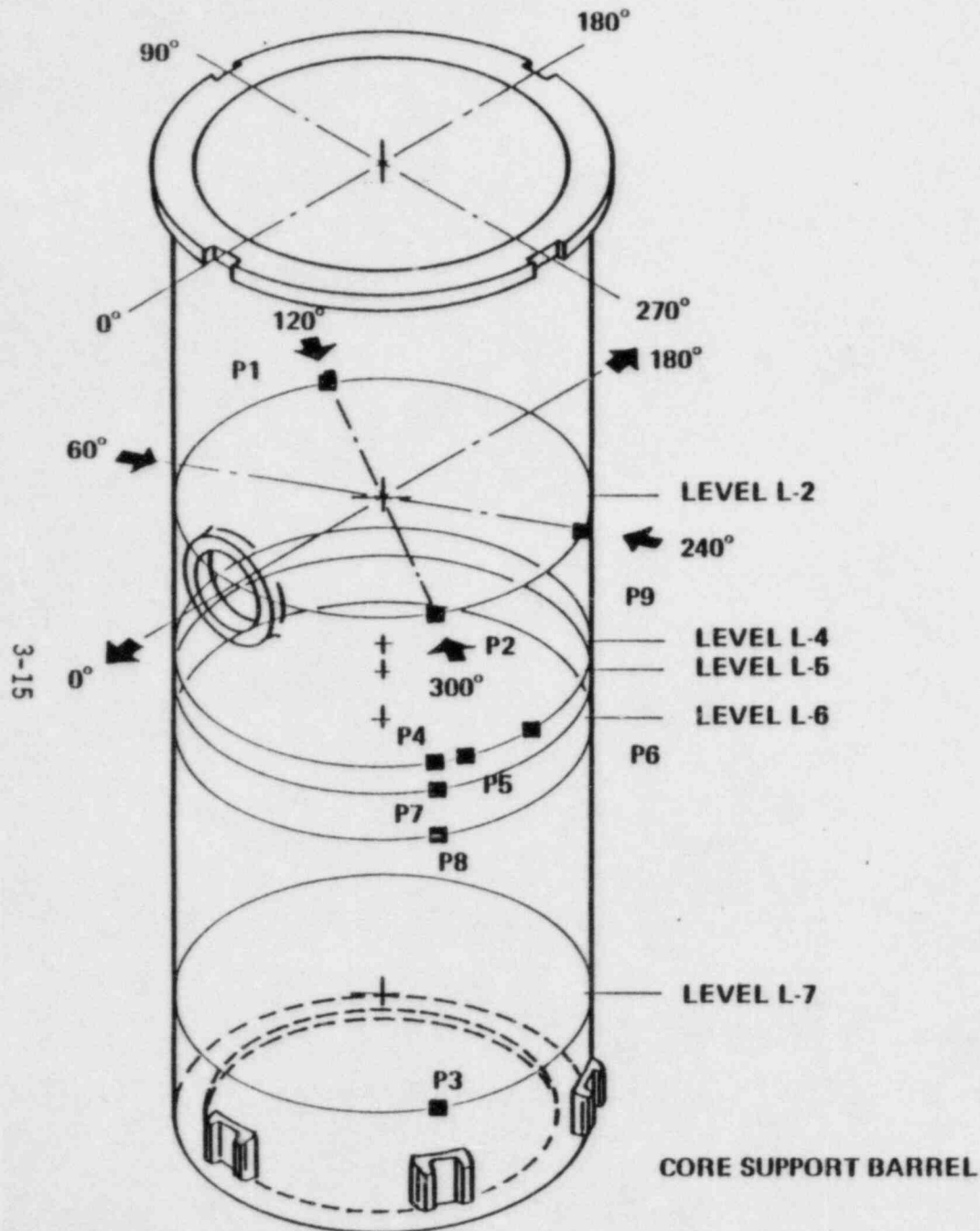


FIGURE 3.2-3  
INPUT FUNCTION MEASUREMENT TRANSDUCERS  
(■)

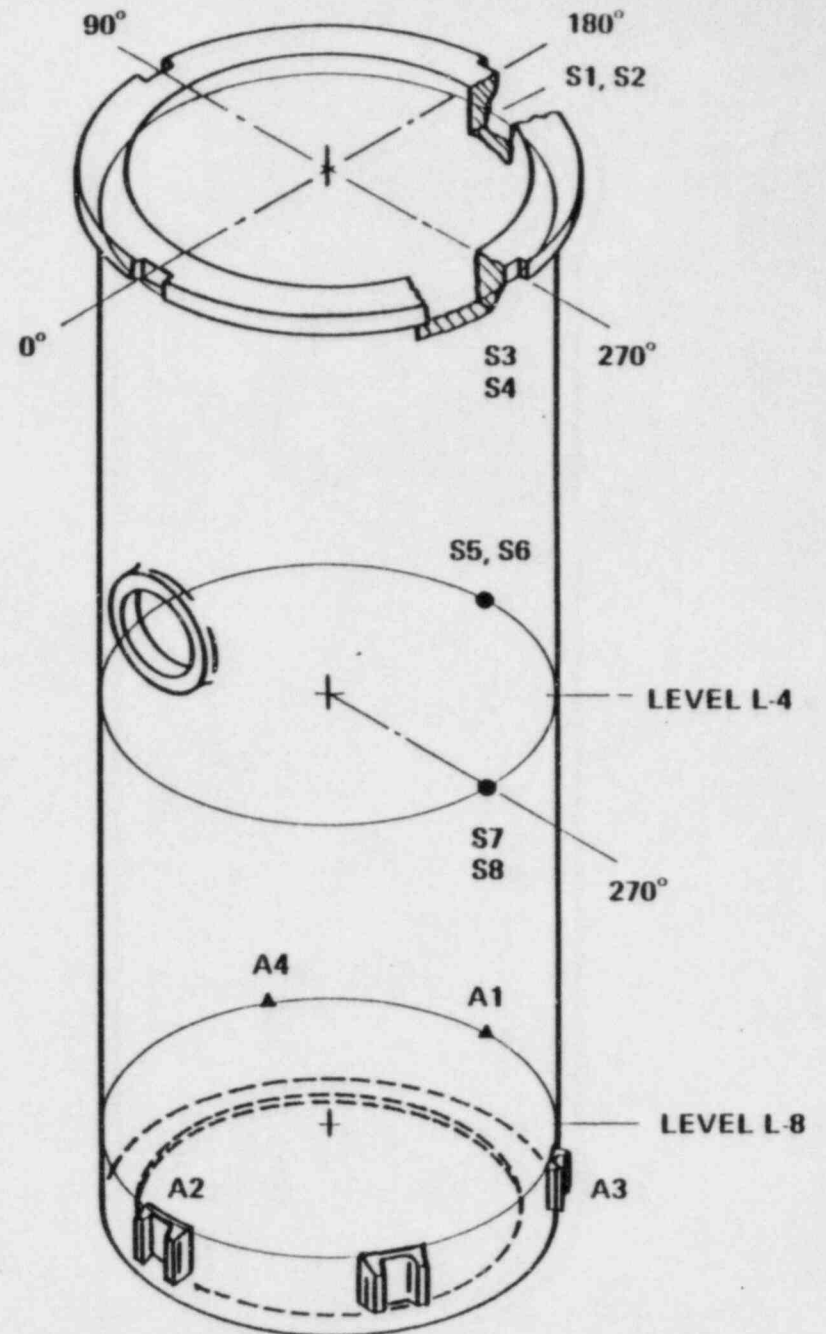
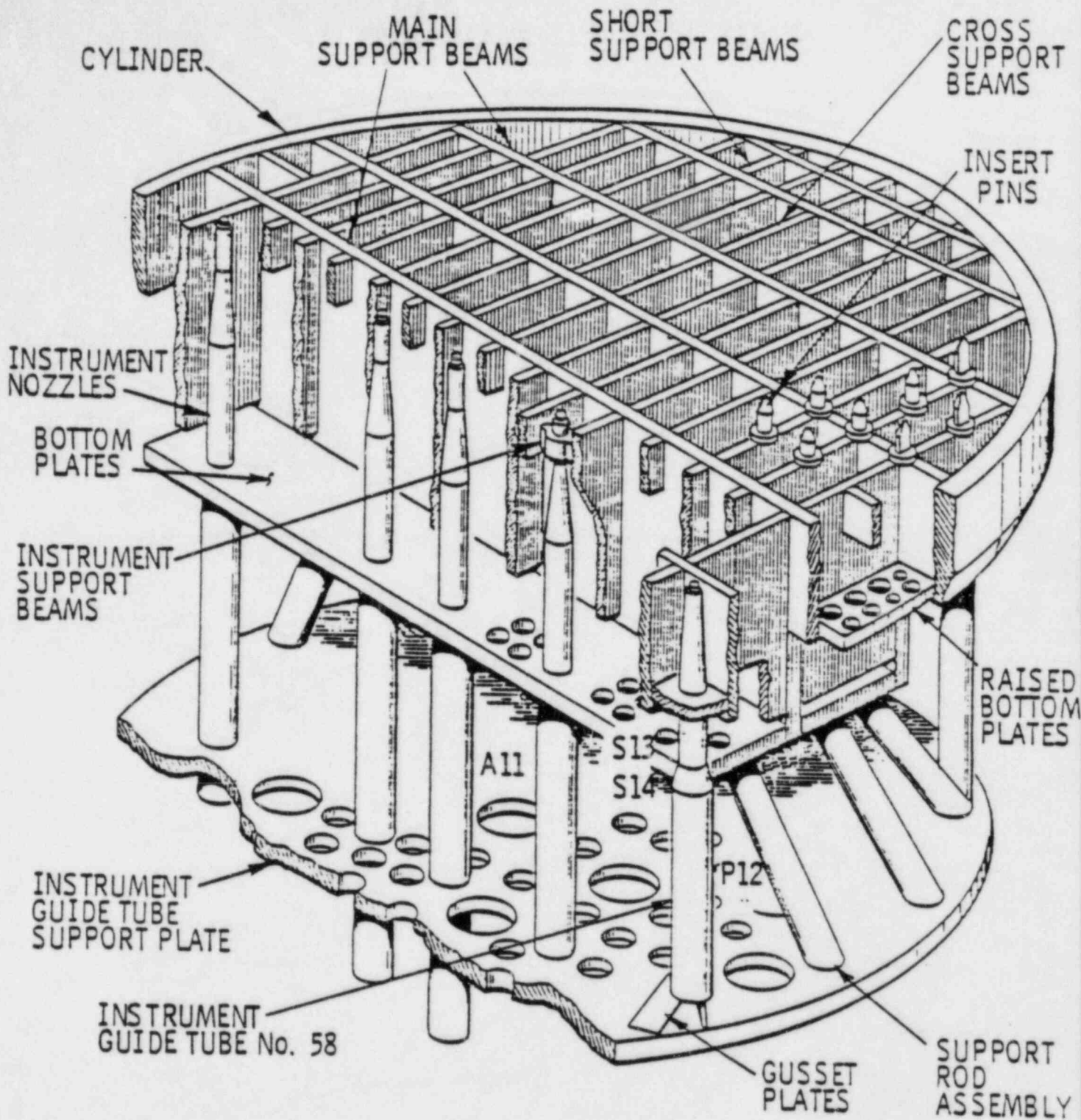
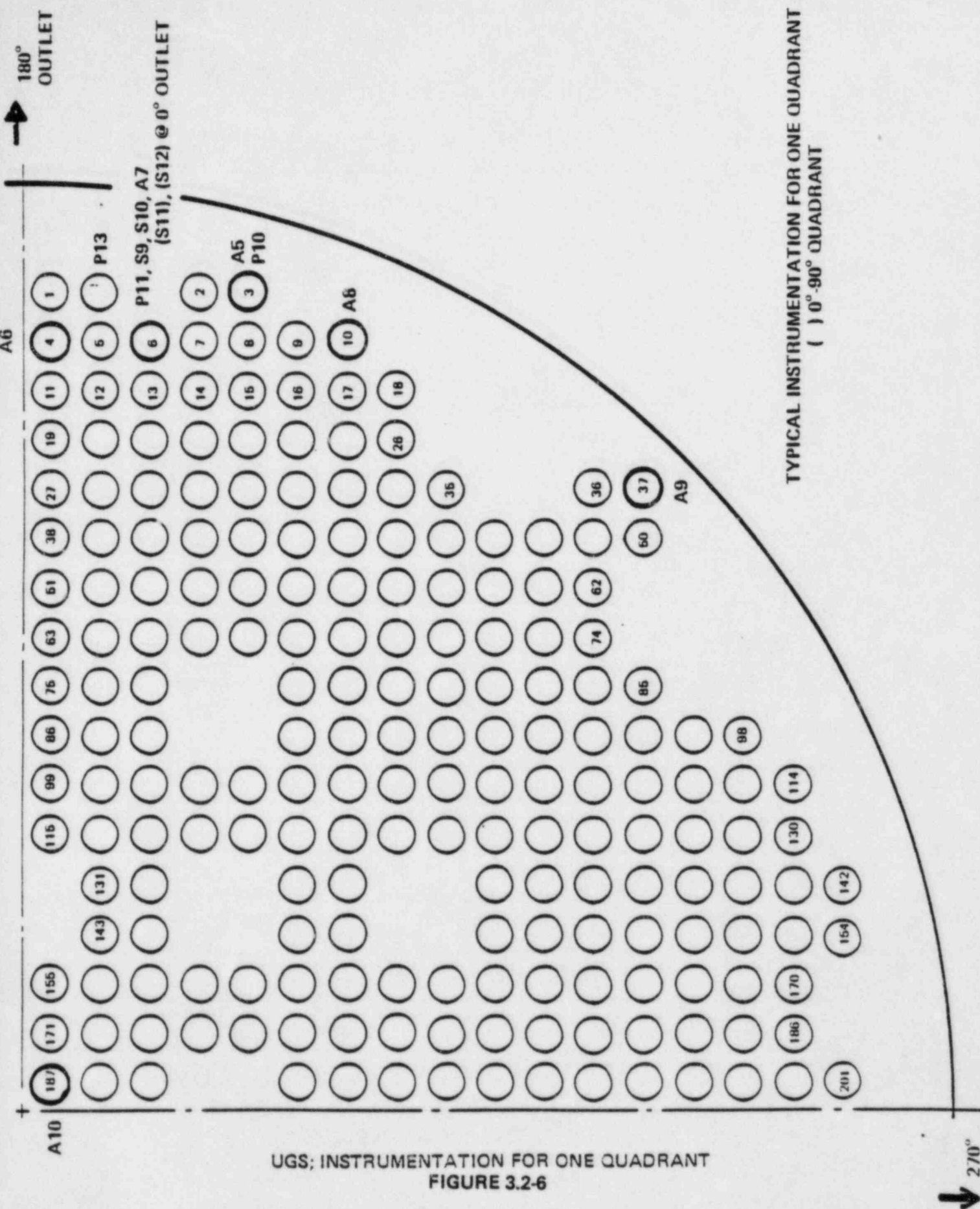


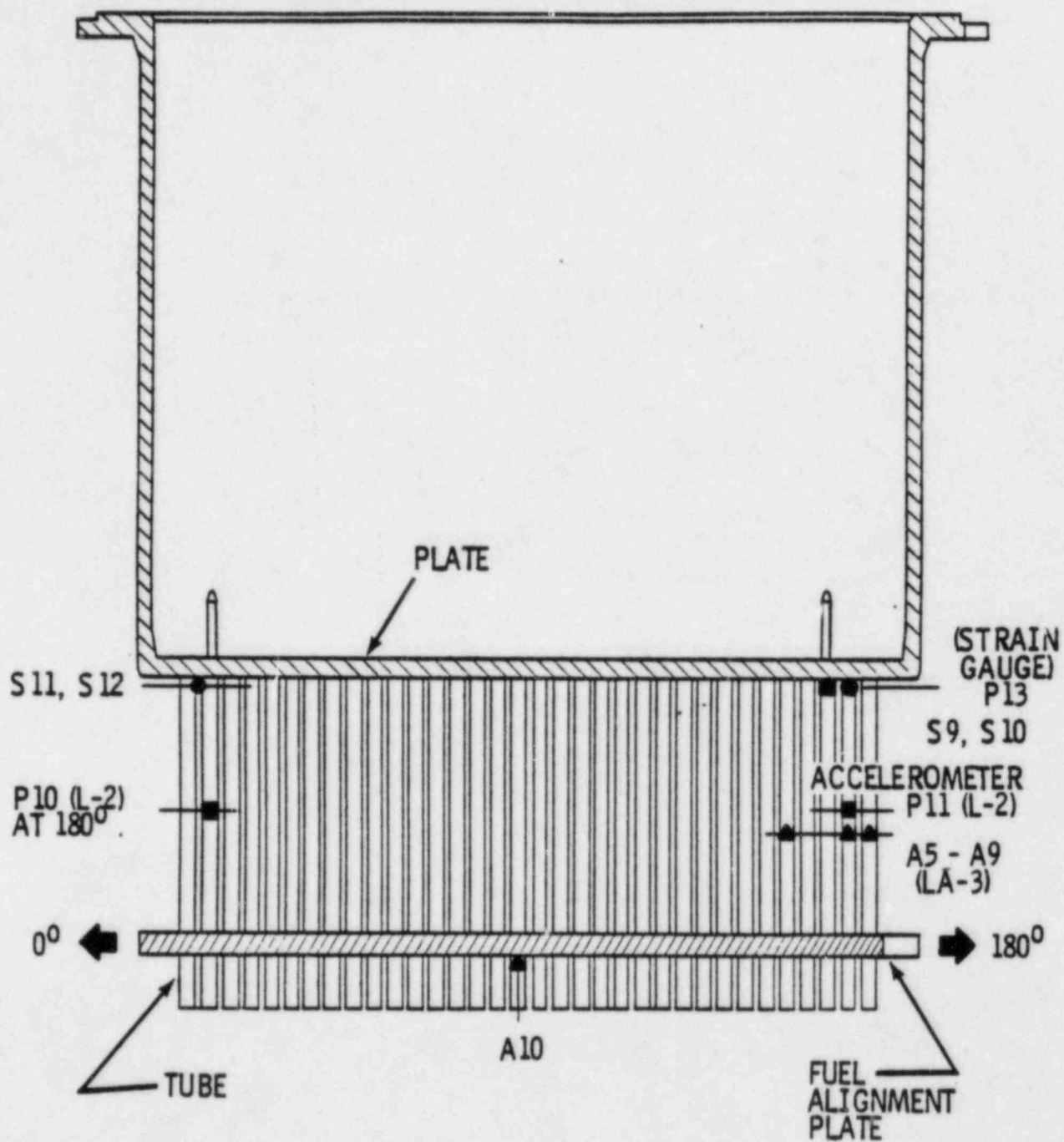
FIGURE 3.2-4  
RESPONSE MEASUREMENT TRANSDUCERS  
STRAIN GAUGE (●)  
ACCELEROMETER & DISP. DEVICE (▲)



LOWER SUPPORT STRUCTURE & INSTRUMENT ASSEMBLY  
 FIGURE 3.2-5



UGS; INSTRUMENTATION FOR ONE QUADRANT  
 FIGURE 3.2-6



UGS; AXIAL LOCATIONS FOR INSTRUMENTATION  
FIGURE 3.2-7

FIGURE 3.3-1  
PALO VERDE DATA ACQUISITION SYSTEM

DATA ACQUISITION (CORE SUPPORT BARREL,  
LOWER SUPPORT STRUCTURE, UPPER GUIDE STRUCTURE)

DATA RECORDING (OFF-LINE REDUCTION)

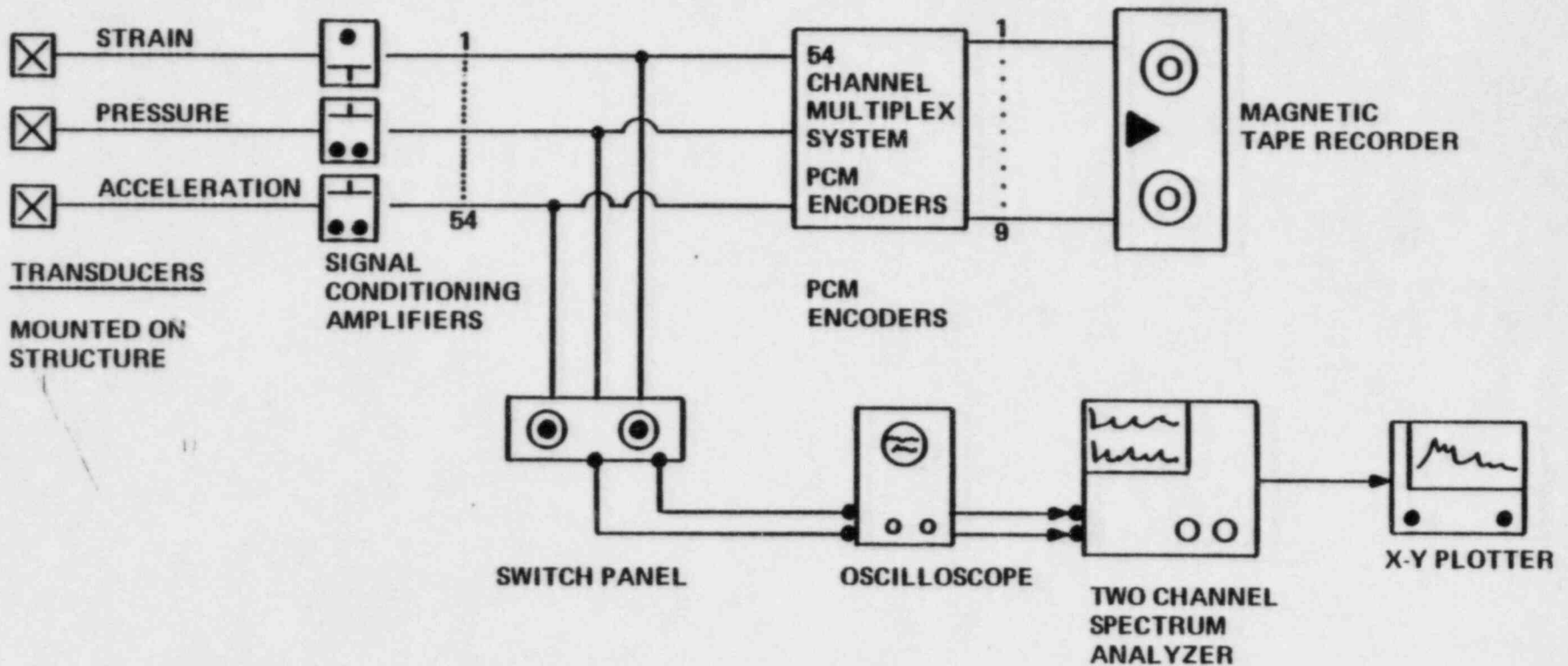
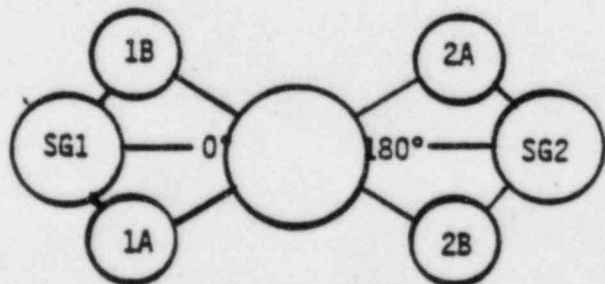


TABLE 3.4-1

ORIGINAL TEST CONDITIONS

<u>SEQUENCE</u> <u>NUMBER</u>	<u>TEMPERATURE</u>		RCP				<u>TEST</u>
			<u>1A</u>	<u>1B</u>	<u>2A</u>	<u>2B</u>	
1	Pump Start	<200°F	S	NO	NO	NO	T
2	Pump Start	200°F	0	NO	S	NO	T
3	Pump Start	200°F	0	S	0	NO	T
4	Pump Shutdown	260°F	0	SP	0	NO	T
5	Hot Shutdown	260°F	0	NO	0	NO	SS
6	Hot Shutdown	260°F	0	S	0	NO	SS
7	Part Loop	500°F	0	SP	0	NO	SS
8	Part Loop	500°F	0	S	0	NO	SS
9	Pump Start	500°F	0	0	0	S	T
10	Max Flow	500°F	0	0	0	0	SS
11	Hot Standby	564°F	0	0	0	0	SS
12	Pump Shutdown	564°F	0	0	0	SP	T
13	Part Loop	564°F	0	0	0	NO	SS
14	Part Loop	564°F	0	SP	0	NO	SS
15	Part Loop	564°F	0	S	SP	NO	SS

KEY: NO - Not Operating  
 0 - Operating  
 S - Start  
 SP - Stop  
 SS - Steady State  
 T - Transient



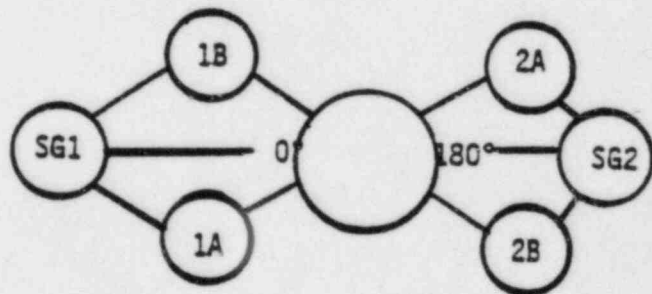
\* All test conditions are PRE-CORE.

TABLE 3.4-2

MODIFIED TEST CONDITIONS

SEQUENCE NUMBER	TEMPERATURE		RCP				TEST	COMMENTS
			1A	1B	2A	2B		
1	Pump Start	<200°F	S	NO	NO	NO	T	
2	Pump Start	200°F	O	NO	S	NO	T	
3	Pump Start	200°F	O	S	O	NO	T	
4	Pump Shutdown	260°F	O	SP	O	NO	T	
5	Hot Shutdown	260°F	O	NO	O	NO	SS	
6	Hot Shutdown	260°F	O	S	O	NO	SS	
7	Part Loop	500°F	O	SP	O	NO	SS	
8	Part Loop	500°F	O	NO	O	S	SS	
9	Pump Start	500°F					T	Deleted
10	Max Flow	500°F					SS	Deleted
11	Part Loop	564°F	O	NO	O	O	SS	
12	Pump Shutdown	564°F	O	NO	O	SP	SS	
13	Part Loop	564°F	O	NO	O	S	T	Deleted +
14	Part Loop	564°F	SP	NO	O	O	SS	
15	Hot Standby	564°F	S	S	O	O	SS	

KEY: NO - Not Operating  
 O - Operating  
 S - Start  
 SP - Stop  
 SS - Steady State  
 T - Transient



\* All test conditions are PRE-CORE.

+ Pumps operated but no data recorded.



TABLE 3.5-1

CVAP TRANSDUCER HISTORY

<u>Accelerometers</u>	<u>Location</u>	<u>Status</u>
A1X	CSB 180° Snubber	OK
A1Y	CSB 180° Snubber	OK
A2	CSB 0° Snubber	Failed prior to test start.
A3	CSB 120° Snubber	OK
A4	CSB 240° Snubber	Failed @ 500°F
A5X	UGS Tube #3	OK
A5Y	UGS Tube #3	OK
A6X	UGS Tube #4	Failed @ 564°F
A6Y	UGS Tube #4	Failed @ 564°F
A7X	UGS Tube #6	Failed @ 564°F
A7Y	UGS Tube #6	OK
A8X	UGS Tube #10	Failed @ 564°F
A8Y	UGS Tube #10	Failed @ 564°F
A9X	UGS Tube #37	Failed @ 564°F
A9Y	UGS Tube #37	Failed @ 564°F
A10X	UGS Tube #187	OK
A10Y	UGS Tube #187	OK
A10Z	UGS Tube #187	OK
A11X	LSS Support Plt	OK
A11Y	LSS Support Plt	OK

TABLE 3.5-1  
CVAP TRANSDUCER HISTORY (Cont'd.)

<u>Pressure Transducers</u>	<u>Location</u>	<u>Status</u>
P1	CSB 120° Inlet	Failed @ 564°F
P2	CSB 300° Inlet	OK
P3	CSB 300° LEV 7	Failed @ 564°F
P4	CSB 300° LEV 4	OK
P5	CSB 292° LEV 4	OK
P6	CSB 270° LEV 4	Failed @ 500°F
P7	CSB 300° LEV 5	OK
P8	CSB 300° LEV 6	OK
P9	CSB 240° Inlet	OK
P10	UGS Tube #3	Failed @ 500°F
P11	UGS Tube #6	Failed @ 564°F
P12	LSS Tube #58	Failed @ 564°F
P13	UGS Plate	OK
<u>Strain</u>		
S1	CSB 180° Keyway	OK
S2	CSB 180° Keyway	OK
S3	CSB 270° Keyway	OK
S4	CSB 270° Keyway	Failed at Program Start
S5	CSB 180° LEV 4	OK
S6	CSB 180° LEV 4	OK
S7	CSB 270° LEV 4	OK
S8	CSB 270° LEV 4	Failed at 500°F
S9	UGS Tube #6	OK
S10	UGS Tube #6	Failed at 500°F
S11	UGS Tube #6*	OK
S12	UGS Tube #6*	OK
S13	LSS Tube #58	Failed @ Program Start
S14	LSS Tube #58	Failed @ 500°F

\* 0° outlet nozzle (SG1); all others are 180° outlet nozzle (SG2).

TABLE 3.5-2

SPECTRAL DENSITY DATA REDUCTION

Assembly	Data Channel A	Data Channel B	Comment		
CSB	P4	P5	Axial & Circumferential coherence for random loading (2)		
	P4	P6			
	P4	P7			
	P4	P8			
	P2	P3	Periodic load, axial & circumferential mode shape		
		P9			
	A2	A3	Displacement pattern & mode shape at CSB snubber level		
		A4			
		A1			
	S1	S5	Axial & circumferential mode shapes between upper flange & midplane. Strain at high response locations on CSB.		
		S3			
		S2			
S4					
LSS	P12	S14	Periodic & random loading Lateral response of LSS Response strain in peripheral instrument tube.		
	A11				
	S13				
UGS	P10	P11	Attenuation, phase of random and periodic pulsations		
	P13				
	S9	S10	Response pattern of Tube 6		
				S11	
	A5	A5	Response pattern of tubes 3, 4, 6, 10, 37		
	A6	A6			
	A7	A7			
	A8	A8			
	A9	A9			
	S9	S10	S22	Determine tube response to random and flow induced forces.	
					A5
					A6
					A7
					A8
					A9

TABLE 3.5-3  
CSB  
TOTAL RMS RESPONSE

MAX-MAX

Test Condition	S1	S2	S3	S5	S6	S7	S8	A1-X	A1-Y	A3	A4	P1	P2	P3	P4	P5	P6	P7	P8	P9	
1																					
2																					
3																					
4																					
5																					
6																					
7																					
8																					
11																					
12																					
14																					
15																					

3-25

TABLE 3.5-4  
 INLET PRESSURE BREAKDOWN  
 TRANSDUCER - P2  
 (PSI)

SENSOR	Test Condition #	RMS AT DIFFERENT FREQUENCY RANGES						TOTAL DETERMINISTIC RMS	TOTAL RANDOM RMS	TOTAL RMS
		20 HZ	40 HZ	120 HZ	240 HZ	360 HZ	480 HZ			
P2 300 Inlet Pressure Trans  " " " " " " " " " " " " " " " "	1									
	2									
	3									
	4									
	5									
	6									
	7									
	8									
	11									
	12									
	14									
	15									

3-26

TABLE 3.5-5  
 SNUBBER DISPLACEMENT BREAKDOWN  
 TRANSDUCER - A3  
 (MILS)

SENSOR	Test Condition #	RMS AT DIFFERENT FREQUENCY RANGES						TOTAL DETERMINISTIC RMS	TOTAL RANDOM RMS	TOTAL RMS
		20 HZ	40 HZ	120 HZ	240 HZ	360 HZ	480 HZ			
A3 120 SNBR Accelerometer	1									
	2									
	3									
	4									
	5									
	6									
	7									
	8									
	11									
	12									
	14									
	15									

3-27

TABLE 3.5-6

UPPER FLANGE STRAIN BREAKDOWN  
 TRANSDUCER - S1  
 (MICRO IN./IN.)

SENSOR	Test Condition #	RMS AT DIFFERENT FREQUENCY RANGES						TOTAL DETERMINISTIC RMS	TOTAL RANDOM RMS	TOTAL RMS
		20 HZ	40 HZ	120 HZ	240 HZ	360 HZ	480 HZ			
S1 Strain Gauge	1									
	"	2								
	"	3								
	"	4								
	"	5								
	"	6								
	"	7								
	"	8								
	"	11								
	"	12								
	"	14								
	"	15								

3-28

TABLE 3.5-7

LSS  
TOTAL RMS RESPONSE

Test Condition	S14	A11-X	A11-Y	P12
1				
2				
3				
4				
5				
6				
7				
8				
11				
12				
14				
15				

(MICRO)  
IN/IN

(MILS)

(MILS)

(PSI)



TABLE 3.5-8

INSTRUMENT TUBE PRESSURE BREAKDOWN  
 TRANSDUCER - P12  
 (PSI)

SENSOR	Test Condition #	RMS AT DIFFERENT FREQUENCY RANGES						TOTAL DETERMINISTIC RMS	TOTAL RANDOM RMS	TOTAL RMS
		20 HZ	40 HZ	120 HZ	240 HZ	360 HZ	480 HZ			
P12 Tube 58 Pressure Trans.  3-30	1									
	2									
	3									
	4									
	5									
	6									
	7									
	8									
	11									
	12									
	14									
	15									



TABLE 3.5-10

INSTRUMENT TUBE STRAIN BREAKDOWN BREAKDOWN  
 TRANSDUCER - S14  
 (MICRO IN/IN)

SENSOR	Test Condition #	RMS AT DIFFERENT FREQUENCY RANGES						TOTAL DETERMINISTIC RMS	TOTAL RANDOM RMS	TOTAL RMS
		20 HZ	40 HZ	120 HZ	240 HZ	360 HZ	480 HZ			
S14 Strain Gauge	1									
"	2									
"	3									
"	4									
"	5									
"	6									
"	7									
"	8									
"	11									
"	12									
"	14									
"	15									

3-32

TABLE 3.5-11

UCS  
TOTAL RMS RESPONSE

Test Condition	S9	S10	S11	S12	A5X	A5Y	A6X	A6Y	A7X	A7Y	A8X	A8Y	A9X	A9Y	A10X	A10Y	A10Z	P10	P11	P13	
1																					
2																					
3																					
4																					
5																					
6																					
7																					
8																					
11																					
12																					
14																					
15																					

TABLE 3.5-12

UPPER PLATE PRESSURE BREAKDOWN  
 TRANSDUCER - P13  
 (PSI)

SENSOR	Test Condition #	RMS AT DIFFERENT FREQUENCY RANGES						TOTAL DETERMINISTIC RMS	TOTAL RANDOM RMS	TOTAL RMS
		20 HZ	40 HZ	120 HZ	240 HZ	360 HZ	480 HZ			
P13 UPR PLT Pressure Trans.	1									
	"									
	"									
	"									
	"									
	"									
	"									
	"									
	"									
	"									
	"									
	"									
	"									
	"									
	"									

3-34

TABLE 3.5-13

TUBE MIDSPAN DISPLACEMENT BREAKDOWN  
 TRANSDUCER - A7  
 (MILS)

SENSOR	Test Condition #	RMS AT DIFFERENT FREQUENCY RANGES						TOTAL DETERMINISTIC RMS	TOTAL RANDOM RMS	TOTAL RMS
		20 HZ	40 HZ	120 HZ	240 HZ	360 HZ	480 HZ			
A7Y Accelerometer	1									
	2									
	3									
	4									
	5									
	6									
	7									
	8									
	11									
	12									
	14									
	15									

3-35

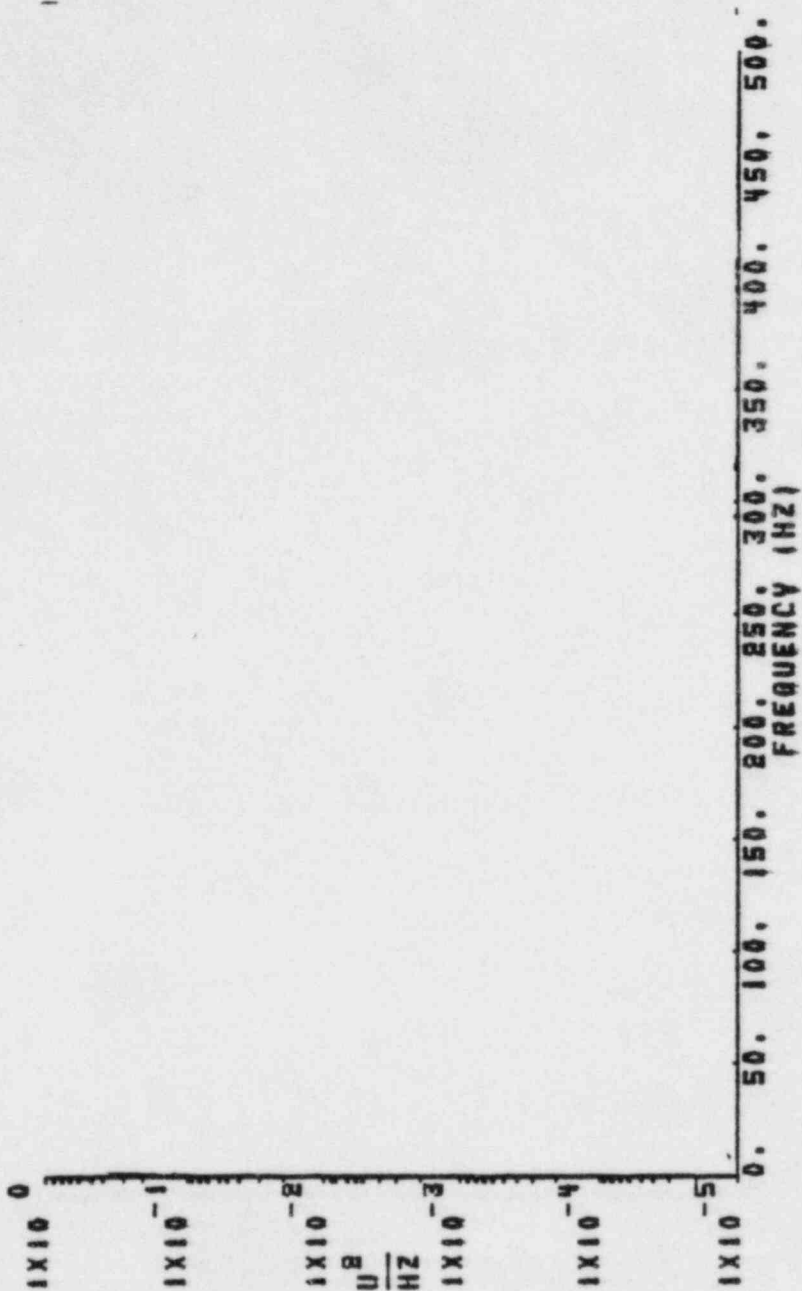
TABLE 3.5-14

GUIDE TUBE STRAIN BREAKDOWN  
 TRANSDUCER - S9  
 (MICRO IN/IN)

SENSOR	Test Condition #	RMS AT DIFFERENT FREQUENCY RANGES						TOTAL DETERMINISTIC RMS	TOTAL RANDOM RMS	TOTAL RMS
		20 HZ	40 HZ	120 HZ	240 HZ	360 HZ	480 HZ			
S9 STRAIN GAUGE	1									
	"	2								
	"	3								
	"	4								
	"	5								
	"	6								
	"	7								
	"	8								
	"	11								
	"	12								
	"	14								
	"	15								

3-36

POWER SPECTRAL DENSITY

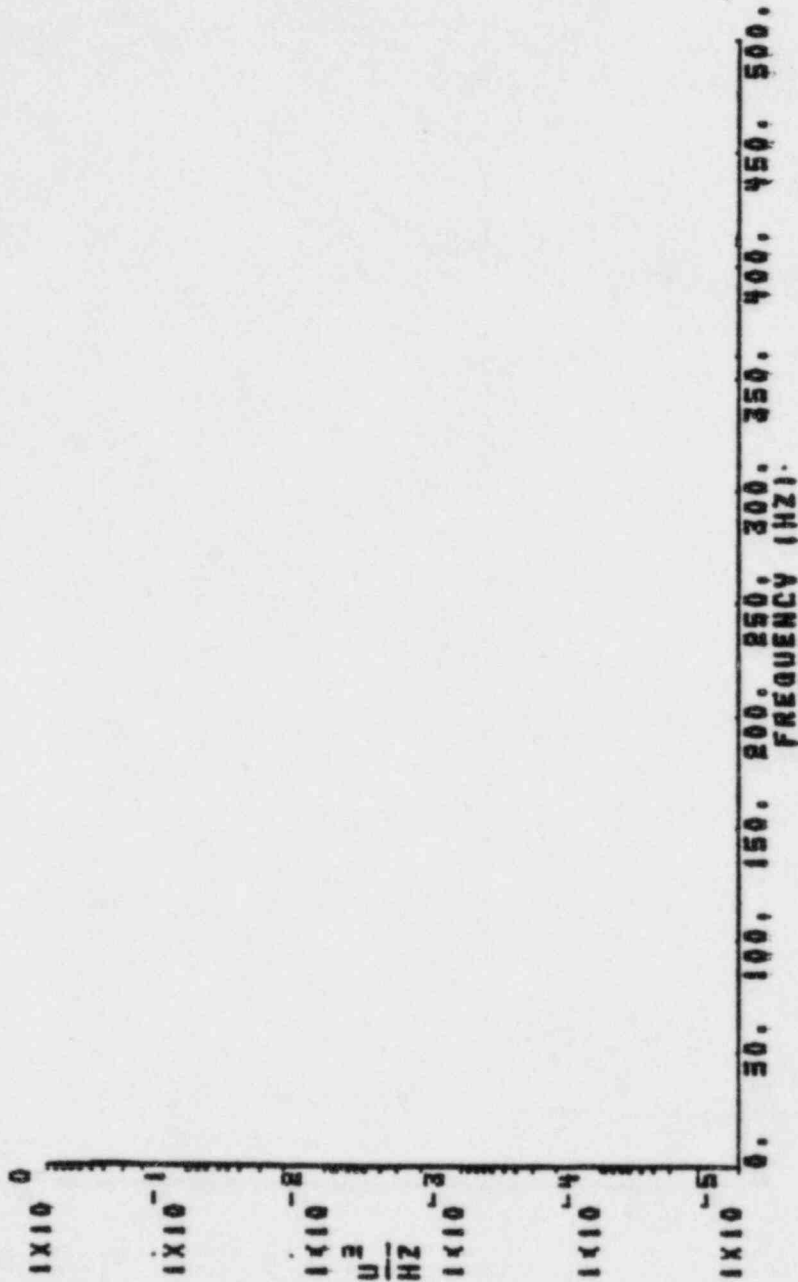


SYSTEM 80 CVAP PALO VERDE UNIT 1  
 PVMP-6  
 TEMP1 2.650E102 PRESSURE1 3.500E102 PUMPS1 A1 0 B1 0 C1 0 D1 MD SS  
 TRANSDUCER GROUP1 PRESSURE ID1 P2 300 IMLT UNITS1 PSI  
 RMS -  
 DL0:PVMP06.PSD TAPE1 T-239 RUN1 13 1.562E103 SFS MW = 2.289E100 MDF = 100.

PRESSURE PSD (P2) - PVMP 6  
FIGURE 3.5-1



POWER SPECTRAL DENSITY



SYSTEM 80 CVAP PALO VERDE UNIT 1  
PVMP-8

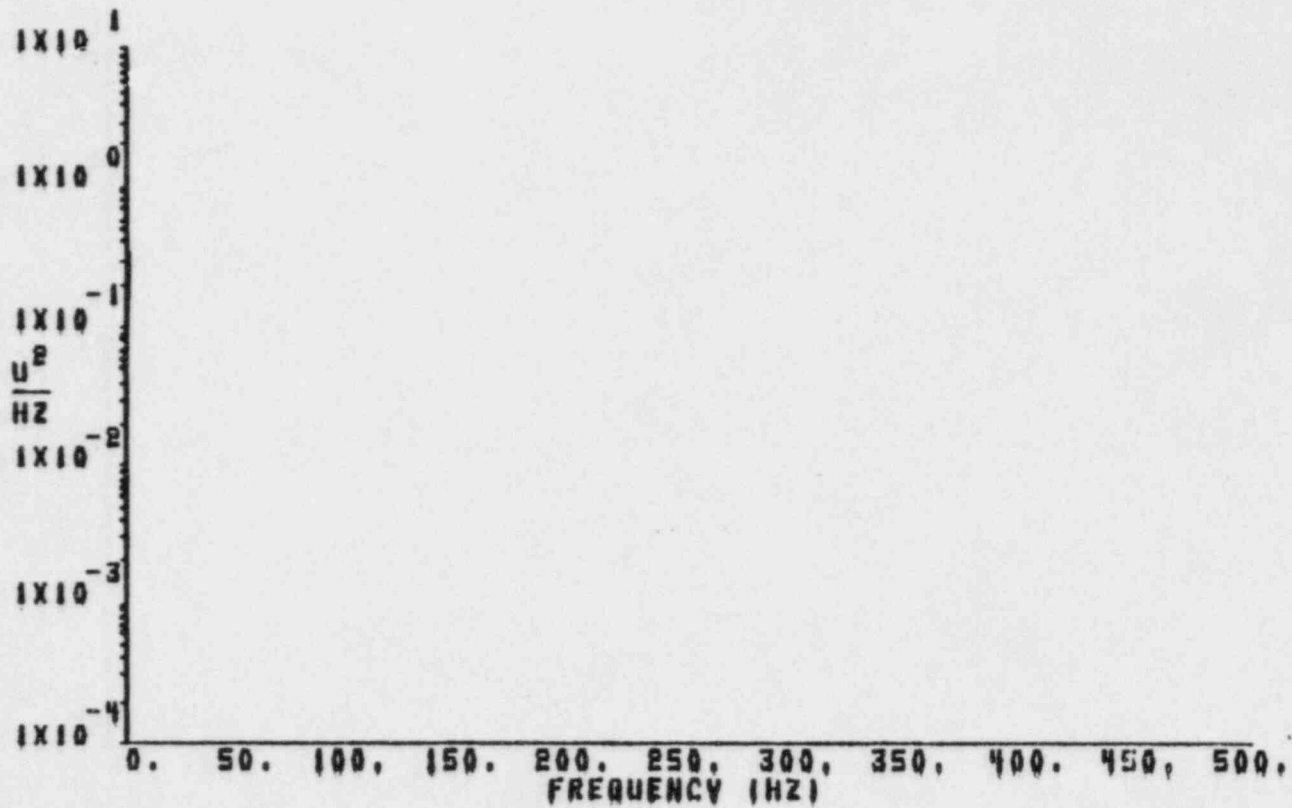
TEMP1 3.000E+02 PRESSURE1 1.550E+03 PUMP81 A1 0 91 MD C1 0 D1 0 88

TRANSDUCER GROUP1 PRESSURE 101 P2 300 INLT UNITS1 PSI  
RMS -

BL01PVMP08.PSD TAPE1 1-241 RUN1 17 1.562E+03 SP8 BM - 2.289E+00 MBF - 100.

PRESSURE PSD (P2) - PVMP 8  
FIGURE 3.5-2

## POWER SPECTRAL DENSITY



3-39

SYSTEM 80 CVAP PALO VERDE UNIT 1

PVMP-11

TEMP:  $5.65E+02$  PRESSURE:  $2.250E+03$  PUMPS: 1A) 0 1B) NO 2A) 0 2B) 0 88

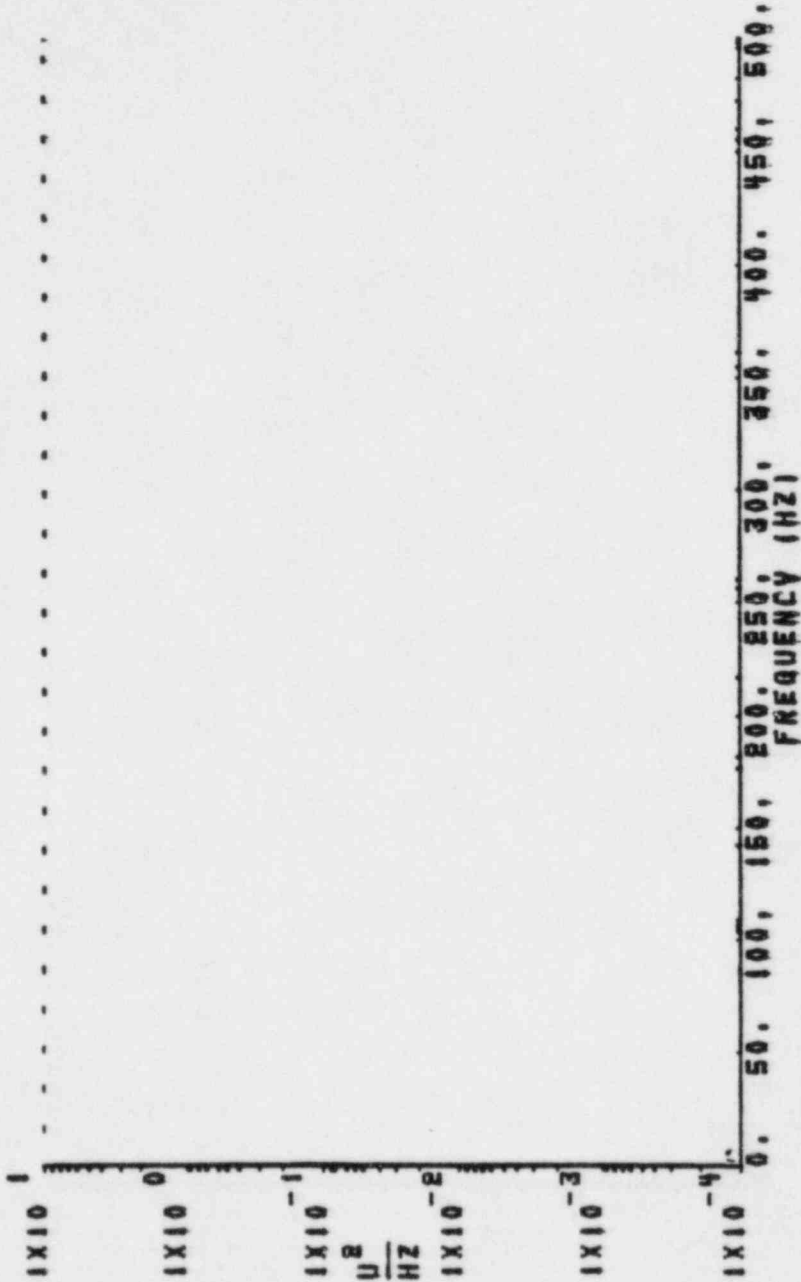
TRANSDUCER GROUP: PRESSURE ID: P2 300 INLT UNITS: PSI

RHS =

DL01PVMP11.PSD TAPE: T-242 RUN: 20  $1.542E+03$  GPH BW =  $2.289E+00$  NBF = 100.

PRESSURE PSD (P2) - PVMP 11  
 FIGURE 3.5-3

# POWER SPECTRAL DENSITY



SYSTEM 80 CVAP PALO VERDE UNIT 1

PUMP-15

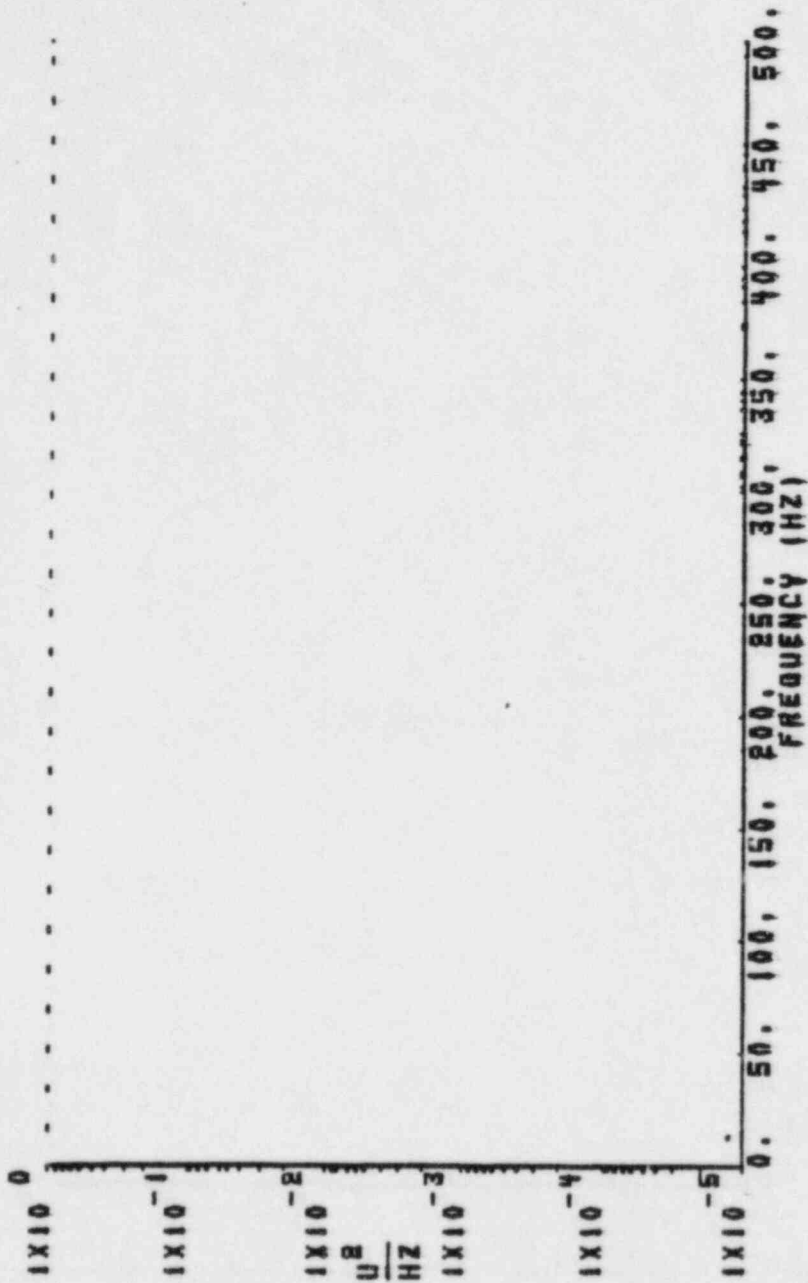
TEMP1 5.650E102 PRESSURE1 2.250E103 PUMPS1 1A1 0 1B1 0 2A1 0 2B1 0 SB

TRANSDUCER GROUP1 PRESSURE 1B1 P2 300 INLT . UNITS1 PSI RMS -

DI01FVNF15.PSD TAPE1 T-245 RUN1 27 1.562E103 SPS BM = 2.289E100 MDF = 100.

PRESSURE PSD (P2) - PVMP 15  
FIGURE 3.5-4

POWER SPECTRAL DENSITY



SYSTEM 80 CVAP PALO VERDE UNIT 1  
PVMP-15

TEMP1 5.650E102 PRESSURE1 2.250E103 PUMPB1 1A1 0 1B1 0 2A1 0 2B1 0 58

TRANSDUCER GROUP1 PRESSURE 1B1 P4 300 1-4 UNITB1 PSI  
RMS =

BL01PVMP15.PSD TAPE1 1-245 RUN1 27 1.562E103 SPS BW = 2.269E100 NDF = 100.

PRESSURE PSD (P4) - PVMP 15  
FIGURE 3.5-6

ANPP PRE-CRITICAL VIBRATION MONITORING PROGRAM (PVMP)  
P2

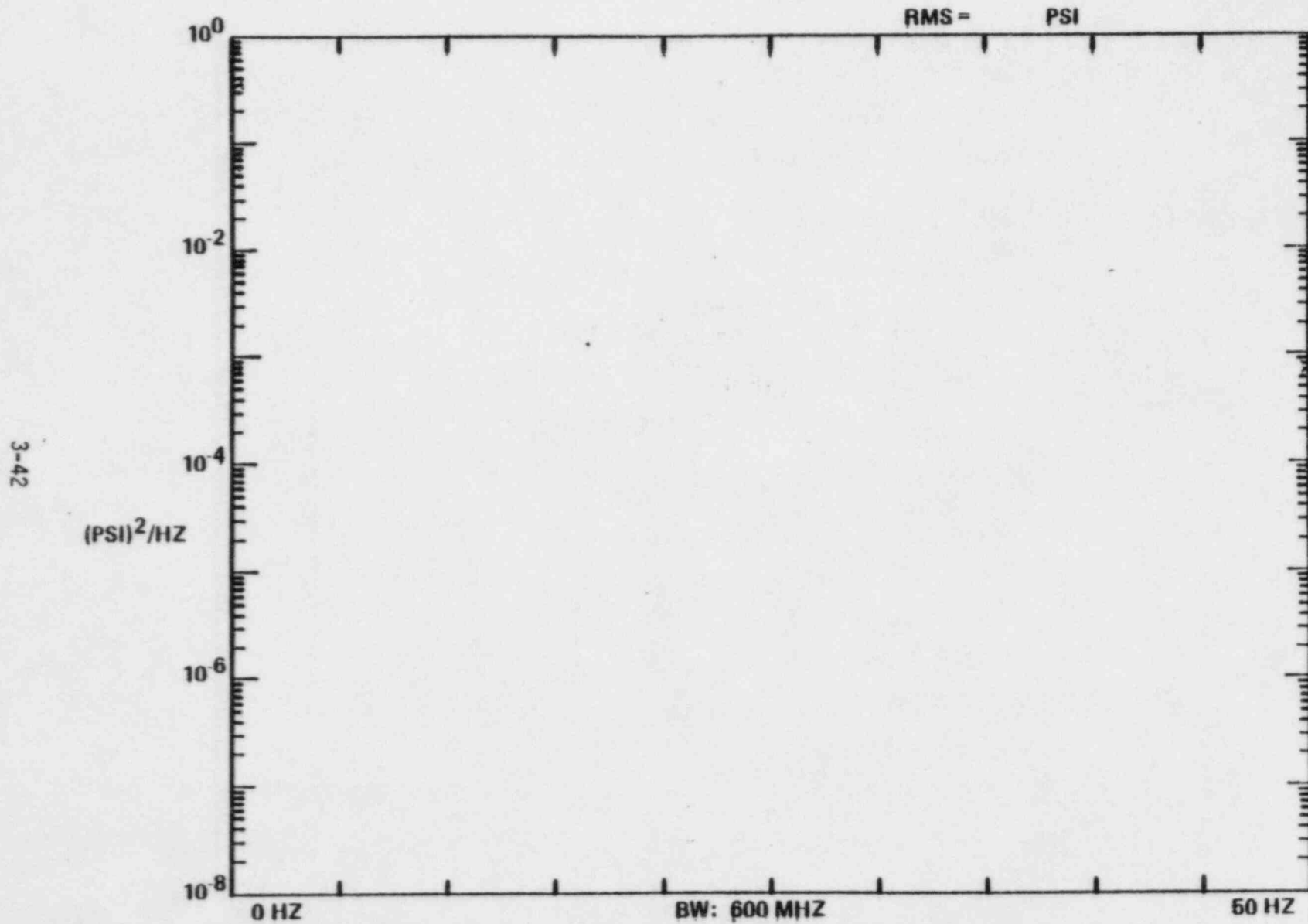


FIGURE 3.5-6  
PRESSURE PSD (P4) - PVMP 15

ANPP PRE-CRITICAL VIBRATION MONITORING PROGRAM (PVMP)  
P4(A) VS P5(B)

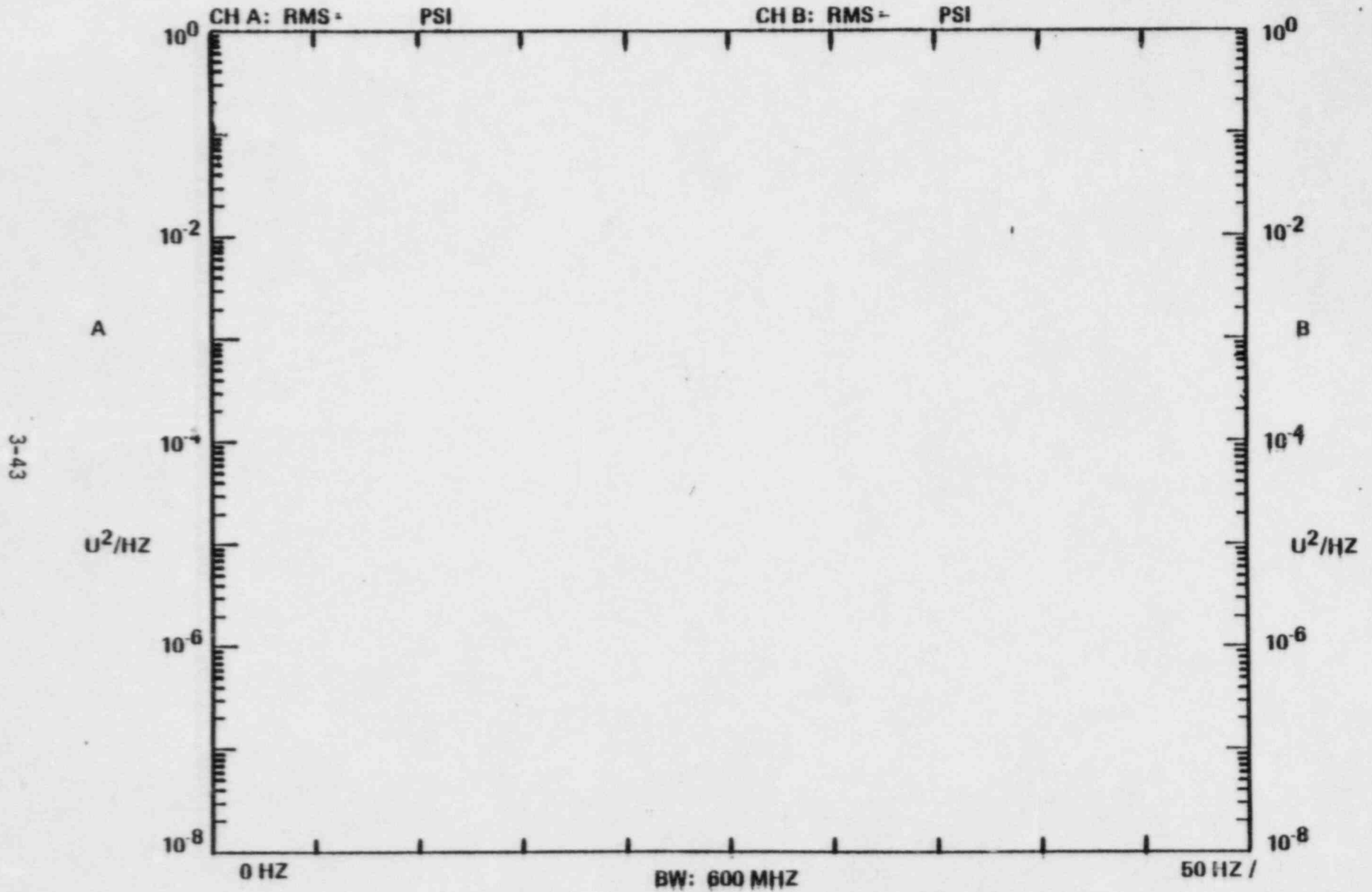
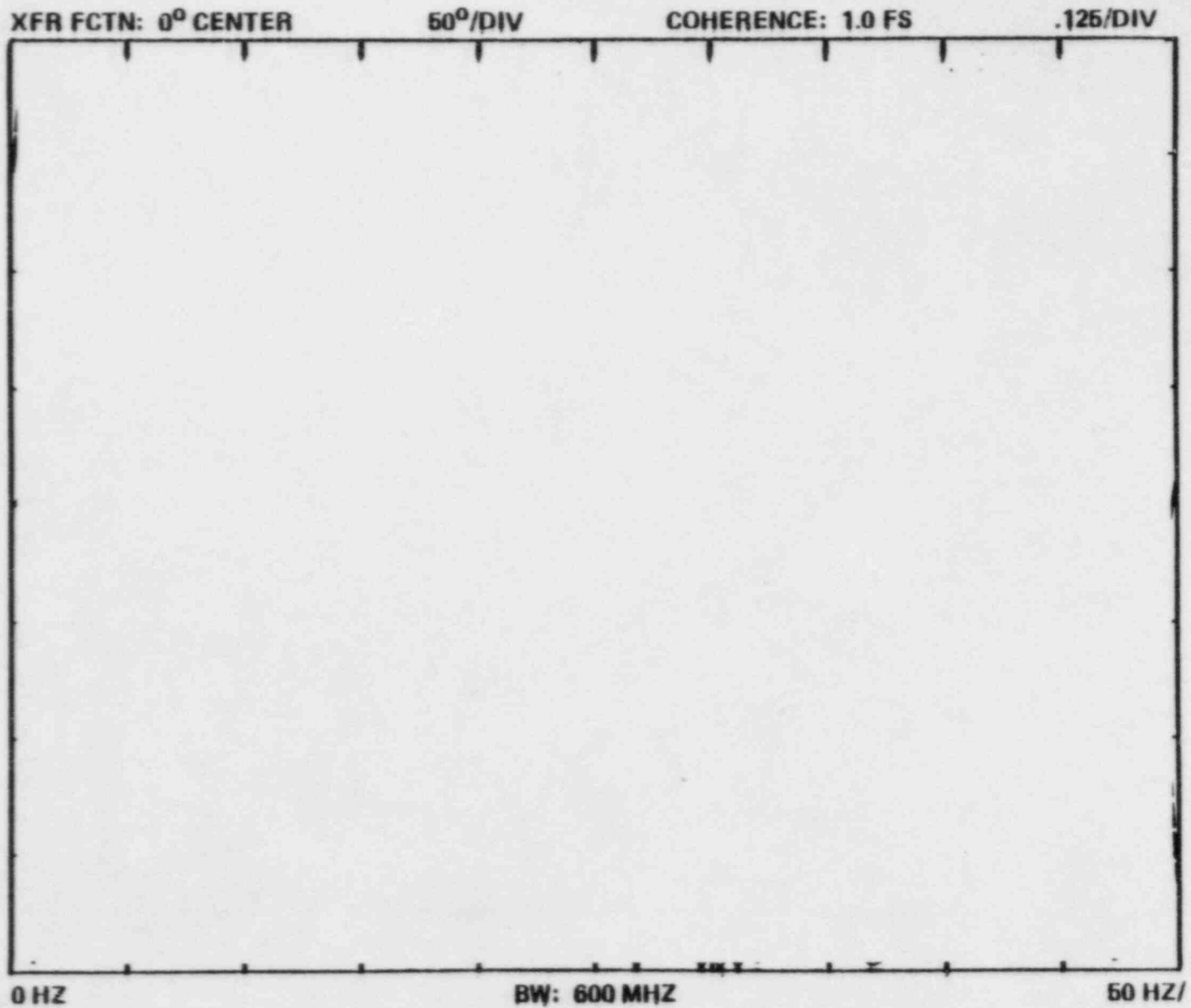


FIGURE 3.5-7  
PRESSURE PSD (P4 & P5) - PVMP 15

ANPP PRE-CRITICAL VIBRATION MONITORING PROGRAM (PVMP)  
PRESSURE TRANSDUCER P4 VS P5



3-44

FIGURE 3.5-8  
COHERENCE/PHASE (P4 & P5) - PVMP 15

ANPP PRE-CRITICAL VIBRATION MONITORING PROGRAM (PVMP)  
P4(A) VS P7(B)

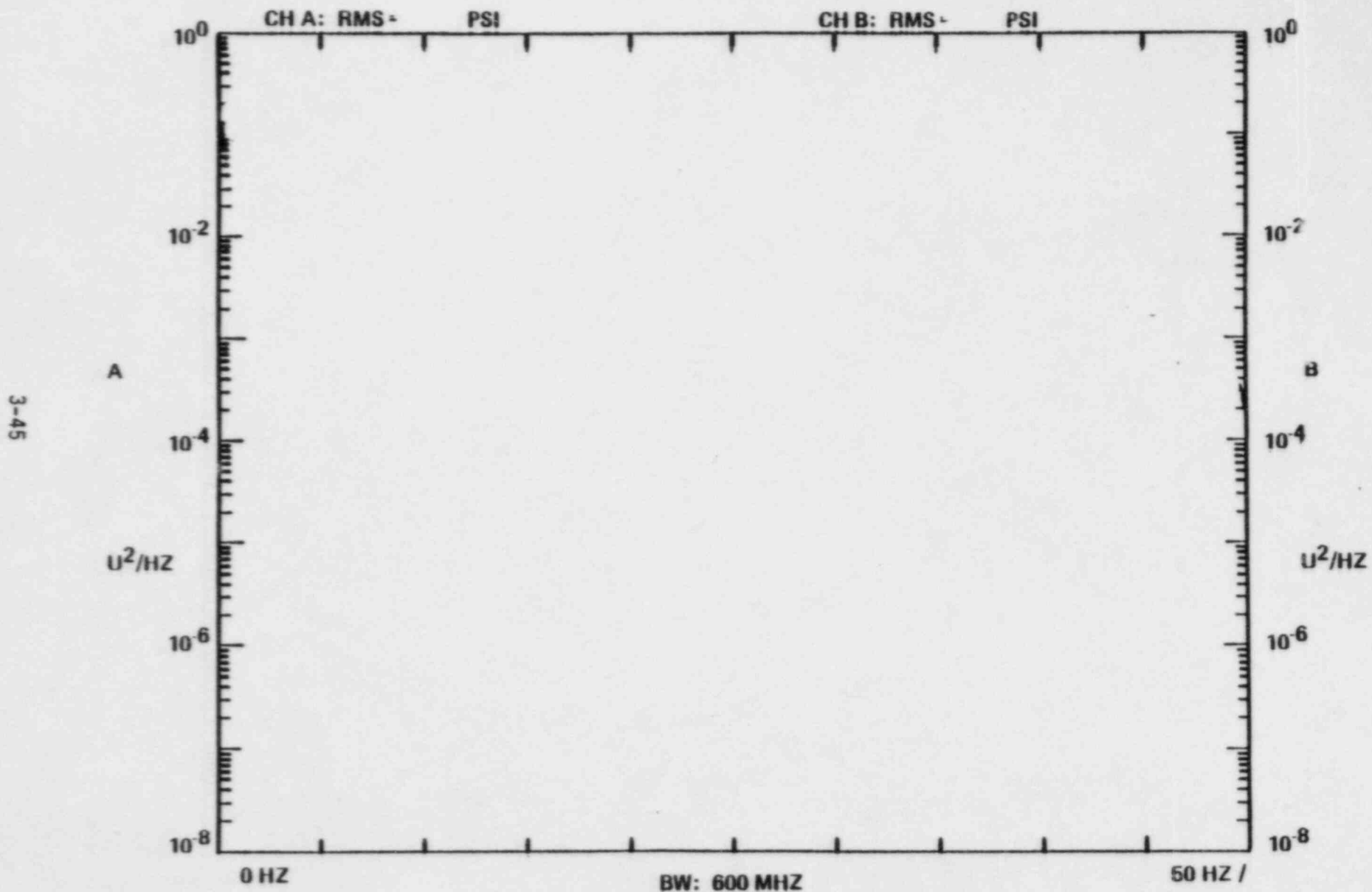
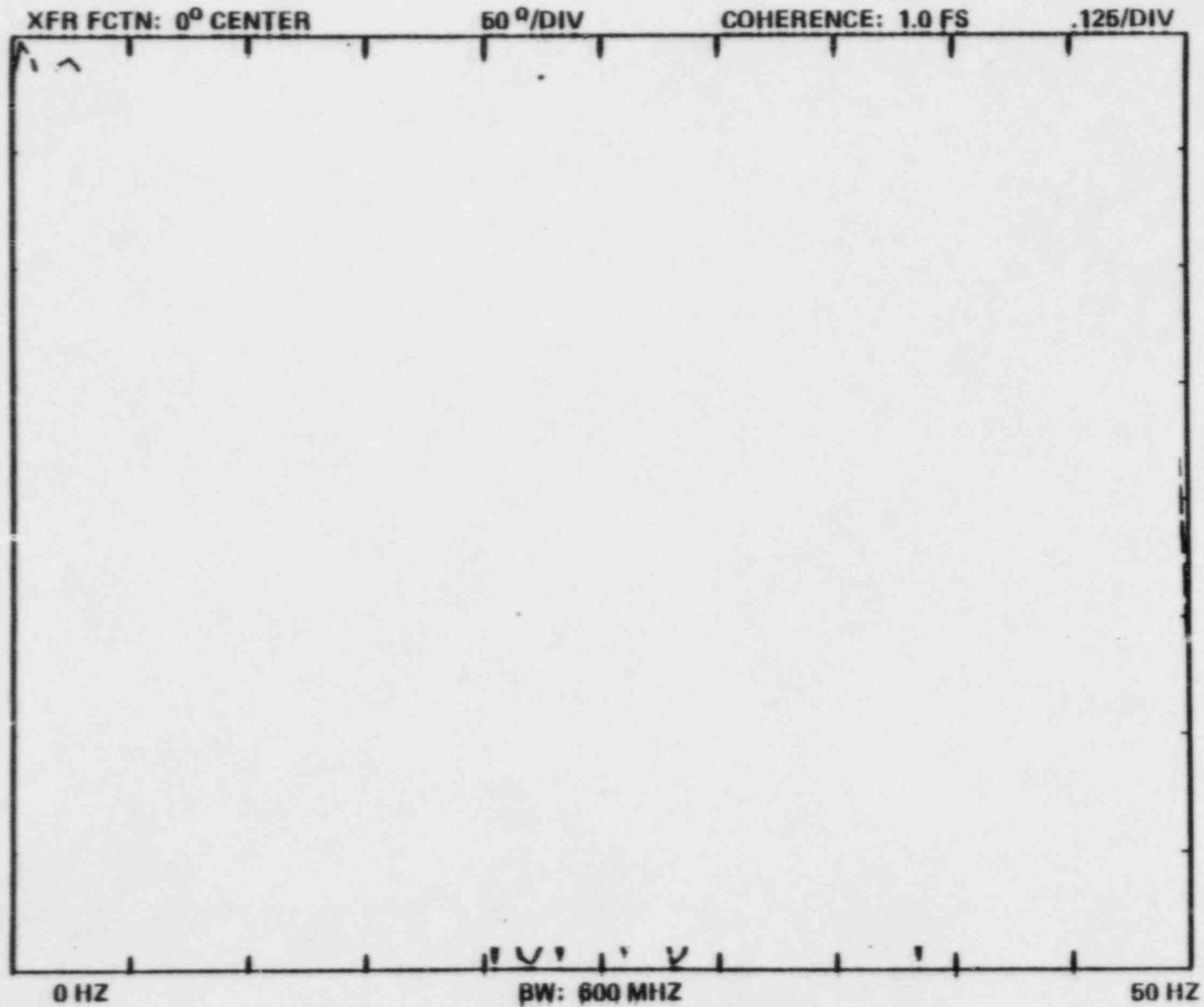


FIGURE 3.5-9  
PRESSURE PSD (P4 & P5) - PVMP 15



ANPP PRE-CRITICAL VIBRATION MONITORING PROGRAM (PVMP)  
PRESSURE TRANSDUCER P4 VS P7



3-46

FIGURE 3.5-10  
COHERENCE/PHASE (P4 & P7) - PVMP 15

ANPP PRE-CRITICAL VIBRATION MONITORING PROGRAM (PVMP)  
P4(A) VS P8 (B)

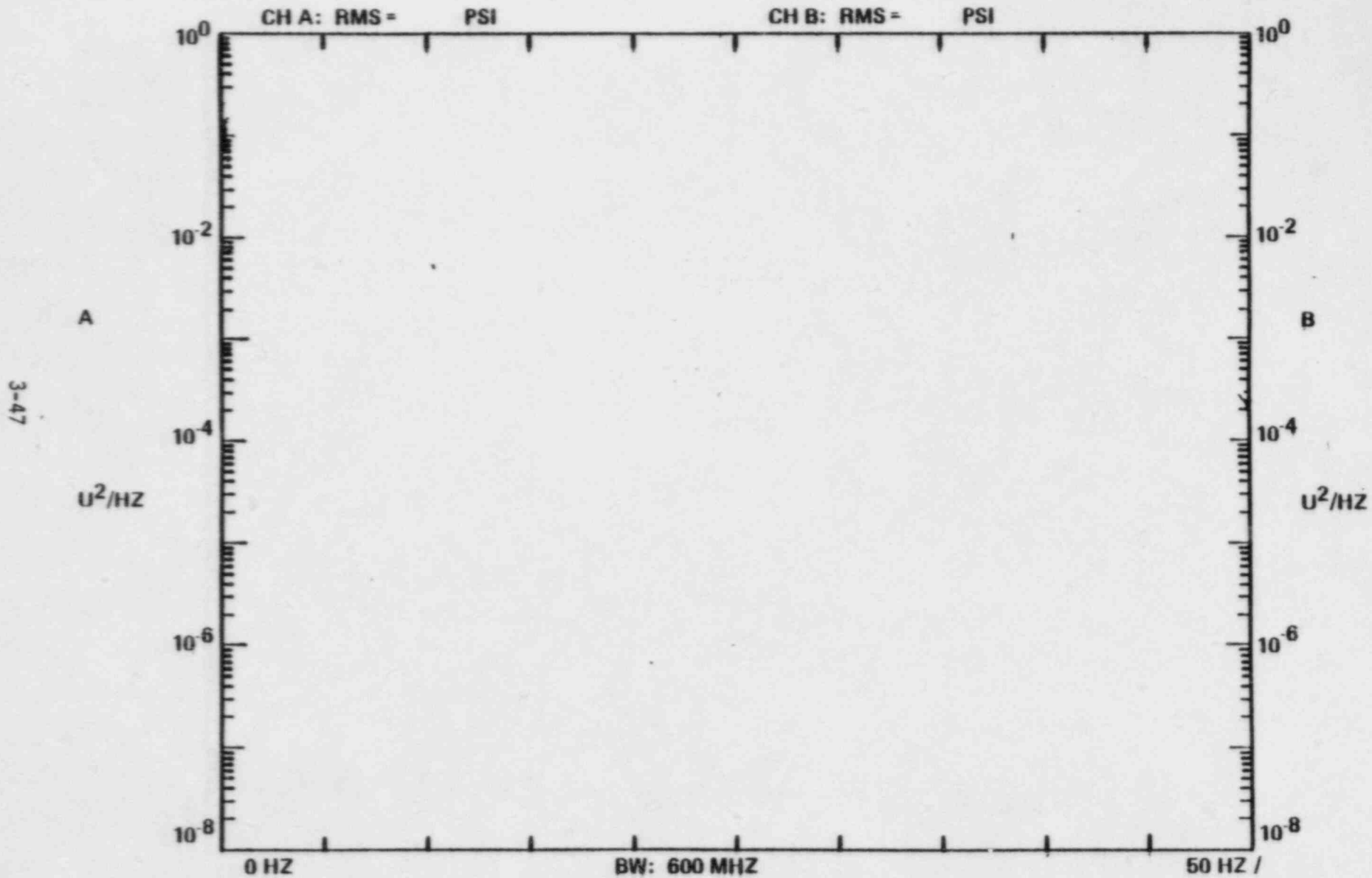
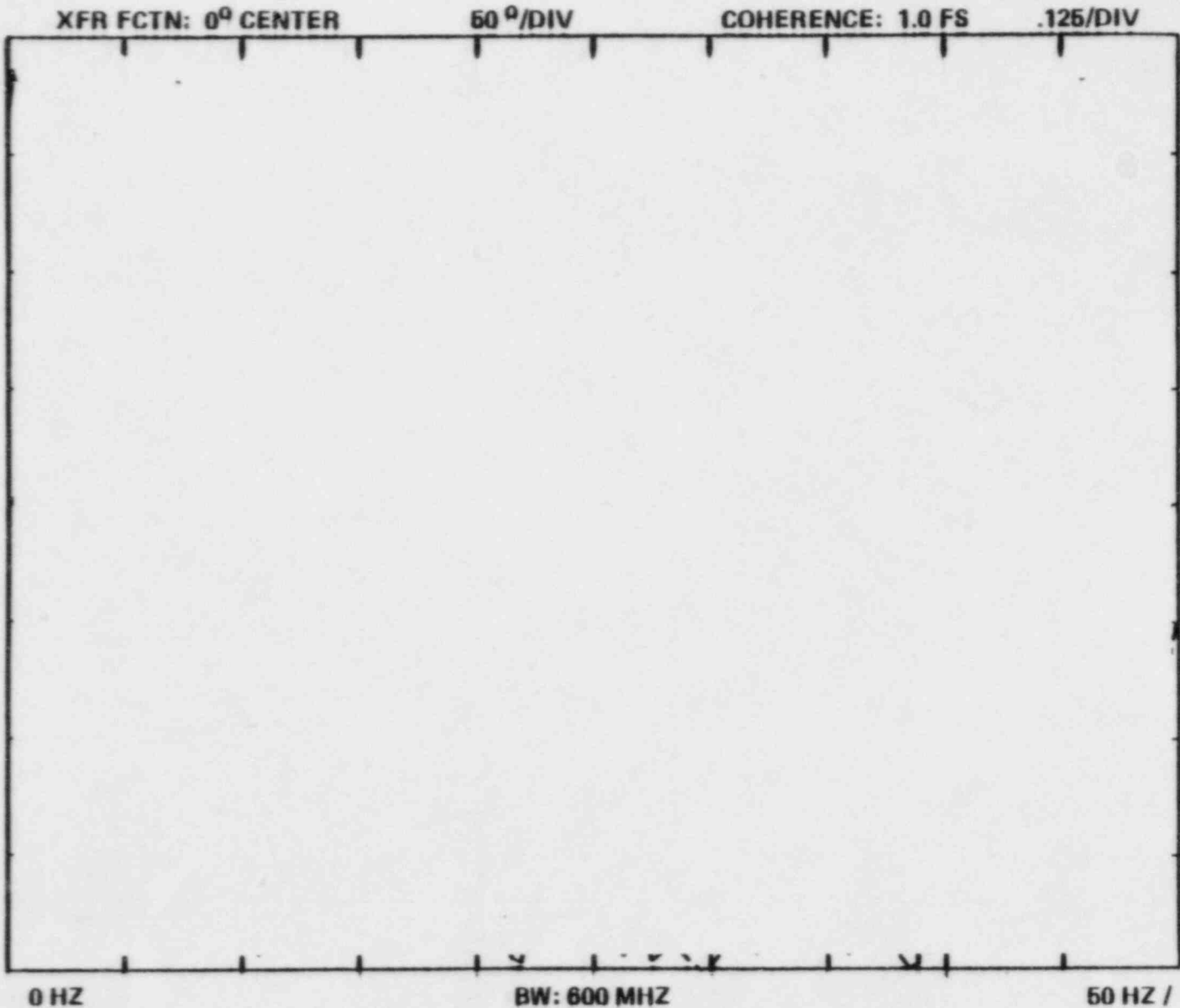


FIGURE 3.5-11  
PRESSURE PSD (P4 & P8) - PVMP 15

ANPP PRE-CRITICAL VIBRATION MONITORING PROGRAM (PVMP)  
PRESSURE TRANSDUCER P4 VS P8



3-48

FIGURE 3.5-12  
COHERENCE/PHASE (P4 & P8) - PVMP 15

SYS 80 CVAP PALO VERDE UNIT 1  
A3 120 SNBR (A) VS A4 240 SNBR (B)

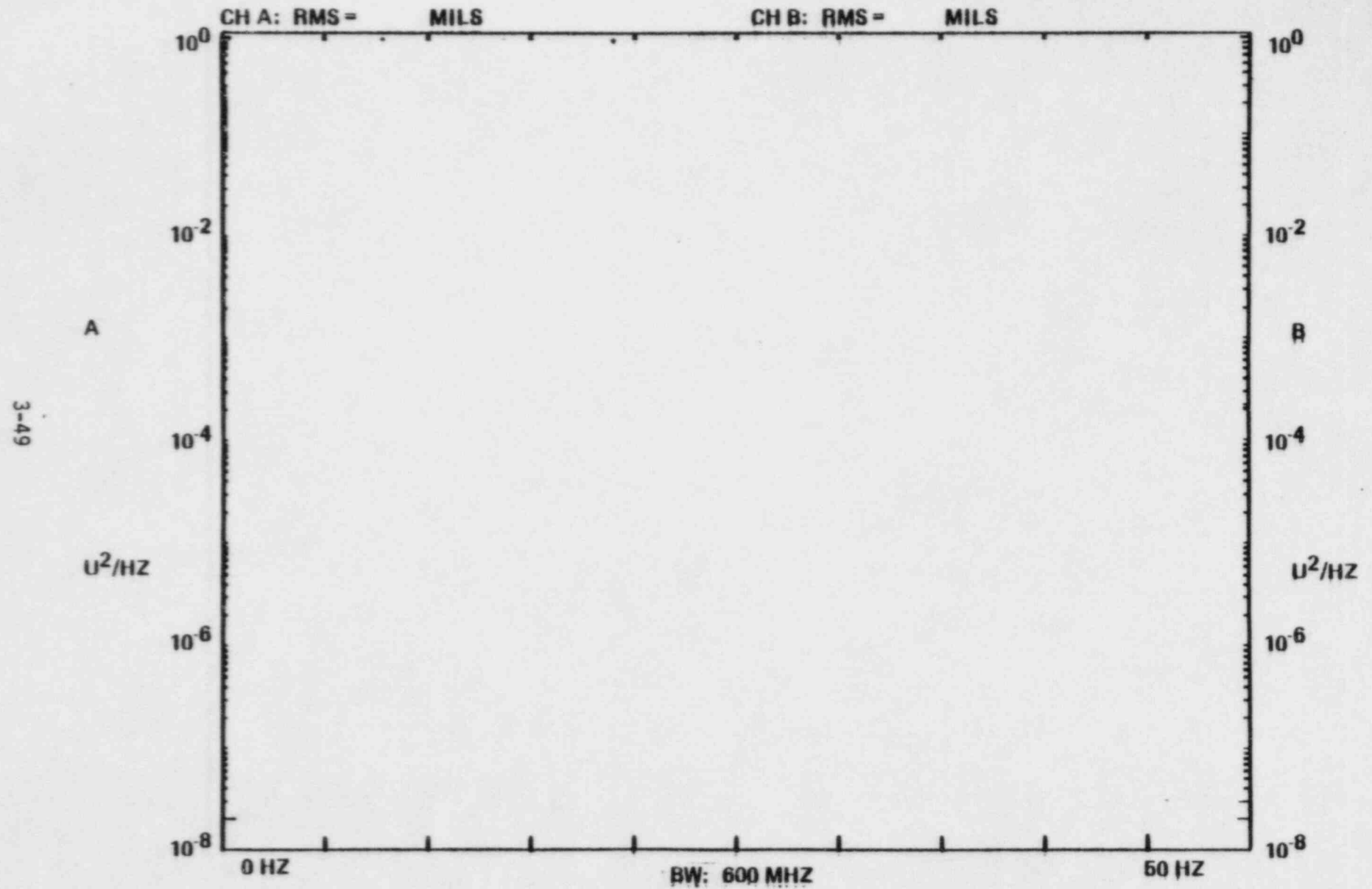


FIGURE 3.5-13  
DISPLACEMENT PSD (A3 & A4) - PVMP 1

SYS 90 CVAP PALO VERDE UNIT 1  
A3 120 SNBR VS A4 240 SNBR

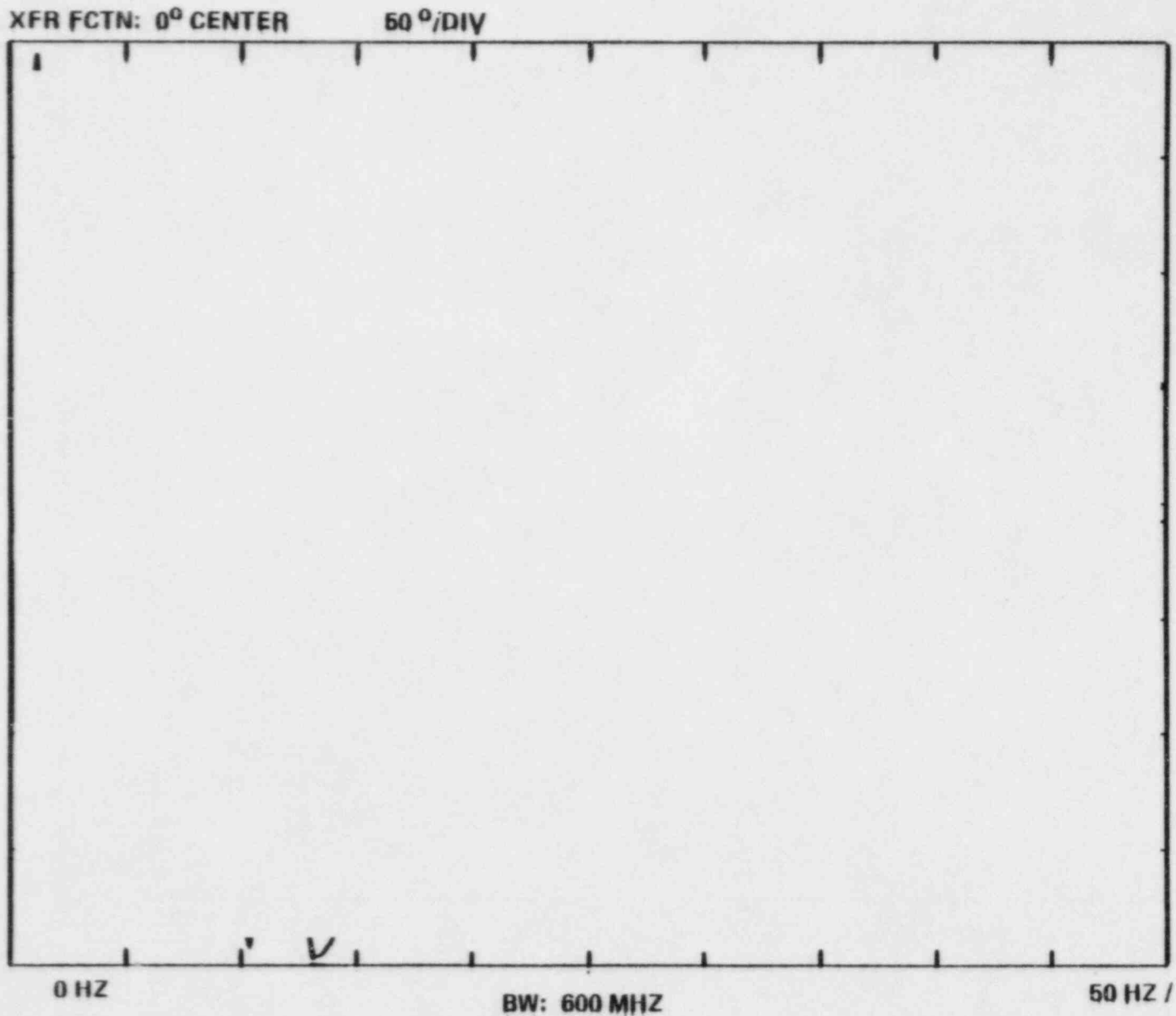
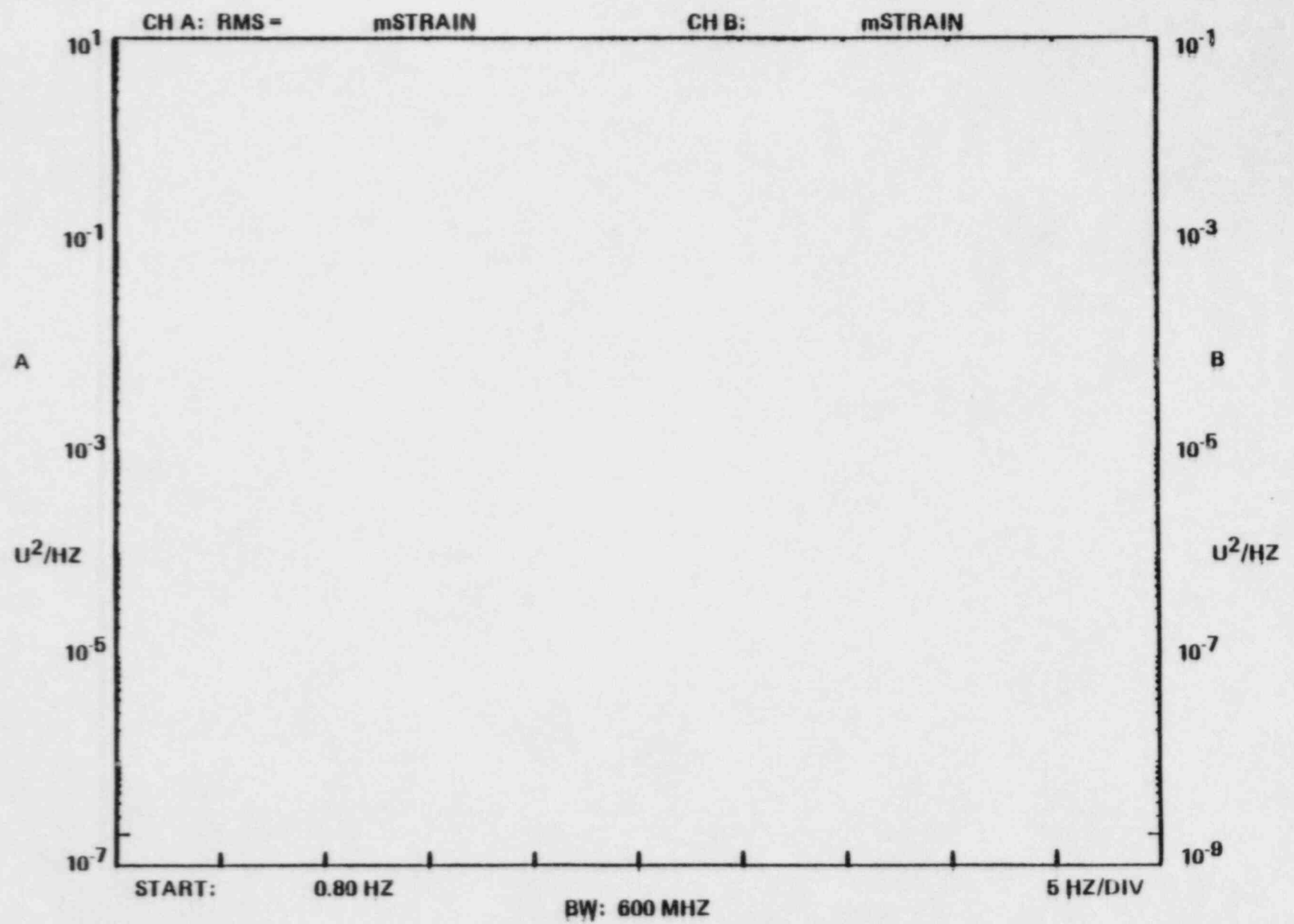


FIGURE 3.5-14  
COHERENCE/PHASE (A3 & A4) - PVMP 1

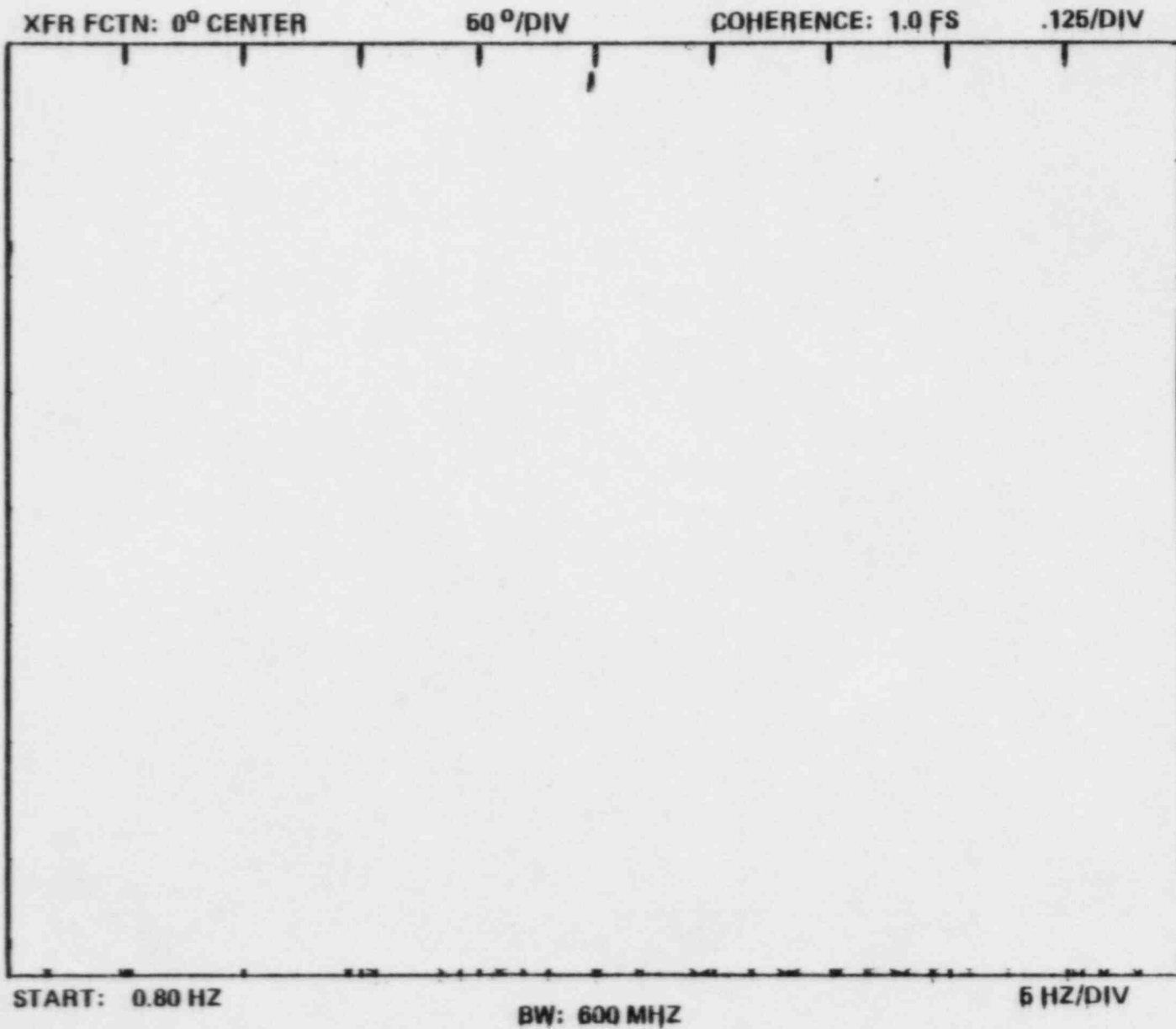
ANPP PRE-CRITICAL VIBRATION MONITORING PROGRAM (PVMP)  
S2(A) VS S6(B)



3-51

FIGURE 3.5-15  
STRAIN PSD - 0 TO 50 HZ (S2 & S6) - PVMP 15

ANPP PRE-CRITICAL VIBRATION MONITORING PROGRAM (PVMP)  
STRAIN GAUGE S2 VS S6



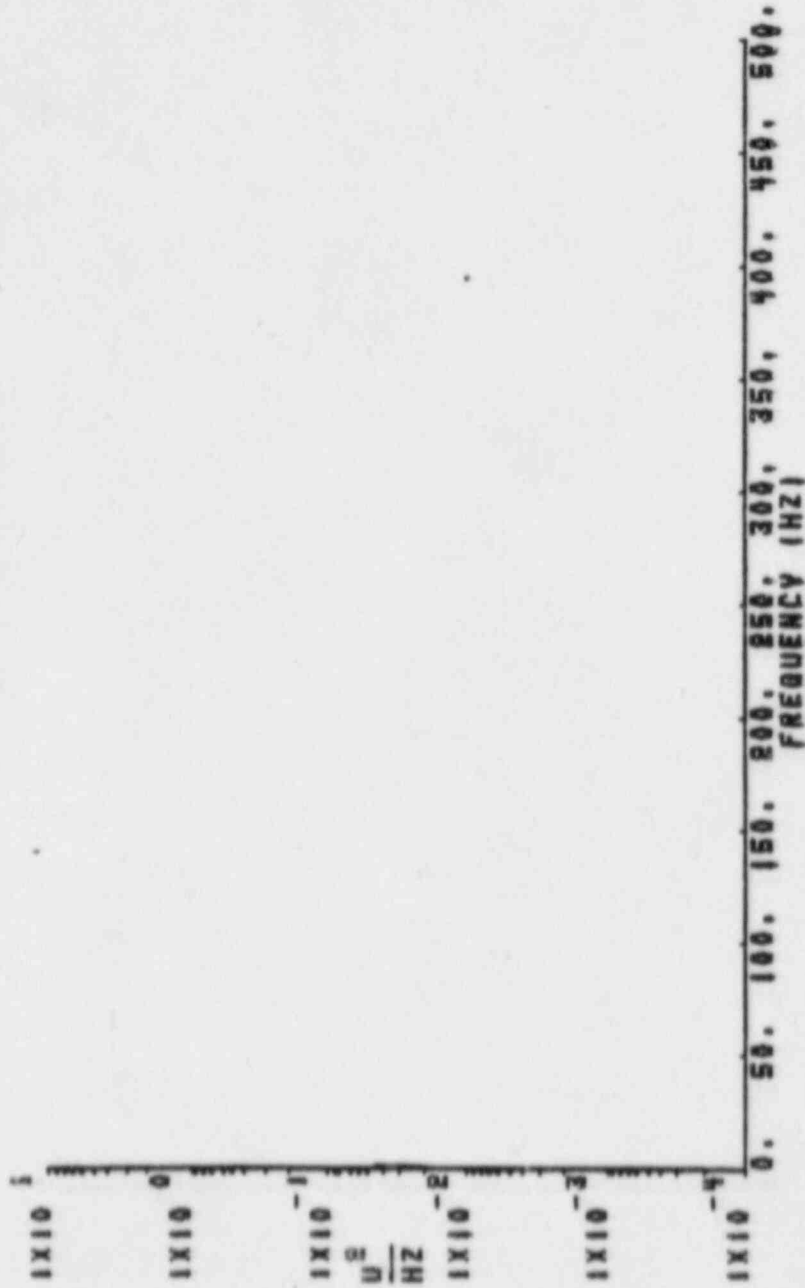
3-52

FIGURE 3.5-16  
COHERENCE/PHASE (S2 & S6) - PVMP 15





### POWER SPECTRAL DENSITY



SYSTEM 80 CMAP PALO VERDE UNIT 1  
PUMP-15

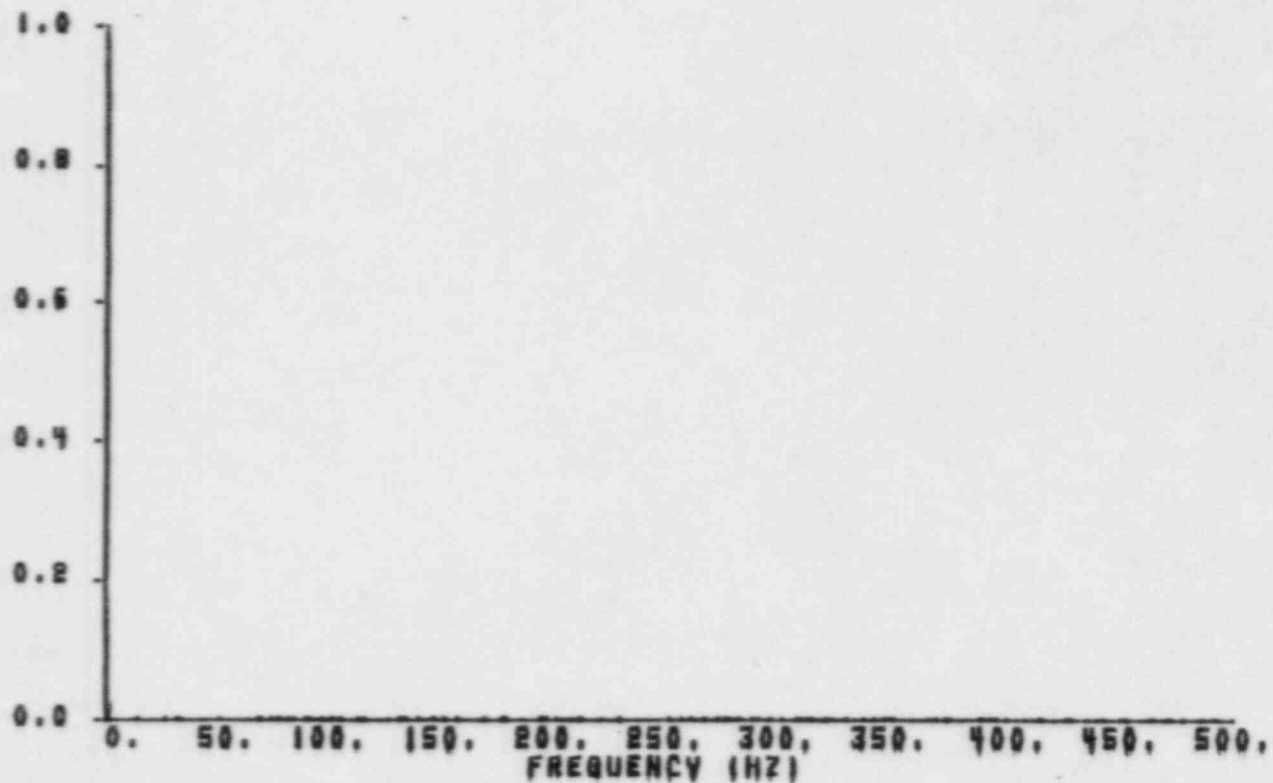
TEMP1 5.450E+02 PRESSURE1 2.250E+03 PUMPS1 1A1 0 1B1 0 2A1 0 2B1 0 88

TRANSDUCER GROUP1 STRAIN 1B1 56 100 L-1 H UNIT81 MICRO IN/IN  
SNS "

DL01PUMP15.PSB TAFE1 T-245 RUN1 27 1.562E+03 SPS BW = 2.289E+00 MDF = 100.

STRAIN PSD - 0 TO 500 HZ (S6) - PVMP 15  
FIGURE 3.5-18

COHERENCE



3-55

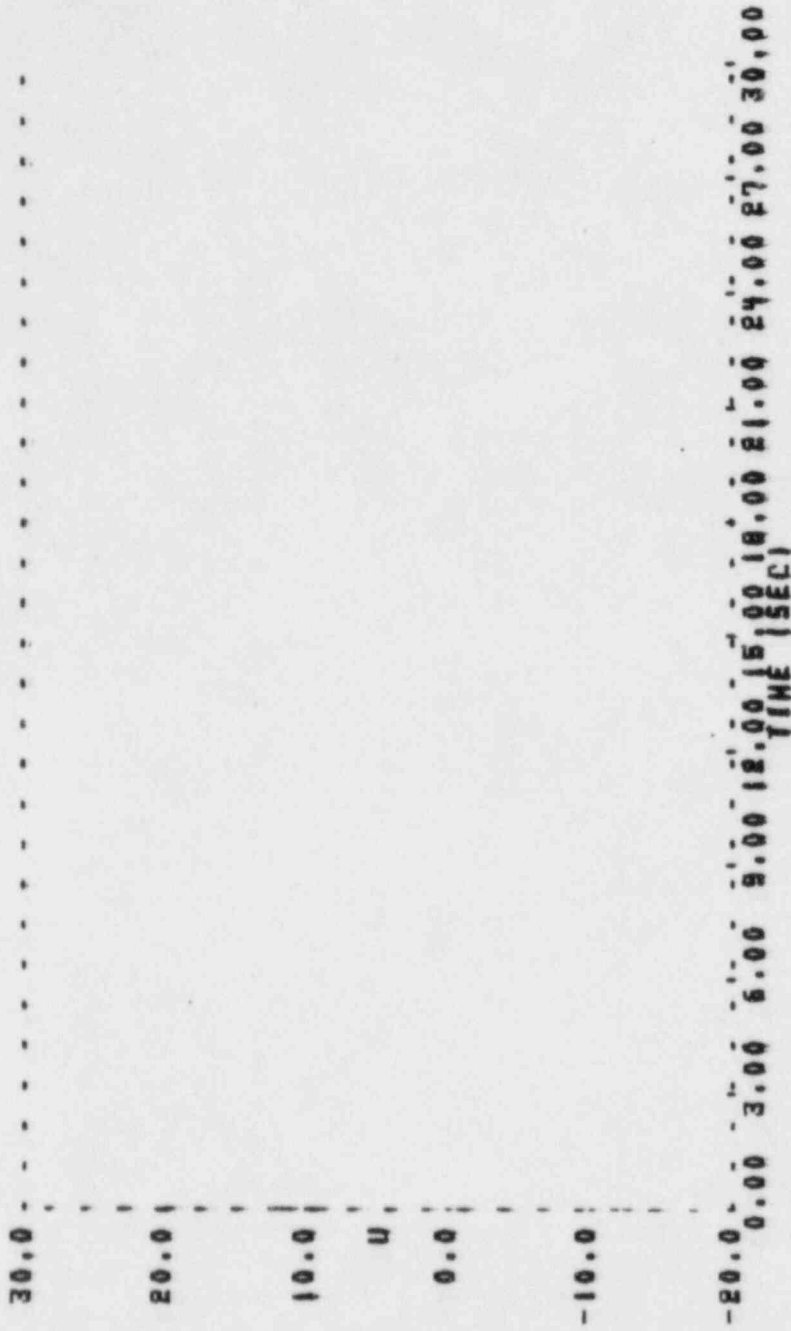
```

SYSTEM 80 CVAP PALO VERDE UNIT 1
PVMP-15
TEMP: 5.450E+02    PRESSURE: 2.250E+03    PUMPBI 1A1 0 1B1 0 2A1 0 2B1 0    SS
TRANSDUCER GROUP: STRAIN    ID1 82 180 L-1 H    UNITS: MICRO IN/IN
TRANSDUCER GROUP: STRAIN    ID1 84 180 L-1 H    UNITS: MICRO IN/IN

BL01PVMP15.PSD    TAPE: T-245    RUN: 27    1.542E+03 SPS    BW = 2.289E+00    NBF = 100.
    
```

COHERENCE - 0 TO 500 HZ (S2 & S6) - PVMP 15  
FIGURE 3.5-19

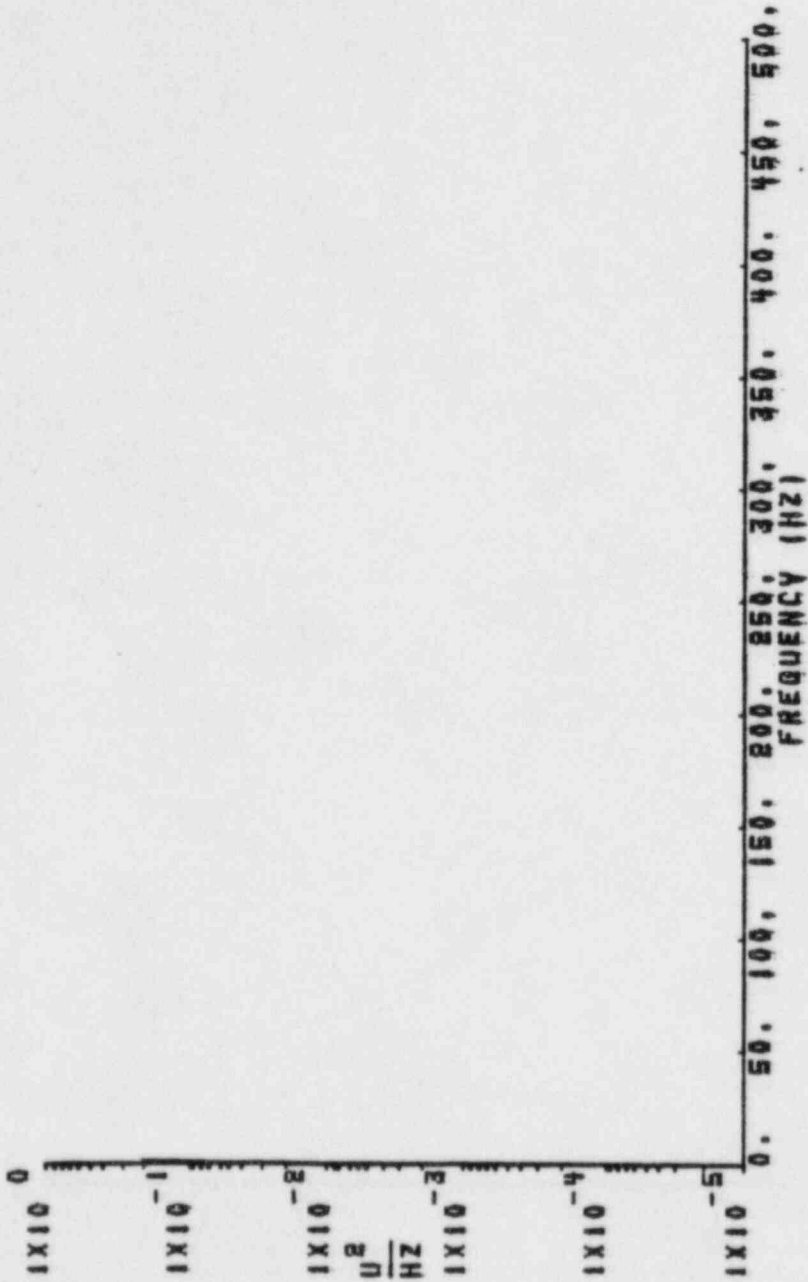
TIME HISTORY  
ENVELOPE



SYSTEM 80 CVAP FALO VERBE UNIT 1  
 FVHP-15  
 IENF1 5.650E102 PRESSURE1 2.250E103 PUMF51 1A1 0 1B1 0 2A1 0 2B1 0 TR  
 TRANSDUCER GROUP1 STRAIN IBI 55 180 1-4 A UNITS1 MICRO IN/IN  
 FVHP15.SIK IAFE1 1-245 RUN1 27 1.562E103 SFS DECIMATION1 500

TIME HISTORY - PUMP START (S5) - PVMP 15  
 FIGURE 3.5-20

# POWER SPECTRAL DENSITY



SYSTEM 80 CVAP FALD VERBE UNIT 1

FVNF-15

1ENF1 5.450E102 PRESSURE1 2.250E103 PUMPS1 1A1 0 101 0 2A1 0 2B1 0 6S

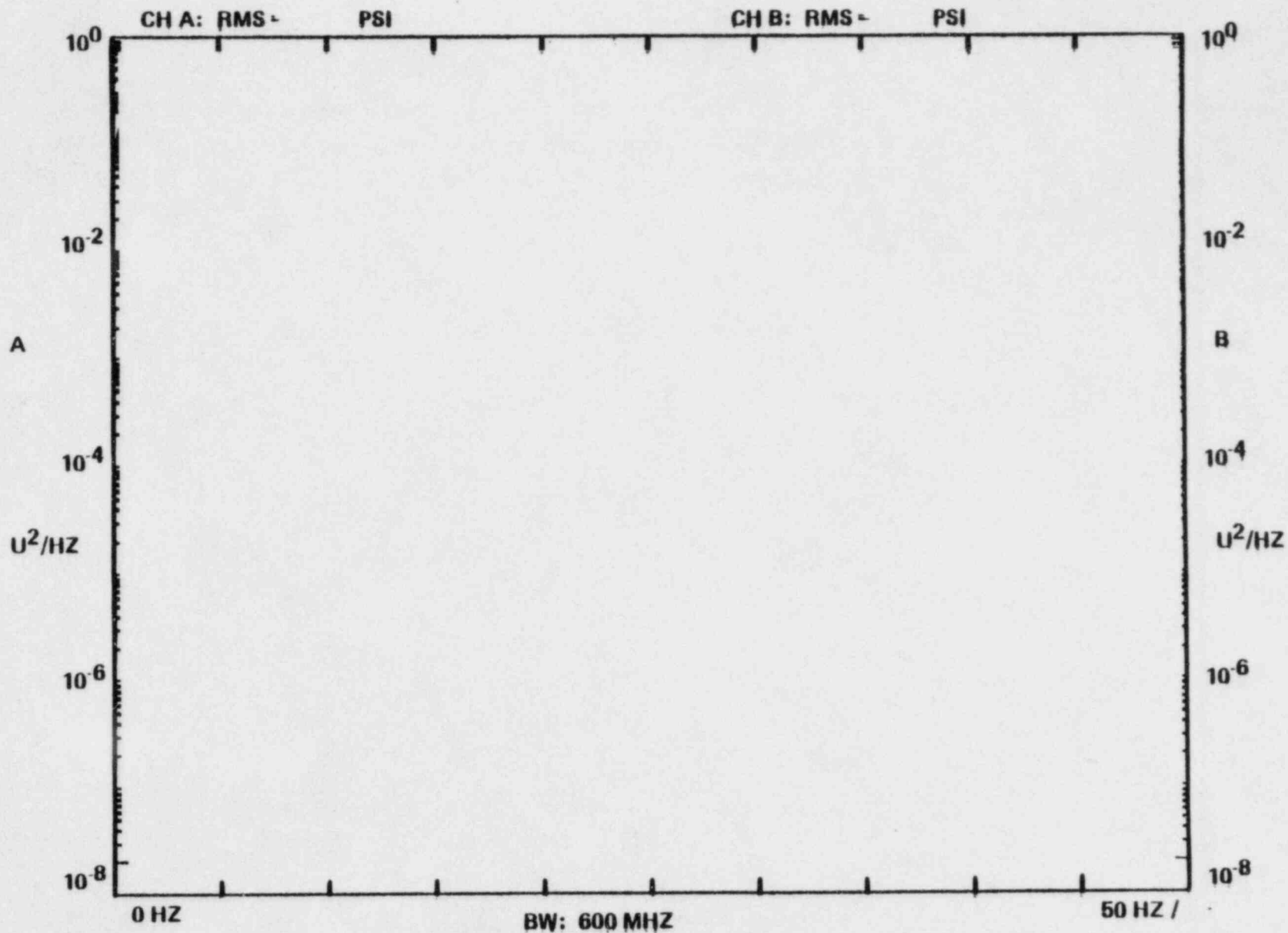
TRANSDUCER GROUP1 PRESSURE ID1 P12 TUBE 50 UNIT1B1 PSI

RMS =

DL01FVNF15.FSD TAPE1 F-245 RUN1 27 1.562E103 SPS BW = 2.289E100 NDF = 100.

PRESSURE PSD - 0 TO 500 HZ (P12) - PVMP 15  
FIGURE 3.5-21

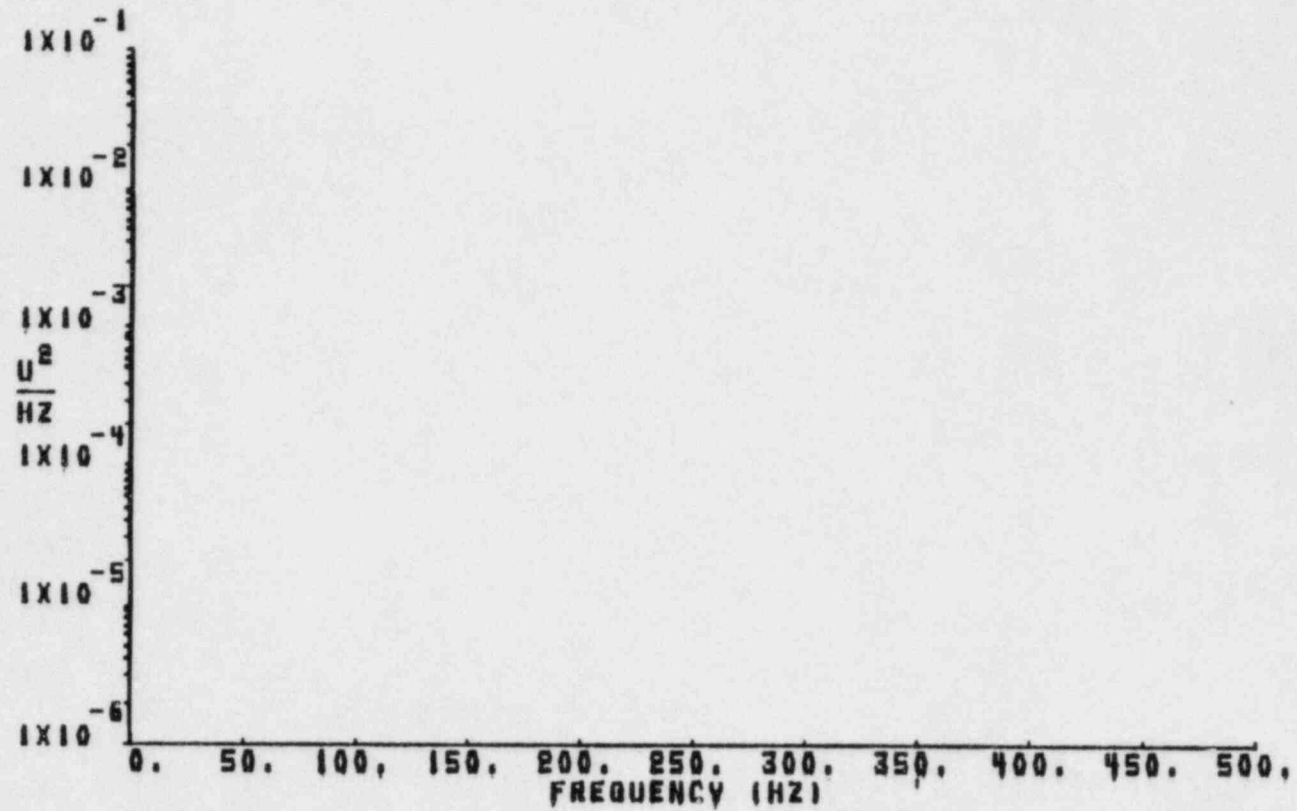
ANPP PRE-CRITICAL VIBRATION MONITORING PROGRAM (PVMP)  
P12(A) VS P13(B)



3-58

FIGURE 3.5-22  
PRESSURE PSD - 0-50 HZ (P12) - PVMP 15

## POWER SPECTRAL DENSITY



3-59

SYSTEM 80 CVAP PALO VERDE UNIT 1

PVMP-15

TEMP: 5.650E+02      PRESSURE: 2.250E+03      PUMPS: 1A 0    1B 0    2A 0    2B 0    SS

TRANSDUCER GROUP: ACCELERATION    ID: A11X LMR PLT    UNIT: 0

RHS =

DLO:PVMP15.PSD    TAPE: T-245    RUN: 27    1.562E+03 SPS    BW = 2.289E+00    NDF = 100.

ACCELERATION PSD - 0 TO 500 HZ (A11) - PVMP 15  
FIGURE 3.5-23

ANPP PRE-CRITICAL VIBRATION MONITORING PROGRAM (PVMP)  
A10X (A) VS A11X (B)

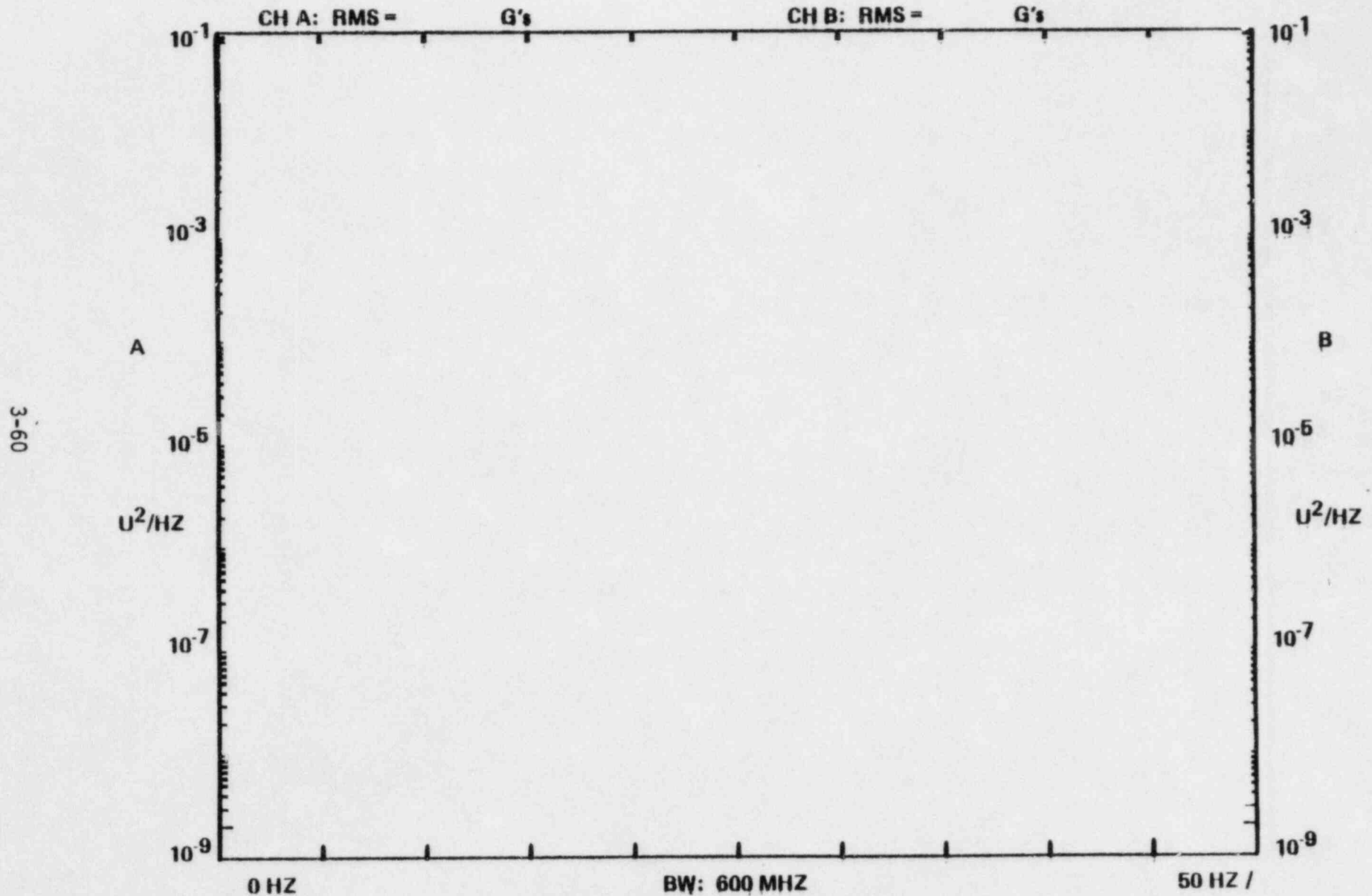
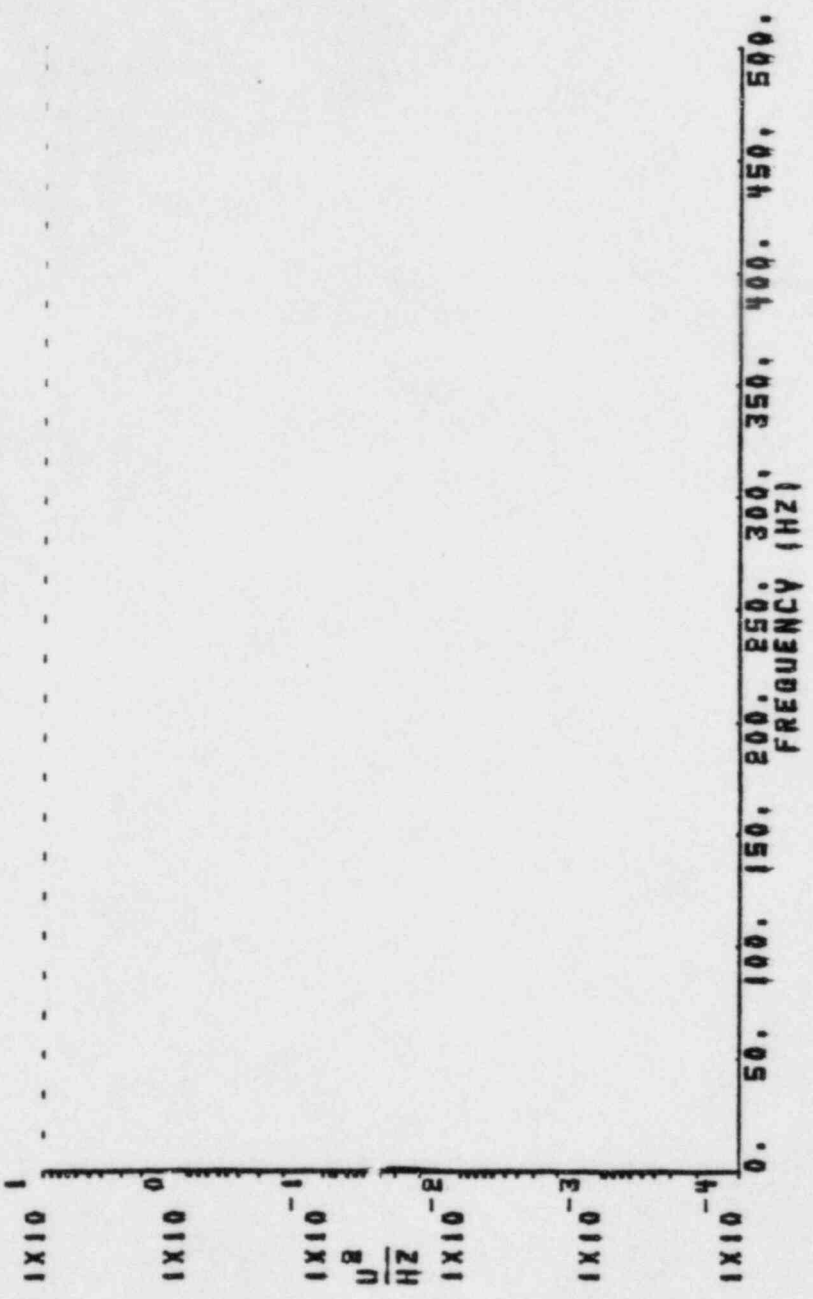


FIGURE 3.5-24  
ACCELERATION PSD - 0 TO 50 HZ (A11) - PVMP 15

POWER SPECTRAL DENSITY

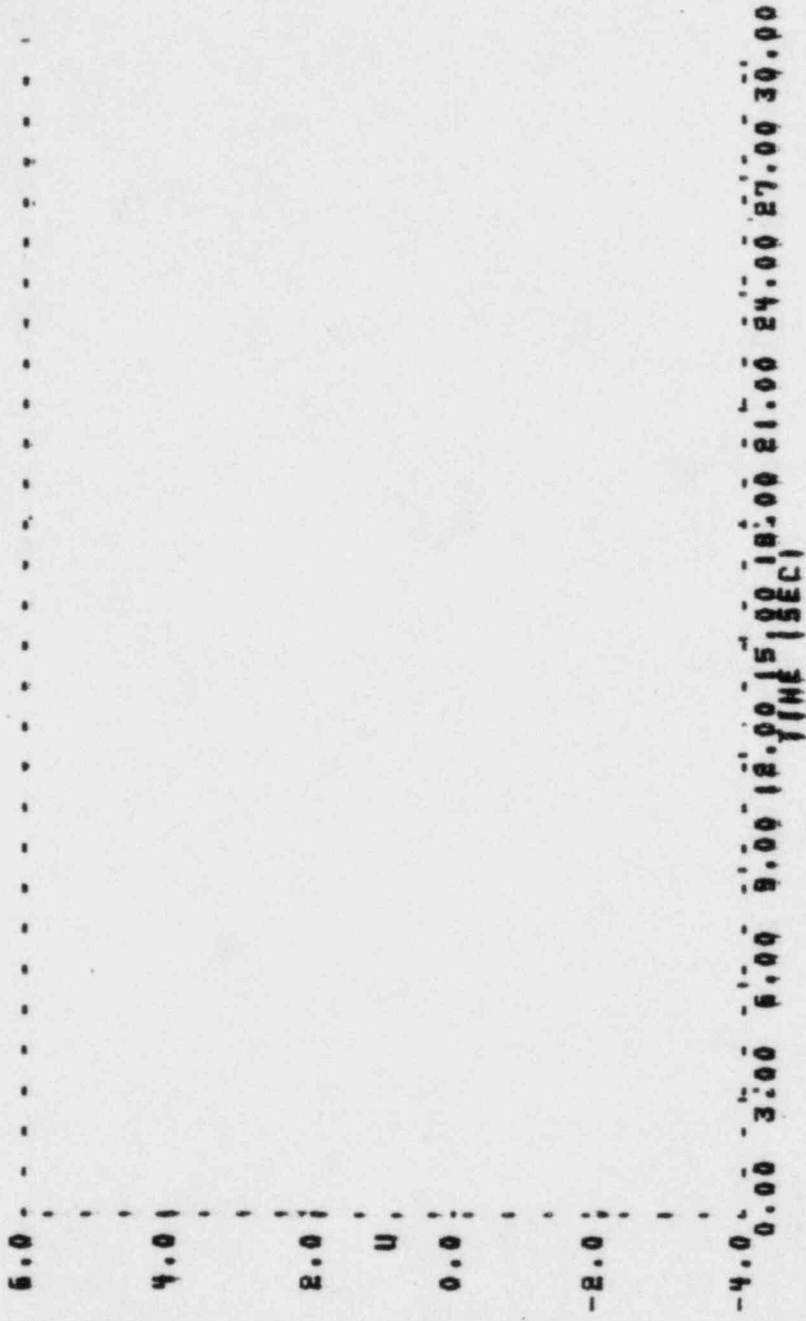


SYSTEM 80 CVAP PALO VERDE UNIT 1  
 PUMP-6  
 TEMPI 2.650E+02 PRESSURE: 3.500E+02 PUMPSI A1 0 B1 0 C1 0 D1 NO 68  
 TRANSDUCER GROUP1 STRAIN ID1 S14 TUBE 58 UNITS1 MICRO IN/IN  
 RMS =  
 D101PVPN06.FSD TAFEI T-239 KUMI 13 1.562E+03 GPS BM = 2.289E+00 NDF = 100.

STRAIN PSD - 0 TO 500 HZ (S14) - PVMP 6  
FIGURE 3.5-25



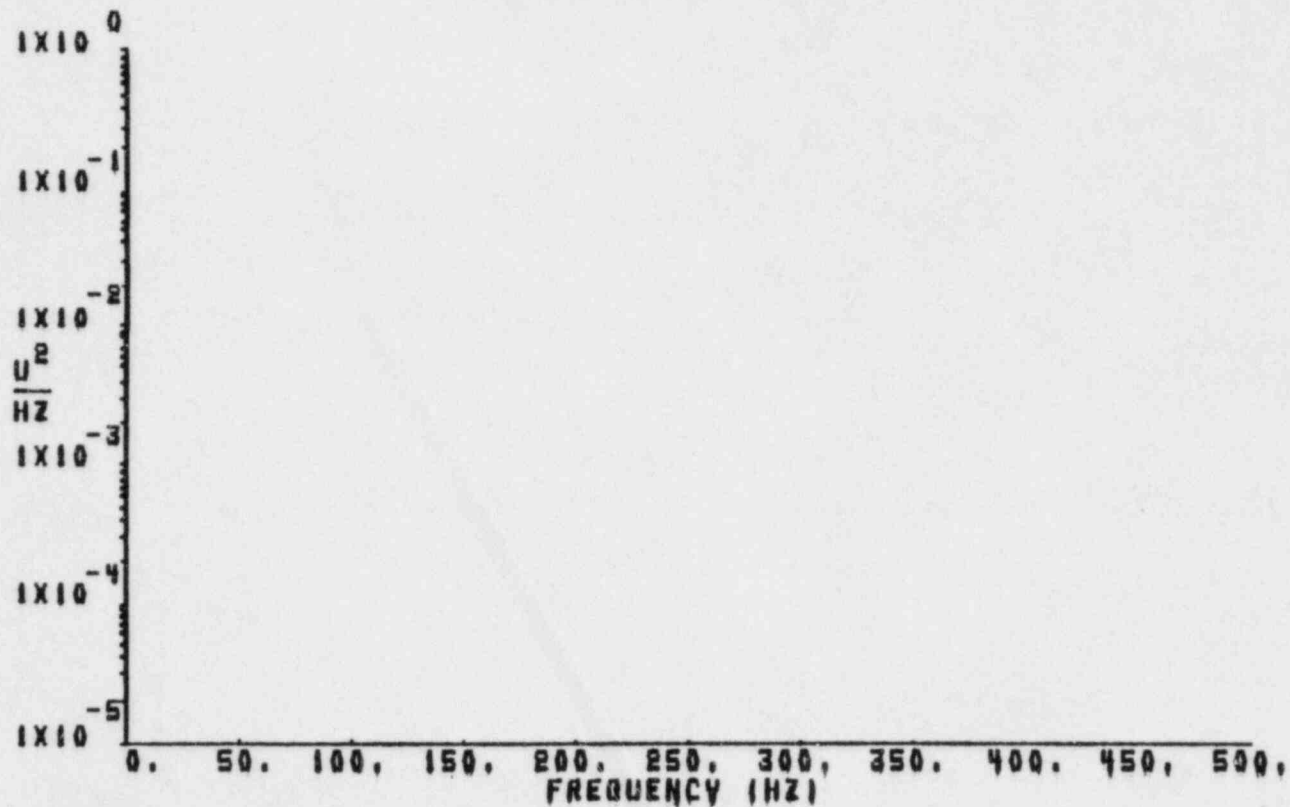
### TIME HISTORY ENVELOPE



SYSTEM 00 CVAP PALO VERDE UNIT 1  
 PVMP-15  
 TENDI 5.650E102 PRESSURE1 2.250E103 PUMPS1 1A1 0 1B1 0 2A1 0 2B1 0 TR  
 TRANSDUCER GROUP1 ACCELERATION 1B1 A11X LWR PLY UNITS1 G  
 PVMP15.BTR TAPE1 Y-245 RUN1 27 1.562E103 SPS DECIMATION1 500

TIME HISTORY - PUMP START (A11) - PVMP 15  
FIGURE 3.5-26

## POWER SPECTRAL DENSITY



3-63

SYSTEM 80 CUAP PALO VERDE UNIT 1

PVMP-15

TEMP1 5.650E+02 PRESSURE1 2.250E+03 PUMPS1 1A1 0 1B1 0 2A1 0 2B1 0 SS

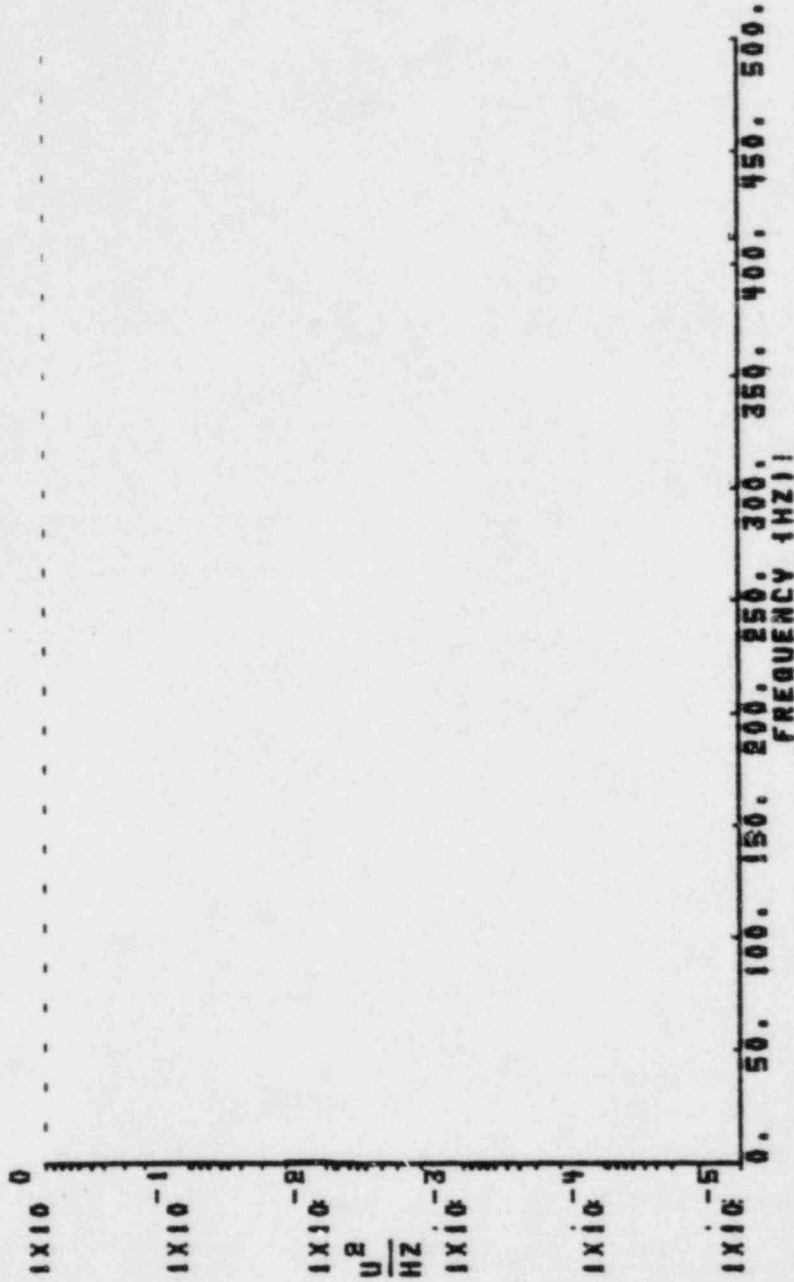
TRANSDUCER GROUP1 PRESSURE ID1 P13 UPR PLT UNIT81 P81

RHS =

DL01PVMP15.PSD TAPE1 T-245 RUN1 27 1.562E+03 8PB BW = 2.289E+00 NDF = 100.

PRESSURE PSD - 0 TO 500 HZ (P13) - PVMP 15  
FIGURE 3.5-27

POWER SPECTRAL DENSITY



SYSTEM 80 CVAP PALO VERDE UNIT 1  
PVMP-11

TEMP1 3.450E+02 PRESSURE1 2.250E+03 PUMPS1 1A1 0 1B1 NO 2A1 0 2B1 0 88

TRANSDUCER GROUP1 PRESSURE 1B1 P11 TUBE 6 UNITS1 PSI  
RMS =

DLO:PVMP11.PSD TAPE1 1-242 RUN1 20 1.562E+03 SPS BW = 2.289E+00 MDF = 100.

PRESSURE PSD - 0 TO 500 HZ (P11) - PVMP 11  
FIGURE 3.5-28

ANPP PRE-CRITICAL VIBRATION MONITORING PROGRAM (PVMP)  
A5Y

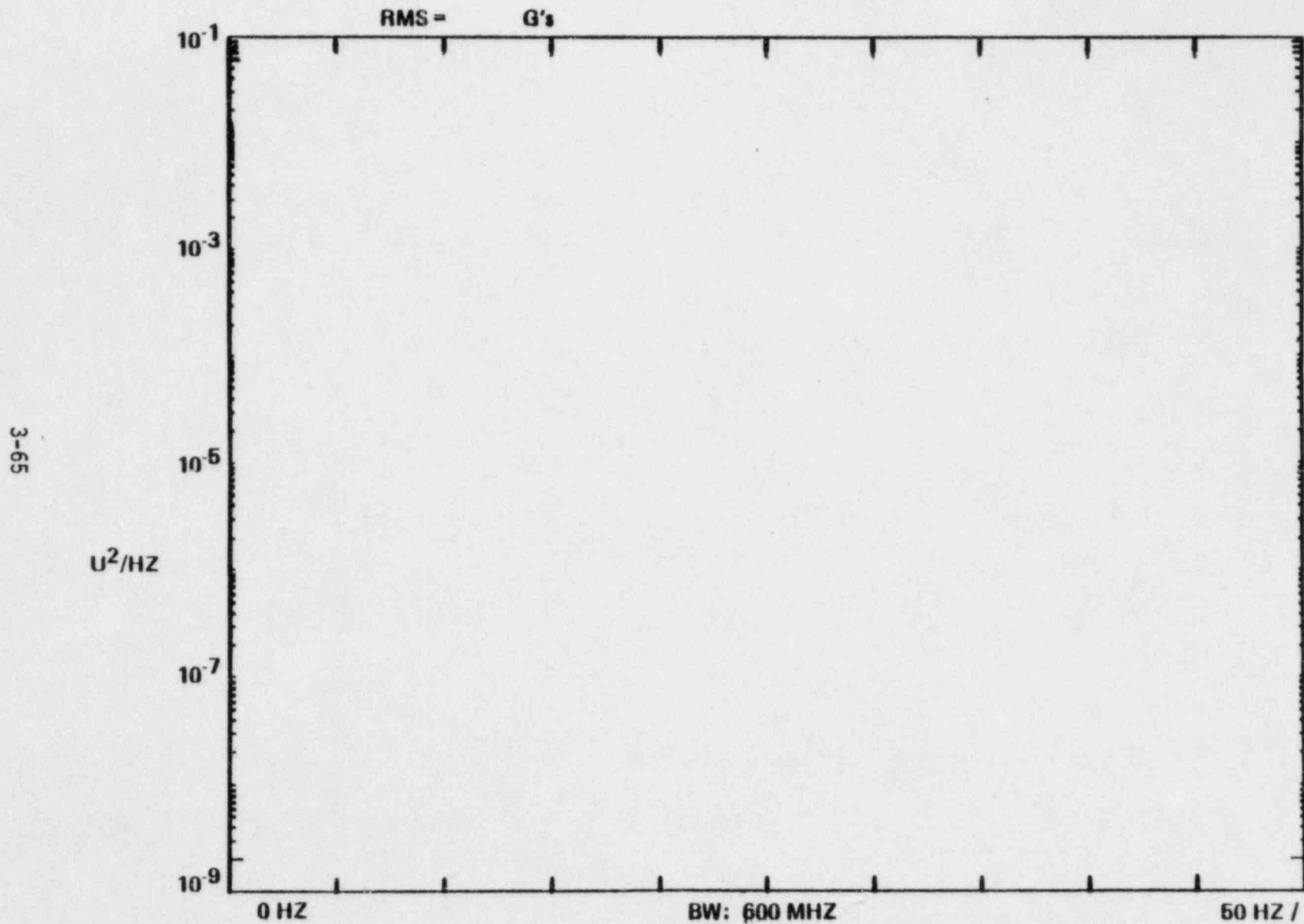
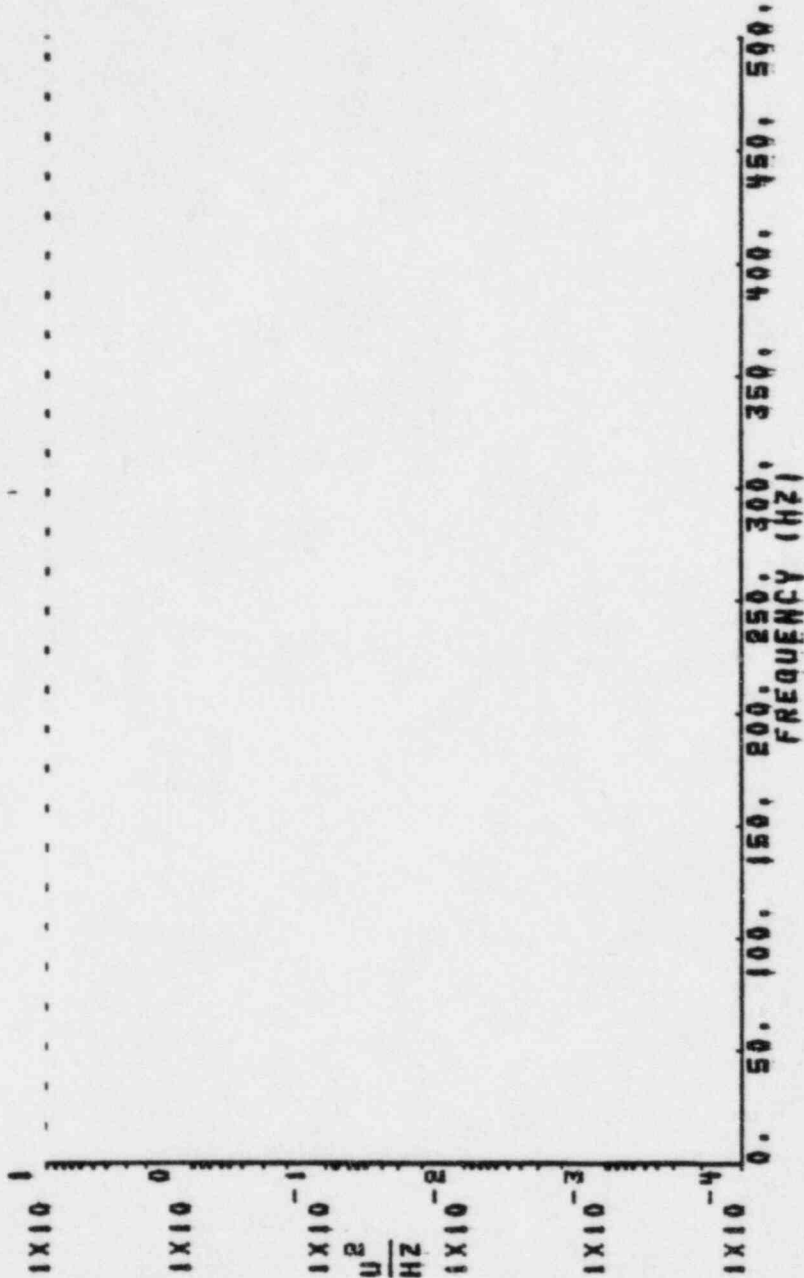


FIGURE 3.5-29  
ACCELERATION PSD - 0 TO 50 HZ (A5) - PVMP 15

POWER SPECTRAL DENSITY



SYSTEM 80 CVAP PALO VERDE UNIT 1

PUMP-15

TEMP1 5.650E+02 PRESSURE1 2.250E+03 PUMPS1 1A1 0 1B1 0 2A1 0 2B1 0 68

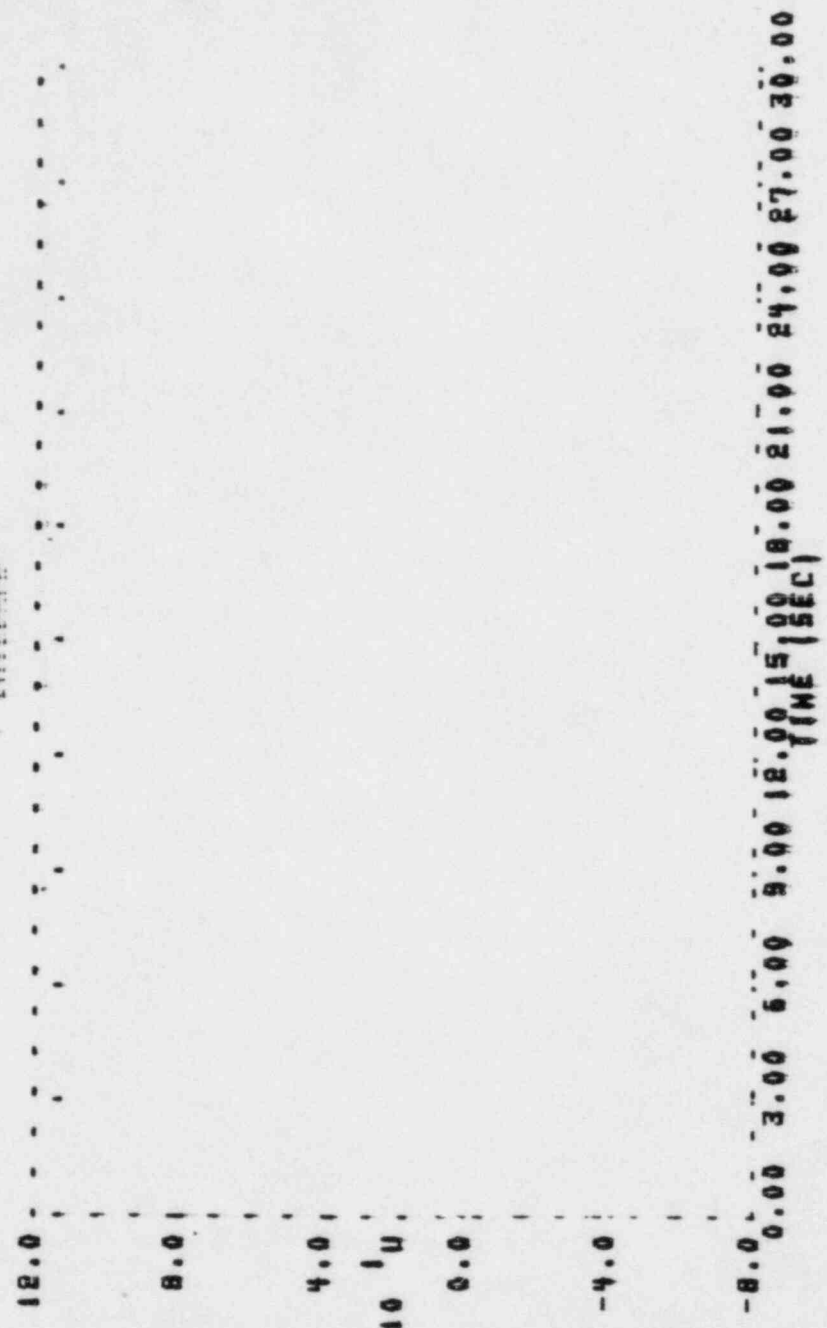
TRANSDUCER GROUP1 STRAIN ID1 811 TUBE 3 UNIT1: MICRO IN/IN

RHS =

BL01FVMP15.P6B TAP1 T-245 RUN1 27 1.562E+03 SP8 BM = 2.289E+00 MDF = 100.

STRAIN PSD - 0 TO 500 HZ (S11) - PUMP 15  
FIGURE 3.5-30

TIME HISTORY  
ENVELOPE



SYSTEM 80 CUAP PALO VERDE UNIT 1  
 PVMP-15  
 TEMPI 5.650E102 PRESSURE1 2.250E103 PUMPS1 181 0 181 0 281 0 281 0 IR  
 TRANSDUCER GROUP1 STRAIN IPI S11 TUBE 3 UNITS1 MICRO IN/IN  
 PUMF15.SIR TAPE1 1-245 RUN1 27 1.562E103 SPS DECIMATION1 500

TIME HISTORY - PUMP START (S11) - PVMP 15  
FIGURE 3.5-31

PVMP-15 4 PUMPS 565/2250  
A5X UGS TUBE 3

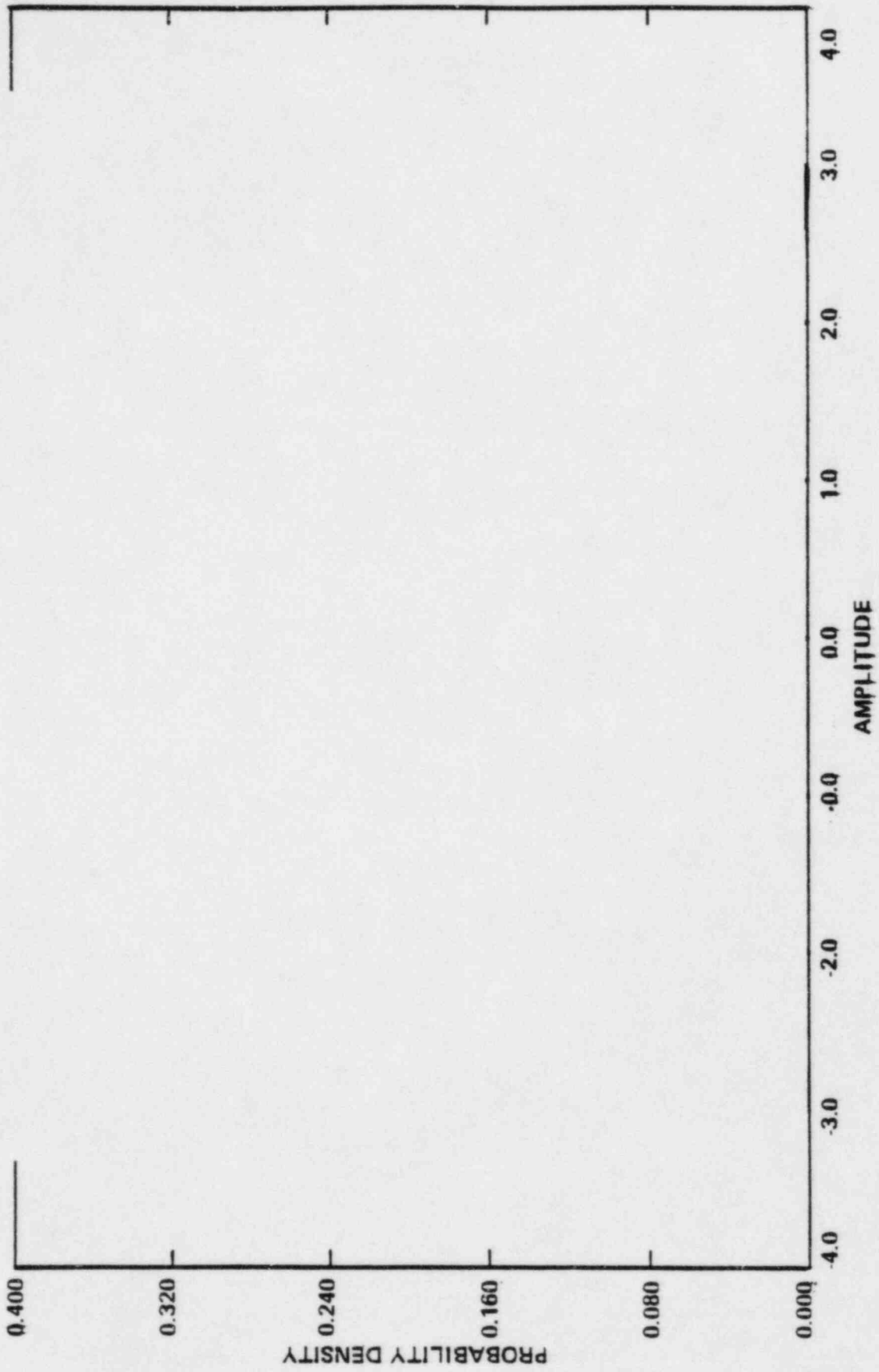


FIGURE 3.5-32  
GUIDE TUBE APD (A5) - PVMP 15

PVMP-15 4 PUMPS 665/2250  
S12 UGS TUBE 3

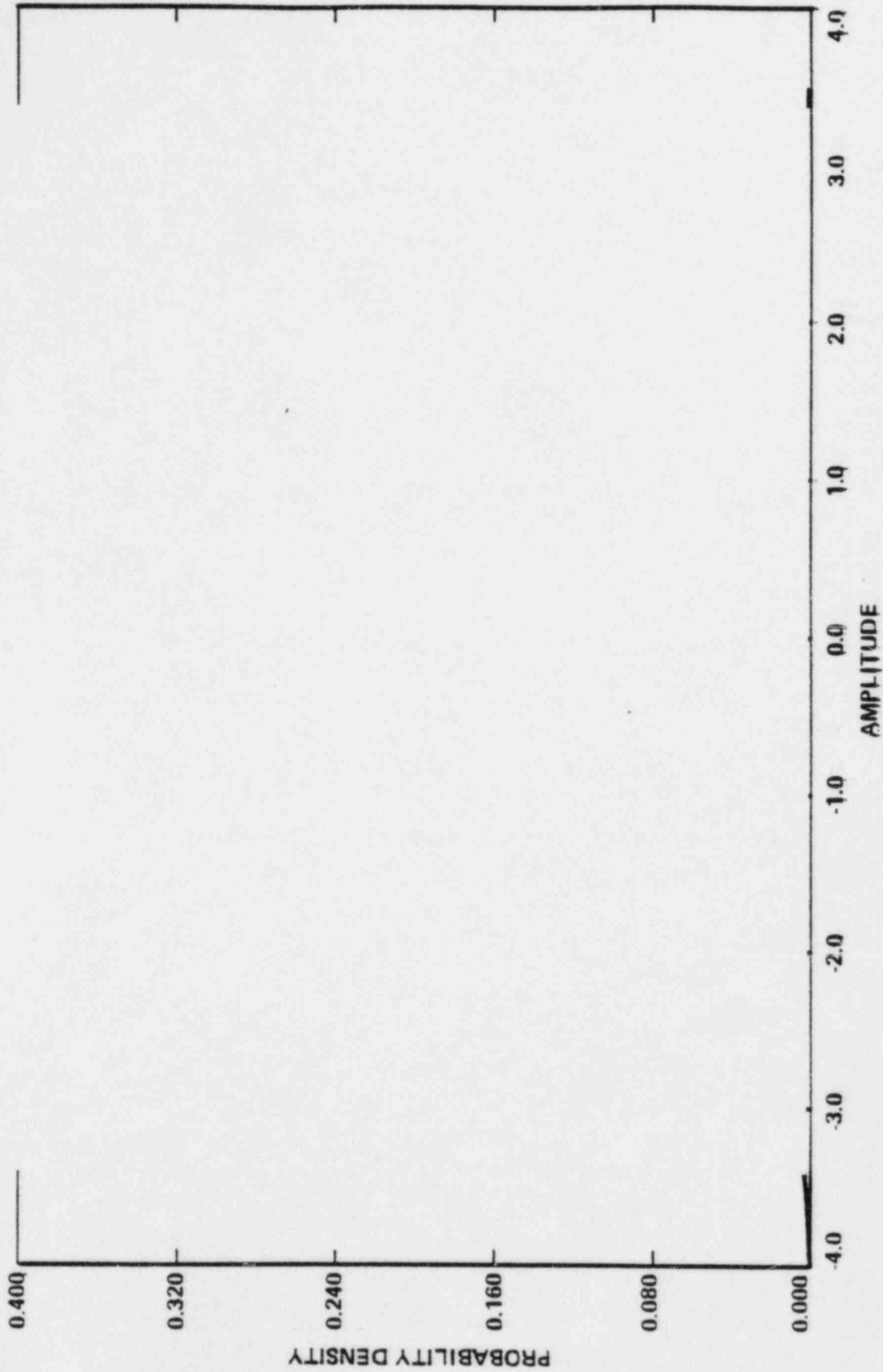


FIGURE 3.5-33  
GUIDE TUBE APD (S12) - PVMP 15



## 4.0 INSPECTION PROGRAM

### 4.1 INTRODUCTION

The Comprehensive Vibration Assessment Program (CVAP) visual inspection for the Arizona Public Service Company Palo Verde Nuclear Generating Station (PVNGS) Unit I was performed in two stages; the Baseline (pre hot functional testing) stage and the Post (post hot functional testing) stage. The Baseline stage inspection is used to establish a foundation which is compared to the results of the Post stage inspection, after the reactor vessel internals have been subjected to the requisite number of cycles of vibration. The net difference between the two stages is an indication of the performance of the reactor vessel internals.

### 4.2 DISCUSSION

The PVNGS Unit I visual inspection program is based on regulatory position C 2.3 of the NRC Regulatory Guide 1.20, Rev. 2 (Ref.1). The inspection of the reactor vessel internals prior to hot functional testing is denoted as the Baseline stage and the inspection following hot functional testing is denoted as the Post stage. The hot functional testing includes all steady-state and transient modes of operation. The Baseline stage inspection for PVNGS Unit I was completed on May 28, 1982 and the Post stage inspection was completed on August 2, 1983. Both were completed successfully without deviation from the specified conditions. NRC Regulatory Guide 1.20, Revision 2 (Reference 1) requires that the duration of hot functional testing be sufficient to ensure the critical reactor vessel internal components be subjected to at least  $10^6$  cycles of vibration. The C-E CVAP Visual Inspection Specification (Reference 6) increased that requirement to  $10^7$  cycles of vibration to establish a meaningful indication of component function. The critical reactor vessel internals component with the lowest natural frequency and thus requiring the longest hot functional testing

duration is the core support barrel, which has a natural frequency of [ ] Hz (Reference 2). The hot functional testing had a duration of 26,576 minutes of cold (less than 350°F) coolant flow and 47,950 minutes of hot (above 350°F) coolant flow for a total duration of 74,526 minutes of steady-state and transient operation. Thus, all critical reactor vessel internals components were subjected to a minimum of [ ] cycles of vibration, exceeding requirements of Reference 1 and Reference 6.

The visual inspection program consisted of the inspection and photography of all elements of the reactor vessel internals so required by regulatory position C 2.3 of Reference 1, both before and after hot functional testing. Throughout the visual inspection program, all surface orientations left (L) and right (R) are as viewed from the reactor centerline. The Baseline stage inspection of the reactor vessel internals revealed the presence of various manufacturing grinding marks and tooling marks along with assembly and disassembly scratches over most of the contact surfaces. These marks are of negligible depth, are considered normal and do not impair the function or integrity of the reactor vessel internals. All welded joints appeared secure. The Post stage inspection revealed a general discoloration of all surfaces due to coolant residue buildup and high temperature operation and specific observations that are summarized below.

#### 4.3 INSPECTION

##### 4.3.1 Reactor Vessel

The core support barrel flange seating surface has a circumferential series of uniform bands of radial scratches at the location of core support barrel contact from the relative thermal growth of the two components. The alignment key slot sides have indications of contact with the alignment keys at the following locations: 0°(R), 90°(L), 180°(R&L) and 270°(R). This corresponds to indications at

contact on the alignment keys. The outlet nozzle faces have a quantity of radial gouges caused by debris from the reactor coolant pump damage as evaluated in Reference 7. The gouges are of negligible depth and do not impair the integrity of the component. The snubber inserts have indications of contact with the core support barrel snubbers at the following locations: 0°(L), 60°(R), 120°(R&L), 180°(R&L), 240°(L) and 300°(L). This corresponds to contact indications on the core support barrel snubbers. The attachment cap screws all appear secure, though the locking pins were missing at the 180°(R) location and loosened at several other locations. The missing locking pins were replaced and the loosened ones resecured. The surveillance capsule holder assemblies, flow skirt attachment points and in-core instrumentation nozzles appeared sound and secure. Debris related to the reactor coolant pump damage (Reference 7) was discovered in the bottom head of the reactor vessel. This included four (4) segments of RCP impeller blades, one (1) two foot long sheet metal thermal sleeve and two (2) resistance temperature detector (RTD) thermowell segments. These items were subsequently removed from the vessel.

#### 4.3.2 Core Support Barrel Exterior

All circumferential girth welds appeared secure. The snubber surfaces have indications of contact corresponding to those on the reactor vessel snubbers. The outlet nozzle faces have a quantity of gouges caused by debris from the reactor coolant pump damage. The gouges have depths up to .010" and have been repaired. Also the nozzles have a 2" wide band of discoloration around the outside diameter of the surface due to the adjacent reactor vessel nozzles. All CVAP instrumentation and instrumentation conduits appeared sound and secure.

#### 4.3.3 Under the Core Support Barrel and the Alignment Keys

The flexure weld at the core support barrel and lower support structure interface appeared sound and secure. The lower support structure bottom plates, flow hole sleeving, CVAP instrumentation and instrumentation conduits, in-core instrumentation support plate, columns and nozzles all appear sound and secure. Debris related to the reactor coolant pump damage (Reference 7) was discovered on the in-core instrumentation plate. This included one (1) segment of an RCP impeller blade which was subsequently removed from the reactor vessel internals. The upper flange and reactor vessel interface surface has indications of contact corresponding to those on the reactor vessel. The alignment keys have indications of contact corresponding to those on the reactor vessel, holddown ring, upper guide structure and reactor vessel closure head key slots except where contact is indicated on the holddown ring 90°(R), the upper guide structure 0°(R) and 90°(R) and the reactor vessel closure head 180°(R) key slots. The lack of indications of contact on the alignment keys at these locations is due to the hardness of the alignment key material compared to the key slot material. The upper flange and holddown ring interface surface has a circumferential band of radial scratches from contact and differential thermal growth with the holddown ring. The transition radii under the core support barrel upper flange appear sound.

#### 4.3.4 Core Support Barrel Interior

Both sides of all the guide lug inserts have indications of contact with the upper guide structure guide lug slots. This corresponds to contact indications on the upper guide structure guide lug slots. The dowel pins, attachment cap screws, locking pins and lockwelds all appear sound and secure. The annulus between the core support barrel and the core shroud top plate is uniform with a gap of [ ] at various circumferential locations and is consistent with Baseline stage measurements. The insert pins,

locking bars and lockwelds all appear sound and secure and the fuel bundle interface surfaces are smooth. The circumferential girth welds, core shroud joints, CVAP instrumentation and instrumentation conduits all appear sound and secure.

#### 4.3.5 Under the Upper Guide Structure

The tube sheet tubes extending below the fuel alignment plate, the fuel alignment plate flow hole sleeving and the flow hole sleeving plugs all appear sound and secure.

#### 4.3.6 Upper Guide Structure Exterior

The guide lug slots have indications of contact corresponding to those on the guide lug inserts. The alignment key slots have indications of contact with the alignment keys at the following locations: 0°(R), 90°(L) and 270°(R). This corresponds to indications of contact on the alignment keys except at the 0°(R) and 90°(R) where the alignment keys have no indications of contact. The holddown ring has uniform gaps and concentricity with the alignment key slots. The stack-up assembly dimensions taken of the core support barrel, holddown ring and upper guide structure; relative to the reactor vessel is uniform, with a height of [ ] at various circumferential locations. This is somewhat less than measurements taken during the Baseline stage, due to the seating-in of the surfaces during hot functional testing, but indicate that the holddown ring exerts sufficient force on the reactor vessel internals to retain them during operation. The CEA shroud assembly tie rod locking strap welds appeared sound and secure. Cracks were noted in seven (7) CEA shroud tubes at locations on the tubes adjacent to the extension shaft guide welds. The above noted damage to the CEA shroud assembly was evaluated in Reference 8, resulting in modifications to the reactor vessel internals, a demonstration test, an analysis program and a vibration measurement program being performed along with a visual inspection program. The upper flange

circumferential girth weld and the tube sheet tubes appeared sound and secure. The upper flange and holddown ring interface has a circumferential band of radial scratches from the holddown ring due to differential thermal growth and a rotation of the holddown ring during reactor vessel closure head tensioning. The upper flange and reactor vessel closure head interface has indications of contact with the closure head. The CVAP instrumentation, instrumentation conduit and covers appeared sound and secure except for one (1) broken and two (2) missing locking pins at tube spring mount assemblies of two (2) vertical conduits, several loosened bolts at the brackets of the horizontal conduit and a missing segment of a tube clip on the horizontal conduit around the outside of the upper guide structure. Debris from this damage was located on the top surface of the upper guide structure support plate and was subsequently removed from the reactor vessel internals. The CVAP instrumentation support stalk assemblies, support stalk legs, fasteners and lockwelds all appeared sound and secure.

#### 4.3.7 Holddown Ring

The holddown ring and core support barrel flange interface surface has indications of contact corresponding to those on the core support barrel flange. The holddown ring and upper guide structure flange interface surface has indications of contact corresponding to those on the upper guide structure flange. The alignment key slots have indications of contact with the alignment keys at the following locations: 90°(L&R) and 270°(R). This corresponds to indications of contact on the alignment keys except at 90°(R) where the alignment key has no indications of contact.

#### 4.3.8 Reactor Vessel Closure Head

The alignment key slots have indications of contact with the alignment keys on both sides of all alignment key slots. This corresponds to indications of contact on the alignment keys except

at 180°(L) where the alignment key has no indications of contact. The reactor vessel closure head and upper guide structure interface has indications of contact corresponding to those on the upper guide structure.

#### 4.4

#### SUMMARY

The visual inspection program was performed to meet the requirements of regulatory position C 2.3 of NRC Regulatory Guide 1.20, Revision 2 (Reference 1). The Baseline stage was completed on May 28, 1982 and established a foundation on which to compare the results of the Post stage, which was completed on August 2, 1983 after the reactor vessel internals were subjected to approximately [ ] cycles of hot functional testing vibration which exceeds the required number of cycles of vibration. The results of the visual inspection are presented in the Reference 6 Combustion Engineering (C-E) Specification which includes photographic documentation books. Reference 10 contains an evaluation of the data presented in the Reference 6 specification and is the Final Report on the Visual Inspection Phase.

The visual inspection program consisted of the inspection of all major load bearing elements, restraint elements, locking components and contact surfaces within the reactor vessel internals. Also the reactor vessel internals were inspected for the presence of loose parts or foreign matter. A comparison of the Baseline stage surface conditions with the Post stage surface conditions indicated that with the exception of damage to the CEA shroud and damage and debris from the reactor coolant pumps, no abnormal flow induced vibration had occurred and that no reduction in the structural integrity of the reactor vessel internals, closure head or reactor vessel had occurred. There were indications of normal amounts of relative thermal growth between the reactor vessel internals and the reactor vessel at the flange surfaces and there were indications of contact between surfaces at the snubbers, guide lugs and alignment keys.

This contact between surface is considered normal, with little wear indicated. All welded joints, threaded fasteners and locking mechanisms appeared secure except for two (2) missing locking pins on the reactor vessel snubber inserts along with several loosened locking pins. These were replaced or resecured. The socket head cap screws being locked at these locations had not loosened. Other items noted during the comparison of the Baseline stage and Post Stage results were the presence of gouges in the core support barrel outlet nozzles caused by debris from the reactor coolant pump damage, which were repaired. Along with this, reactor coolant pump debris was found in the reactor vessel and subsequently removed. For further information related to the reactor coolant pump damage, Reference 7 should be consulted. Also noted was damage to temporary CVAP instrumentation conduit, all of which was removed from the reactor vessel internals as previously scheduled.

Damage to the CEA shroud was evaluated and modifications were made to the reactor vessel internals to maintain the structural adequacy of the shroud. A Baseline stage visual inspection was performed on the modified CEA shroud, followed by a Demonstration Test to subject the modified reactor vessel internals to cycles of vibration, along with a vibration measurement program and an analysis program. The results of a Post stage visual inspection revealed no evidence of unacceptable motion, excessive or undue wear or deviation from the predicted results of the analysis program. For further information related to the CEA shroud damage, reactor vessel internals modification, Demonstration Test, analysis program, vibration measurement program or visual inspection program results, Reference 8 should be consulted.

The stack-up assembly dimensions taken of the core support barrel, holddown ring and upper guide structure; relative to the reactor vessel indicate that the holddown ring exerts sufficient force on the reactor vessel internals to retain them during operation.



## 5.0 EVALUATION PROGRAM

The Evaluation Program includes a critical review and analysis of the data obtained in both the Measurement and Inspection programs and comparison of these data with predictions of the Analysis program. This evaluation includes an assessment of the methods used to predict the response of the internals to dynamic forces and the resulting margins of safety.

### 5.1 INTRODUCTION

The predicted and measured quantities which are compared and evaluated in this program may be grouped in three categories: forcing functions, structural characteristics, and dynamic response. The forcing functions of interest are hydraulic in nature and contain both periodic and random characteristics. The measurement of the forcing functions is done using pressure transducers. Natural frequencies and modeshapes are the quantities of concern in the area of structural characteristics. These items are measured using both strain gages and accelerometers. Dynamic response refers to the strains and displacements which occur in the structure as a result of the hydraulic loading. The responses are measured using strain gages and accelerometers.

### 5.2 COMPARISON OF PREDICTIONS AND MEASURED DATA

#### 5.2.1 Core Support Barrel

Knowledge of the acoustic fluctuating pressure exiting the reactor coolant pumps is of importance in evaluating the response of all the reactor internals. Pressure transducers P1, P2 and P9 were specifically located in front of the inlet pipe/reactor vessel interface to monitor these deterministic acoustic pulsations which occur at the pump rotor frequency of 20 HZ, its harmonic of 40 HZ, the blade passing frequency of 120 HZ and its harmonic of 240 HZ.

The predicted peak inlet pressures are given in Table 2.2-1 and the RMS measured values are found for P2 in Table 3.5-4. Multiplying the measured RMS values by  $\sqrt{2}$  yields peak values. Comparison of measured and predicted peak values shows good order of magnitude agreement. Since Table 2.2-1 assumes ideal pump phasing it is an upper bound on the pump pulsations.

Table 3.5-4 and Figures 3.5-1 to 3.5-5 show the existence of higher harmonics of the blade passing frequency at 360 HZ and 480 HZ. These were not predicted in the analysis phase. These forcing frequencies of 360 HZ and 480 HZ will be addressed in Section 5.3.

The pump pulsation pressures acting on the CSB are dependent on the inlet pressures, the reactor vessel/CSB annulus and end conditions of closed end at the top of the annulus and open end at the bottom. The resulting pressure distribution is verified based on pressure transducers P1 thru P8. The axial pressure distribution is in good agreement compared to that which was predicted in Figure 2.2-2. This axial distribution does not vary much with temperature or pump combination.

The predicted random hydraulic forcing function on the core support barrel was developed from semi-empirical methods. An analytical expression was developed to define the turbulent pressure fluctuation for fully developed flow. Based on the results of scale model testing, the expression was modified to account for the fact that the flow in the downcomer is not fully developed.

This semi-empirical relationship was used to provide best estimate predictions for the random pressure PSD for the CVAP testing given in Table 2.2-1. Data from transducers P2, Fig. 3.5-4 at the 300° (RCP1A) inlet nozzle location and P4, Fig. 3.5-5 at 300° level 6 were reduced at the 4-pump, 565°F operating condition for comparison with the best estimate prediction values.

Since the P2 transducer was located opposite the pump 1A inlet duct, it is assumed that the higher than predicted PSD below 50 HZ is due to the inlet nozzle jet effect. It is also noted that the magnitude of the random spectra decreases with frequency and is well below the predicted white noise level at frequencies above 50 HZ.

The random turbulence of interest for the CSB is in the low frequency range shown in Figure 3.5-6. Note that the pump rotor frequency of 20 HZ and it's harmonic of 40 HZ do not appear and are therefore below the turbulence level.

A cluster of pressure transducers P4 thru P8 were monitored to verify the coherence length assumed for the random response due to turbulence. A coherence length of the annulus gap of [ ] was assumed. Figures 3.5-7 thru 3.5-12 consisting of 0 to 50 HZ PSD's coherence and phase demonstrate this coherence length to be conservative. The low frequency 0 to 10 HZ coherence is not fully developed between the circumferential P4 & P5 or axial pair P4 & P7 but they are very much alike, thus demonstrating that the axial and circumferential coherence lengths are approximately equal. The spacing between P4 & P5 is [ ] and P4 & P7 is [ ]. The larger spacing of [ ] exists between P4 & P8. The PSD's, coherence and phase for this pair are shown in Figures 3.5-11 and 3.5-12 where coherence has decreased. Thus the coherence length both axially and circumferentially is evident between [ ], and the value of [ ] used for the analytical predictions is therefore conservative.

The response PSD of a structure subjected to random loading exhibits a peak response at the natural frequency of the structure. A deterministic loading, on the other hand, produces a PSD which contains peaks, not at the structures natural frequencies, but at the forcing frequency. Thus in order to determine natural frequencies from the CVAP data, random loading is required. Since strong turbulence only exists in the low frequency range, the only

identifiable frequency is the CSB beam mode predicted in Figure 2.2-3 to be [ ] HZ. Figure 3.5-13 shows this response mode at a frequency of [ ] HZ in the displacement transducers A3 and A4 at the first CVAP test condition. Strong coherence is seen between these instruments for this mode in Figure 3.5-14. This frequency was apparent throughout the CVAP data acquisition and reduction program. From Table 3.5-3 it is clear that the CSB response is low. The maximum strain occurs at S2 for Test Condition 12 and is equal to [ ] micro in./in. RMS. For a random response this represents a peak stress of [ ] psi. This is well below both the fatigue endurance limit of 26,000 psi for  $10^6$  cycles (the fatigue curve used for design) and 21,850 psi at  $10^{11}$  cycles (the ASME extended fatigue curve). The displacements are low, the maximum occurred during Test Condition 4 at displacement transducer A4 and was equal to [ ] mils RMS. This is well below the acceptance value of 30.0 mils given in Table 1.3-1.

Tables 3.5-5 and 3.5-6 demonstrate that the CSB motion is dominated by random response. Figures 3.5-15 thru 3.5-19 show typical strain gage (S2 & S6) response for 0 to 50 HZ and 0 to 500 HZ. Strong coherence is noted in Figure 3.5-16 for the beam mode frequency of [ ] HZ. In Figures 3.5-17 and 3.5-18, care must be taken since the strain gages exhibited electrical noise at all multiples of 60 cycles. This was eliminated from the tabulated results, such as those in Table 3.5-6, as discussed in Section 3.5.1.

High coherence of instrument groups S1 & S5, and S2 & S6 at [ ] HZ coupled with the lack of coherence in S3 & S7, S4 & S8 and A1X and A1Y suggests an apparent favored beam mode response in the 0 to 180° direction. This is in agreement with snubber inspection findings.

The CSB response data was also examined during pump transients, i.e. pump starts and stops. This was performed to verify that no resonance response occurs as the pump frequency changes. Analysis indicated that the pump frequency changes during pump start up and shutdown occur too rapidly to cause any structural resonance. A number of pump time histories were examined. A typical CSB time history envelope is shown in Figure 3.5-20. The pump start occurred at approximately 9 seconds and reached normal speed at approximately 18 seconds. During this time no abnormal excursions were in evidence, thus verifying the original pump transient assumption.

### 5.2.2 Lower Support Structure

The hydraulic forcing function is measured by transducer P12, the response of which is listed in Table 3.5-7. The largest overall RMS pressure in this listing occurs at the normal operating condition of four pumps, 565°F (Test Condition 15). A more detailed breakdown of these responses is shown in Table 3.5-8 wherein the periodic and random components of the pressure are delineated. The periodic pump pressure pulsations at 120 HZ and 240 HZ in Table 3.5-8 are found to be in good agreement with the predicted values in Table 2.2-4. Pump pulsations at 360 HZ and 480 HZ are strong but were not predicted. The values in Table 3.5-8 indicate the major portion of the pressure loading is due to random turbulence. This random turbulence is predicted in Table 2.2-5 as wide band white noise. Typical plots of the pressure (P12) are found in Figures 3.5-21 and 3.5-22 and show that the magnitude of random turbulence is higher than predicted below 50 HZ and lower than predicted at all frequencies above 50 HZ. Furthermore the magnitude decreases with increasing frequency in contrast to the flat white noise spectrum predicted in Table 2.2-5. Because the natural frequencies in the Lower Support Structure are all above 100 HZ the predicted random levels are conservative. The higher random turbulence below 50 HZ apparently masks the expected vortex shedding pressure predicted in Table 2.2-4 as these are not seen in the typical response plots for P12 shown in Figures 3.5-21 and 3.5-22.

Natural frequencies and modeshapes of the Instrument Nozzle Assembly and ICI Tube 58 were predicted as shown in Figures 2.2-7 and 2.2-8 respectively. The first and second modes of the assembly can be seen in Figure 3.5-23 as the peaks at [ ] HZ and [ ] HZ respectively. This is in good agreement with predicted values of [ ] HZ and [ ] HZ. Other prominent peaks and build ups in response energy are due to pump pulsations at 120, 240, 360, and 480 HZ; response of other types of ICI tubes which have frequencies scattered from [ ] HZ and can cause the plate, to which A11 is mounted, to respond locally; and electrical noise at 60, 180, 300, and 420 HZ. Natural frequencies of ICI Tube 58 should most clearly be seen in the response plot for strain gage S14 shown in Figure 3.5-25. Strain gages, however, show both odd and even multiples of electrical noise and these signals appear to mask the predicted responses at [ ] HZ. In addition these high frequency modes will not be very strongly excited by the low levels of random turbulence found above 250 HZ. Periodic loading will not cause response at frequencies other than those of the forcing function itself, and thus low random levels will not show the natural frequencies well. Indications of these tube modes do appear in the plot of accelerometer A11 shown in Figure 3.5-23.

Response displacement and strain in the LSS region is shown in Tables 3.5-9 (A11) and 3.5-10 (S14) respectively. The response is seen to be mostly random which is in good agreement with the predictions of Reference 8. The predicted values of response in Figures 2.2-10 (S14) and 2.2-11 (A11) are conservative, but in fair agreement with the measured values of Table 3.5-7. This difference is attributed to the large percentage of response to random loading and the overprediction of that loading as well as the low damping used in the prediction analysis. The loss of both strain gages in the LSS region is acceptable in view of the early data obtained and the correlation of that data with pressure and acceleration readings

in the same area. The trend of response strain can be inferred from the pressure and accelerometer data and since this shows no significant increase beyond Test Condition 7, when the last strain gage failed, the response strains for Test Condition 1 thru Test Condition 6 are considered sufficient. Maximum response strain is [ ]  $\mu\epsilon$  in Table 3.5-7. This corresponds to a peak stress of [ ] psi which is far below the fatigue endurance limit of 26,000 psi. A typical pump start up transient response is shown in Figure 3.5-26. The plot shows no significant displacements as predicted.

### 5.2.3 Upper Guide Structure

The hydraulic forcing functions are measured using pressure transducers P10, P11 and P13 the responses of which are shown in Table 3.5-11. The table shows an increase in pressure with the number of pumps operating (Test Condition 1 to Test Condition 2) as predicted by analysis in Reference 2. Relative components, deterministic and random, of the total response are shown in Table 3.5-12. Indications are that random and deterministic contributions are about equal. Predicted values of pump pulsation deterministic loading are given in Table 2.2-6. Comparison with measured data shows the 40 HZ and 120 HZ values are overpredicted while the 20 HZ and 240 HZ values are underpredicted. In addition, relatively significant pump pulsations occur at 360 HZ and 480 HZ which were not predicted.

Figures 3.5-27 and 3.5-28 show pressure PSD's from 0 to 500 HZ at the upper plate (P13) and on a guide tube (P11) respectively. The two plots are virtually identical except for the [ ] HZ frequency range where only the guide tube transducer (P11) shows a pressure rise. This frequency range is the first beam mode of the guide tubes and it appears as a pressure loading which is actually due to motion of the tubes themselves.

The predicted pressure spectral density for the Random Forcing Function is based upon test data from a quarter-scale CEA tube bank test with a pressure transducer mounted on the upper guide structure support plate downstream of the CEA tubes near the outlet nozzle. Test data for P13, on the bottom plate of the UGS cylinder were reduced for the 4-pump, 565°F operating condition (Test Condition 15) for comparison with the predicted PSD in Table 2.2-7. The reduced data are shown in Figure 3.5-27. This Figure is repeated with the predicted PSD superimposed, see Figure 5.2-1.

The spectra for P13 decreases with increasing frequency similar to the spectra used in the analysis based on scale model tests for the tube bank. It is noted that the random pressure variations used in computing the dynamic response of the tube bank are larger than the measured magnitude at frequencies above 50 HZ.

Natural frequencies and modeshapes in the UGS region were predicted as shown in Figures 2.2-12 through 2.2-14. Figure 3.5-29 shows the first lateral assembly mode through the response of a typical guide tube accelerometer (A5). The frequency measures [ ] HZ, as compared to the predicted value of [ ] HZ. This frequency peak of [ ] HZ was also observed in the Demonstration Test of Reference 8. The difference in frequencies can be attributed to the variation in predicted hydrodynamic mass effects which are highly dependent on the methods and assumptions used, and the simplified spring mass modelling employed. Other predicted modes of the tube bank and assembly are not seen in the data. The first and second modes of the guide tubes are seen in the response peaks at [ ] HZ and [ ] HZ shown in Figure 3.5-30. These show good agreement with the predicted values of [ ] HZ and [ ] HZ respectively. The second mode response is verified by the strain gages showing an increase due to the [ ] HZ pump pulsations while the accelerometers, which are at node points for the second mode, show no increase.



These frequencies and levels of vibration were also found in the data taken during the Demo Test (Reference 8). This not only demonstrated the repeatability of the test but supplemented the CVAP by providing data for Test Condition 13 which was deleted in the CVAP but obtained during the Demo Test.

Typical response strain in the UGS guide tubes is shown in Table 3.5-14 and Figure 3.5-30. These indicate the response to be primarily due to random turbulence, [ ] HZ first mode response, with a secondary contribution from deterministic loading, pump pulsations at [ ] HZ and [ ] HZ exciting first and second tube modes. Even though the [ ] HZ pump pulsation was not used in the prediction of response strains, the total measured response in the UGS is small compared to that which was predicted. Table 3.5-11 shows the maximum strain to be [ ]  $\mu\epsilon$  in strain gage S12 during Test Condition 15. This represents a peak stress of [ ] PSI which compares with the predicted value of [ ] psi (Figure 2.2-16). Maximum displacements shown in Table 3.5-11 are [ ] mils for a guide tube (A7) and [ ] mils for the fuel alignment plate (A10). These compare very well with the predicted values of [ ] mils (Figure 2.2-17) and [ ] mils (Figure 2.2-18, 2 pump, 260°F).

Transient response strain in the guide tubes during pump startup is shown in Figure 3.5-31 which is typical. The overall strain is seen to increase but no large excursions are noted during the duration of the transient.

Guide tube acceleration and strain response are found to be primarily random and deterministic respectively (Tables 3.5-13 & 3.5-14). This is also reflected in the Amplitude Probability Distributions (APD) in Figures 3.5-32 & 3.5-33. These APD plots are smooth and show no signs of the deterministic traits of fluid structure instabilities.

### 5.3 EVALUATION

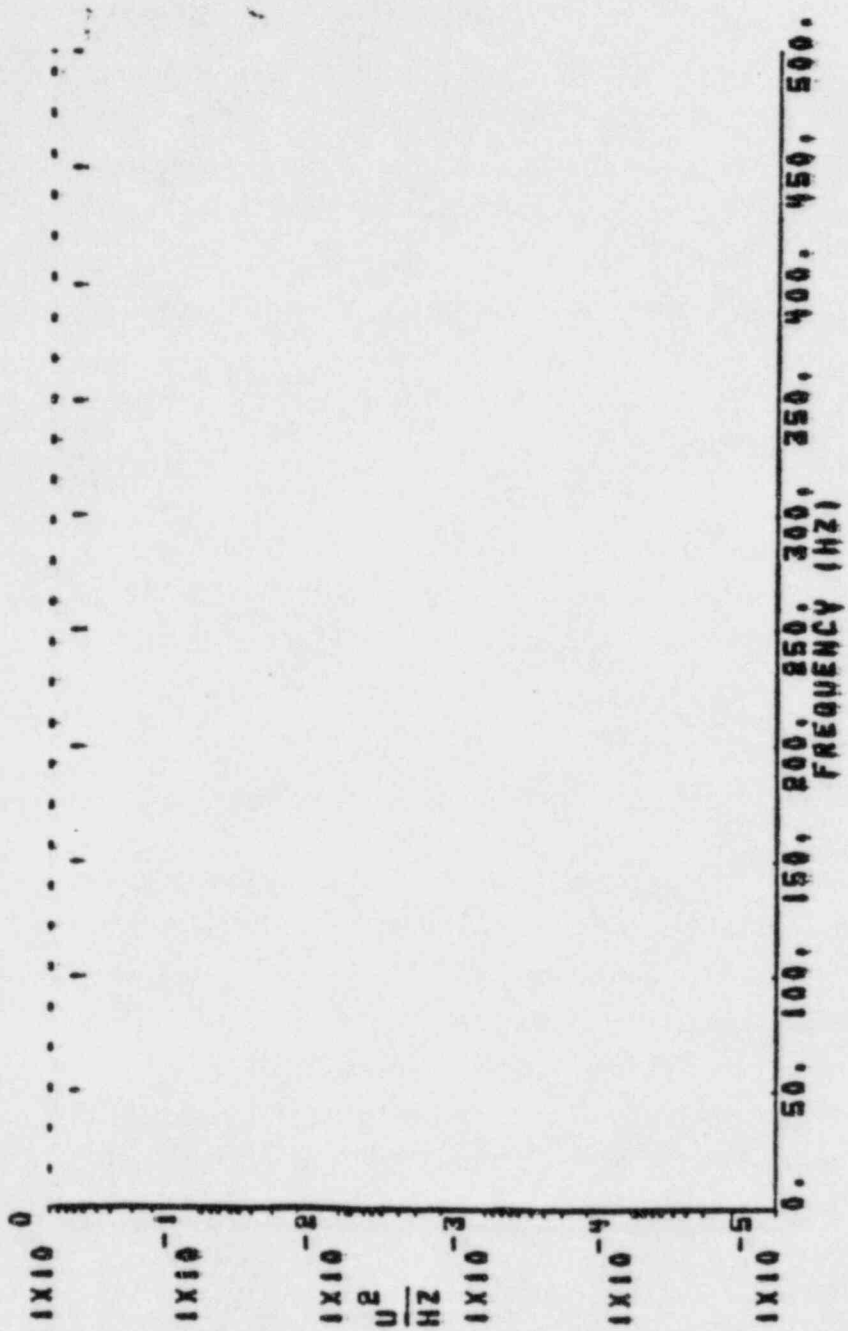
#### 5.3.1 Structural Adequacy of Reactor Internals

Evaluation of the comparisons of analytical predictions, test measurements, and visual inspection results leads to the conclusion that the ANPP System 80 Reactor Internals are structurally adequate and acceptable for long term operation.

This conclusion is based upon the following:

1. All design limits of Section III of the ASME code (Ref. 4) have been met by means of analysis. (Ref. 12)
2. Measured response frequencies agreed well with predicted values in all areas of the reactor internals. Measured forcing functions were less than predicted except for the pump pulsations at 360 and 480 HZ, and some random turbulence below 50 HZ, neither of which cause any meaningful response of the structure.
3. Measured response strains and displacements were all smaller than predicted and well under the acceptance criteria.
4. The acceptance criteria of Table 1.3-1, based upon ASME code fatigue allowables, and the reduced values based on the ASME code Winter 1982 Addenda shown in Section 1.4, were at no time exceeded during testing.
5. Inspection of the reactor internals was performed after acquiring a minimum of  $10^7$  cycles of vibration. No indications of failure or abnormal wear were found in the core support structural components. Cracks found in the CEA Shroud Assembly and the Reactor Coolant Pumps were corrected through structural modifications and the integrity of the modifications was verified by demonstration testing as described in References 7 and 8.

### POWER SPECTRAL DENSITY



SYSTEM 80 CVAP PALO VERDE UNIT 1  
 PUMP-13  
 TCMPI 3.450E102 PRESSURE1 2.250E103 PUMPS1 1A1 0 1B1 0 2A1 0 2B1 0 58  
 TRANSDUCER GROUP1 PRESSURE 1B1 P13 UPR PL1 UNIT101 PSI  
 RMS -  
 DL01PUMF13.PSB TAP1 1-245 RUN1 27 1.562E103 SP8 BW - 2.289E100 MDF - 100.

UGS RANDOM PRESSURE COMPARISON (P13) - PUMF 15  
 FIGURE 5.21

6. Measurements taken during the Inspection phase indicate that the holddown ring exerts sufficient force on the reactor vessel internals to retain them during operation.

### 5.3.2 Margins of Safety

The predicted and measured stress levels in the reactor internals components under steady state normal operation conditions are presented in Table I. A broader summary of maximum response stresses for all test conditions is shown in Table 5.3-1. It is obvious from both of these tables that the response stress levels are quite low and well below the acceptance and ASME code allowables.

### 5.3.3 Analytical and Test Methods

A review of the comparisons of predictions, measurements and inspection results lead to the following observations on the analytical and test methods employed in this CVAP.

1. Analytical methods to predict frequencies and modeshapes for the reactor internals were very good.
2. Prediction methods to determine the hydraulic forcing functions, while good in most cases, did not provide the pump pulsations found at 360 HZ and 480 HZ. These were found to be of the same order of magnitude as the 120 HZ and 240 HZ pulsations in many cases, but were not found to cause meaningful response despite their omission. Random loading was in general overpredicted at frequencies above 50 HZ and underpredicted below 50 HZ.

3. Response strains and displacements predicted were in good agreement with measurements considering the variations in predicted and measured forcing functions.
4. Instrumentation used in the tests were sufficient to provide redundancy and obtain the required data for comparison with predictions.
5. Repeatability of the testing was very good as found in the comparison of CVAP and Demo Test data.
6. Inspection methods, which are part of the CVAP, worked very well in uncovering problem areas which were not instrumented. These areas, CEA Shroud and Coolant Pumps, were successfully modified and tested to demonstrate their adequacy as explained in References 7 and 8.

In general it can be stated that the methods employed in the analysis and test phases of this CVAP are valid and sufficient to meet the objectives of Reg. Guide 1.20 (Ref. 1).

#### 5.4 CONCLUSIONS

The comparison and evaluation of the predictions, measurements and inspection results leads to the following conclusions:

1. The requirements and intent of Reg. Guide 1.20 (Ref. 1) have been satisfactorily met and completed in this Comprehensive Vibration Assessment Program for the ANPP Unit 1 prototype.
2. The reactor internal structures have been found to be adequate and acceptable for long term operation.
3. The methods used in the analysis and test phases of this CVAP are valid and sufficient to meet the objectives of Ref. 1.

TABLE 5.3-1

SUMMARY OF PEAK STRESSES AND FATIGUE MARGINS

Component	Stress Concentration Factor	Peak Stress (psi)	Location (Instrument)	CVAP Test Condition; Maximum Stress Normal Op.	Fatigue Margin
CSB					
LSS					
UGS					

5-15

Peak Stress = Measured Stress x Stress Concentration Factor

Fatigue Margin =  $\frac{\text{Endurance Limit}}{\text{Peak Stress}}$

Endurance Limit = 26,000 psi (see also Section 1.4)

\* Extrapolated

\*\* Same Steam Generator (Test Condition 12)

REFERENCES:

- (1) Regulatory Guide 1.20, Rev. 2, "Comprehensive Vibration Assessment Program for Reactor Internals During Preoperational and Initial Startup Testing."
- (2) "A Comprehensive Vibration Assessment Program for the Prototype System 80 Reactor Internals Palo Verde Nuclear Generating Station Unit 1," CEN-202-(V)-P.
- (3) "A Comprehensive Vibration Assessment Program for Palo Verde Nuclear Generating Station Unit 1 (System 80 Prototype) Preliminary Evaluation of Pre-Core Hot Functional Measurement and Inspection Programs", CEN-263(V)-P.
- (4) ASME Boiler and Pressure Vessel Code, Section III, 1977.
- (5) "Precore Reactor Internals Vibration Measurements", Procedure No. 92HF-1RX 01, Rev. 1, 5/9/83.
- (6) "Comprehensive Vibration Assessment Program Visual Inspection Data on the Reactor Vessel Internals for Arizona Public Service Company Palo Verde Nuclear Generation Station Unit Number One", Combustion Engineering Specification Number 14273-RCE-457, Revision 02, November 1984; including photographic documentation books; Combustion Engineering, Inc.
- (7) "Final Report on Palo Verde Nuclear Generating Station Reactor Coolant Pumps," CEN-271(V)-P, Revision 1-P; August 1984; Combustion Engineering, Inc.
- (8) "Final Report on the Performance Evaluation of the Palo Verde Control Element Assembly Shroud," CEN-267(V)-P, Rev 1-P.
- (9) Interim Report - E. E. Van Brunt (APS) to USNRC (Region 5) NAPP-27598, August 19, 1983.



- (10) "CVAP Visual Inspection of the Reactor Vessel Internals for Arizona Public Service Company Palo Verde Nuclear Generating Station Unit Number One (System 80 Prototype)", CEN-290(V)-P.
- (11) "Pump-Induced Acoustic Pressure Distribution in an Annular Cavity Bounded by Rigid Walls", M.K. Au Yang, Journal of Sound and Vibration, 1979, 62(4), pg. 577-591.
- (12) "Evaluation of Reactor Core Support Structures for Arizona Nuclear Power Project Palo Verde Unit I", Stress Report No. 14273-MD-001, Combustion Engineering, June 17, 1981.
- (13) SYSTEM 80 CESSAR/FSAR
- (14) ASME Boiler and Pressure Vessel Code, Section III, Winter 1982 Addenda.

**COMBUSTION ENGINEERING, INC.**